THE EFFECTS OF ANGLED INSOLES ON SHORT RADIUS FLAT-TRACK RUNNING MECHANICS

by

Christopher David Bianchini

A thesis submitted in partial fulfillment
of the requirements for the degree

of

Master of Science

in

Mechanical Engineering

MONTANA STATE UNIVERSITY
Bozeman, Montana

December 2023

DEDICATION

This paper is dedicated to my wife, Alexus Bianchini.

ACKNOWLEDGEMENTS

I would first like to thank my graduate committee Dr. Corey Pew, Dr. Scott Monfort, and Dr. James Becker for their continued support throughout the research process. I would also like to thank Dr. David Graham for his support. Lastly, I would like to thank my colleagues in the Montana State University Neuromuscular Biomechanics Laboratory for supporting my research.

TABLE OF CONTENTS

TABLE OF CONTENTS CONTINUED

LIST OF TABLES

Table Page

LIST OF FIGURES

Figure Page

LIST OF FIGURES CONTINUED

Figure Page

LIST OF FIGURES CONTINUED

Figure Page

LIST OF FIGURES CONTINUED

Figure Page

LIST OF FIGURES CONTINUED

Figure Page

LIST OF FIGURES CONTINUED

Figure Page

LIST OF FIGURES CONTINUED

Figure Page

ABSTRACT

While indoor track allows athletes to compete during the winter period of December to February, injury rates during the indoor track and field season are 16% higher than the outdoor season. Increases in injury rates are often attributed to the shorter turn radii experienced by athletes when competing on a 200m indoor track as opposed to the longer turn radii of a 400m outdoor track. A common method of counteracting these asymmetries is to bank the turns of a 200m indoor track. Aligning the athlete's resultant force vector perpendicular to the running surface can alleviate many of the running form abnormalities caused by turn running. However, the high cost of implementing a banked indoor track can be prohibitive to many programs who currently have a flat track facility.

To this end, we have developed two experimental insoles designed to alleviate the asymmetries experienced during turn running: a physically angled foam insole and an insole containing an angled stiff mid-plate. Insole function was tested through human participant running trials to identify their effects on indoor flat track running mechanics. 12 NCAA Division 1 track and field athletes (6 male, 6 female, age: 21 ± 2 years, mass: 61.4 ± 11.4 kg, height: 1.77 ± 0.17 m) who specialize in distance and mid-distance running provided informed consent to participate in this Institutional Review Board-approved protocol. Kinematics, muscle activation, and ground interaction variables were monitored during running trials and used to compare the effects of the insoles on running biomechanics.

The physically angled insole produced positive results for ankle joint angles and ground interaction variables for turn running. The angled plate insole positively affected right-side ankle joint angle positioning and did not significantly impact straight running mechanics. Both insoles produced higher levels of muscle activation asymmetry, indicating that this may be a required effect of turn running regardless of joint angle positioning and ground interaction. While the angled plate insoles showed almost no impact on straight or turn running mechanics, the wedge insoles functioned effectively to alleviate several asymmetries related to turn running.

CHAPTER ONE

INTRODUCTION

Over 30,000 athletes compete in National Collegiate Athletic Association (NCAA) outdoor track[1]. Over 27,000 of these athletes also compete during the indoor season[1]. 1.1 million high schoolers compete in outdoor track and field, with over 127,000 also competing in indoor track[1]. While indoor track allows athletes to compete during the winter period of December to February[2], injury rates during the indoor track and field season are 16% higher than the outdoor season[3]. Specifically, distance and mid-distance runners report 1.7 times higher incidence of overuse injuries than other event groups (sprinters, jumpers, or throwers), require 168% more time-loss than other event groups[3], and cost an average of $334,115 in injury related events to a university in a single season[4]. In addition, running related injuries can cause extreme emotional hardship and negatively impact the day-to-day wellbeing of athletes[5].

Several theories as to why indoor track and field injury rates are higher than outdoor, particularly in distance running, have been proposed. First, because indoor track takes place prior to outdoor track season, it is thought that a more sudden increase in running volume is a primary cause for increased injury rates[6]. Another possible cause is that indoor track and field takes place from December to early March, which is typically a colder and darker time of year than outdoor track season (late March to June). Winter training conditions can lead to vitamin D deficiency in athletes and an increased rate of overuse injuries[7,8]. Lastly, it has been proposed that increases in injury rates during indoor season may be influenced by the shorter turn radii [9–12] experienced by athletes when competing on a 200m indoor track (17.2m turn radius)[13] as opposed to the longer turn radii of a 400m outdoor track (36.5m turn radius)[13] (fig. 1). No epidemiological data exists

comparing injury incidence between flat track and banked track facilities, but studies have shown that biomechanical asymmetries like those seen between the inside and outside legs while running on an indoor track may be related to injury[12,14–19] It is also important to note that athletes competing on a track will always run counterclockwise, meaning the left leg is always the inside leg and the right leg is always the outside leg. While externally caused gait asymmetries are not dangerous in the short-term, long-term training and competition with consistently altered running mechanics can lead to strength asymmetries and alterations to an athlete's natural running gait[20–23].

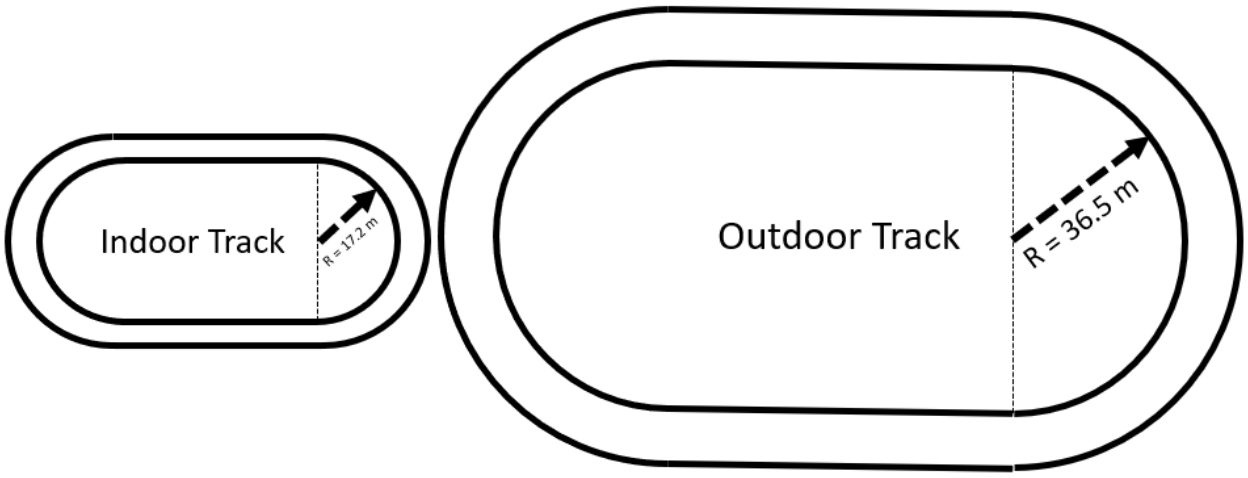

Figure 1. Scale drawings of an indoor and outdoor track. The shorter turn radius of an indoor and outdoor track. The shorter turn radius of an indoor track may be the cause of higher injury rates.

Some of the first studies regarding flat turn running were conducted by Peter R. Greene in the 1980s. Greene developed an extensive body of research regarding turn running, both on banked and flat surfaces. His primary goal was to classify how different turn radii and turn conditions affect the maximum speed attainable by athletes. By recording athletes running with a high-speed 16mm camera, Greene was able to compare each athlete's velocity, stride length, and

ground contact time for straight and curved paths[24]. He found that for curves of decreasing radii, an athlete will have a reduced maximum speed and increased ground contact time, but stride length and stride time remain unchanged. He also discovered that the magnitude of these effects is dependent on each individual athlete's height, weight, and velocity, due to the changes of reaction forces as seen in fig. 2. This study was one of the first to show that short radius turns can negatively impact a runner's performance and paved the way for future studies that investigate more specific gait metrics.

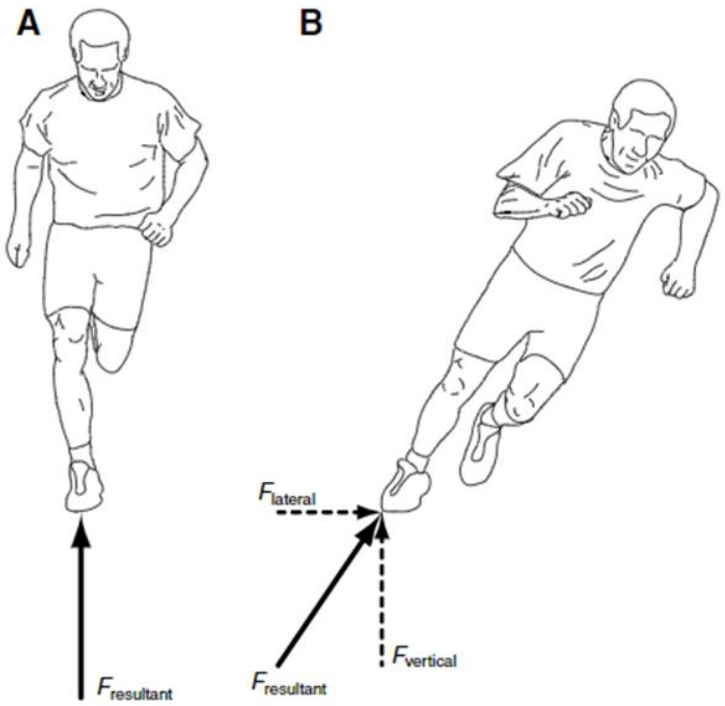

Figure 2. The difference in ground reaction forces between straight and corner running, from the frontal plane. From Chang, et al.[16].

Further studies have attempted to investigate the potential causes of decreased running performance around track turns[9,14,16,17,19,25–27]. While most studies regarding turn running are focused on performance metrics, their findings indicate that certain biomechanical changes in

running form will occur that may also be correlated with higher rates of injury. Specifically, maximum left ankle eversion[19] (fig. 3, fig. 4), right ankle inversion at initial contact[19], maximum left hip adduction[17], right gluteus medius activation[11], left gastrocnemius medialis activation[26], ground contact time asymmetry[28], and ground reaction force asymmetry[19] have been shown to significantly increase when an athlete runs a track turn. Interestingly, the epidemiology of indoor track and field injuries among distance runners aligns with injuries that these changes may be related to[3,29–31].

Figure 3. A photograph from an NCAA indoor track and field meet demonstrating the extreme values of left ankle eversion that can be achieved when running a track turn.

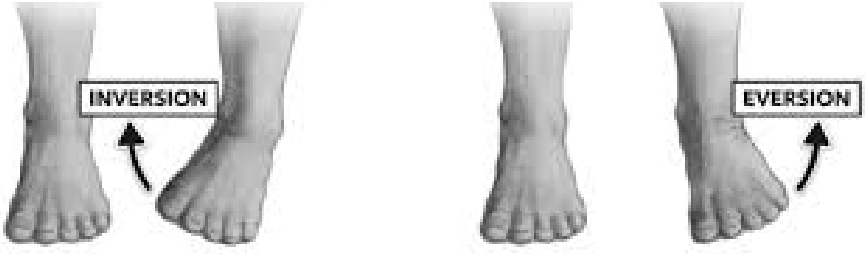

Figure 4. Ankle inversion vs. eversion.

One of the first studies to follow Greene's research came from Hamill, et al.[19]. Their investigation into the effects of track turns on lower extremity function showed significant differences in ankle angle at initial contact, mediolateral and vertical ground reaction force variables, and maximum eversion of the left ankle during midstance (fig. 5). In this study, when running a track turn, the left ankle reached a maximum eversion angle of 22.56˚ (compared to 11.48˚ when straight running) during midstance and the right ankle experienced 12.76˚ of inversion (compared to 7.09˚ when straight running) at initial contact.

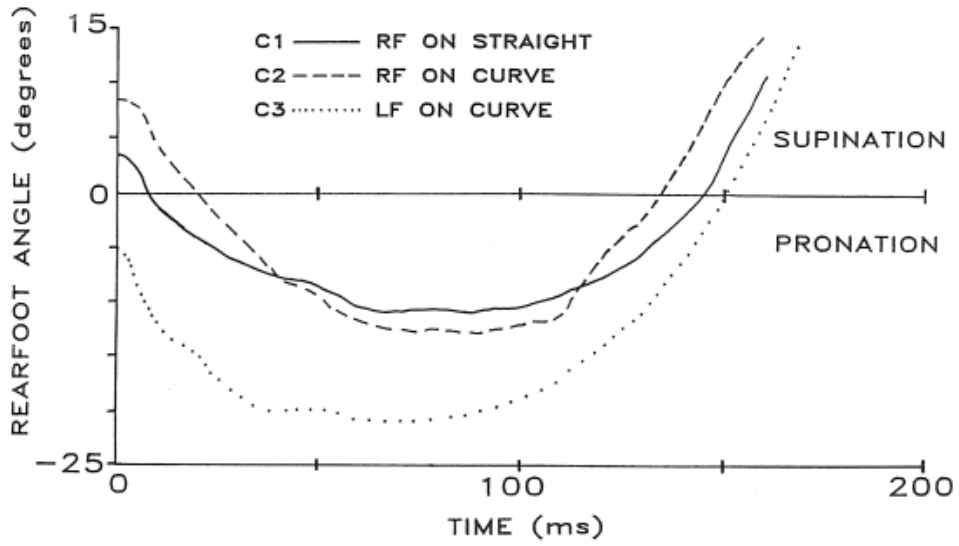

Figure 5. Eversion (pronation) and inversion (supination) angles of the left and right ankles, respectively, when running a turn[19]. Note that the left ankle eversion on the curve is higher, and the right ankle has a larger total range of motion and inversion angle at initial contact than straight running conditions. (C1: condition 1, C2: condition 2, C3: condition 3, RF: right foot, LF: left foot).

The correlation between repetitive ankle eversion during running and injury likelihood is highly debated. Historically, excessive ankle eversion was defined as an eversion angle greater than 13-15˚, and in one study athletes with eversion-related injuries displayed 2-4˚ more eversion during running than healthy controls[32,33]. However, comprehensive reviews of the literature

indicate that absolute eversion angle alone may not correlate with running injury incidence[34]. Another study indicated that coupling peak eversion angle and hip adduction angle may be a predictor of tibial stress fractures[35]. In addition, a greater duration of time spent in eversion during the stance phase functions as an effective predictor for the development of medial tibial stress syndrome and Achilles tendinopathy[36]. Track injury epidemiology suggests that the left leg may experience more injuries like plantar fasciitis, metatarsalgia, medial tibial stress syndrome, and tibialis posterior tendonitis[3], which may also be correlated with ankle eversion[33].

The clinically significant definition of "excessive" inversion is also not well defined, but a foot that is forced into a more inverted position and restricted from naturally everting at midstance may exhibit a lesser ability to absorb impact[32]. Because ankle eversion functions as a shock absorber during running[37], some studies have suggested that an ankle that is forced into a more inverted position, such as the right ankle while running a track turn, may be more likely to cause knee and hip compressive injuries[19,38]. This again aligns with indoor track and field injury epidemiology[3,31].

In addition to ankle angle modification, an athlete also experiences significant changes in hip angles when running a track turn[17] (fig. 6). Alt et al. found that when running straight, an athlete will experience around 7-9˚ of hip adduction. When turning left around a track, left hip adduction values increased from7.7˚ to 13.8˚. The peak values for hip adduction occurred during midstance, which may be related to injury likelihood. Hip adduction during the stance phase can be indicative of medial limb collapse that can lead to patellofemoral pain syndrome, iliotibial band (ITB) friction syndrome, and patellar tendinopathy[39]. In prospective studies, athletes with iliotibial band injuries exhibit significantly higher levels of hip adduction than healthy controls[40],

and athletes with rehabilitated IT band injuries exhibit 2.2˚ less hip adduction than their injured counterparts[41].

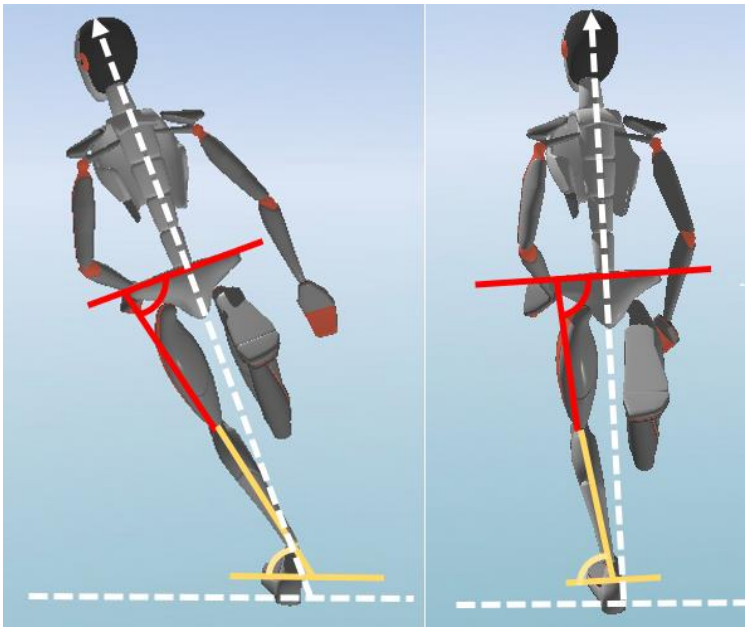

Figure 6. Joint angle differences experienced when turning (left) and running straight (right). The red lines demonstrate hip angle, and the yellow lines represent ankle angle.

Because of the requirement to generate asymmetrical force when running a track turn, athletes are not only forced to position their lower extremity joint angles in an abnormal manner, but also asymmetrically activate running-related muscles[11,26]. Whenever a specific muscle is repeatedly activated at a higher rate than others, morphological and physiological adaptations in muscle structure and function may occur, which contribute to a risk of overloading, asymmetry, and consequently, injury[42]. Pietraszewski, et al.[26] found that the left gastrocnemius medialis (MG) activates at a significantly higher level than the right MG during a 400m indoor time trial. The MG is primarily a muscle that contributes to ankle plantarflexion, but it also functions as an ankle invertor when the ankle is in a neutral or inverted position. The Achilles tendon sits slightly medial to the subtalar joint and has a slight inversion moment arm on the subtalar joint,

allowing the MG to contribute to ankle inversion[43,44]. Asymmetry of muscle activation can lead to overuse of the muscle that is being activated at a higher level, as well as eventual strength asymmetries that can lead to elevated injury risk[45]. Corroborating these findings, Beukeboom, et al. found that athletes training consistently on a small radius indoor track will develop significant strength increases of the left ankle invertor and right ankle evertor muscle groups[9]. Consequently, athletes that consistently train and compete on short-radius indoor tracks may be more susceptible to the development of muscle asymmetries and related injury[9].

Similarly, Nevison, et al.[11] showed that the gluteus medius (GM) muscle of the right (outside) leg will also activate at a significantly higher level than the left (inside) when an athlete is running an indoor track turn. When an athlete runs a consistent left turn, Nevison et al. suggest that their findings indicate that the athlete would be required to activate their right GM more than their left in order to abduct the right hip to produce lateral force, possibly leading to the development of strength asymmetries from repetitive asymmetrical movements over time. For hip abductors like the GM, muscle activation asymmetry of 16% is associated with a higher incidence of patellofemoral pain syndrome[46] and GM strength asymmetry has been shown to negatively impact performance and running economy[46,47]. Athletes that consistently train and compete on a short radius indoor track may be more susceptible to the development of GM strength asymmetry.

Some of the earliest research regarding track turn running mechanics indicates that overall ground contact time (GCT) and ground reaction force (GRF) increase when an athlete is running a turn[12,15,17]. Greene noted that GCT may be higher for the left side than the right when running a track turn[12]. Agreeing with Greene's preliminary findings, Ammann, et al. found that,

over the course of a 5 km time trial on a 400m track, GCT was approximately 2.57% longer on the left side[28] (fig. 7). Ground contact time asymmetry has been tied to decreased running economy, leading to a higher rate of fatigue and overuse injuries[48].

	Overall	Women	Men
5-km time	17:06	18:54	15:55**
[min:ss]	±01:39	±00:56	±00:35
Speed	4.92	4.42	5.24**
[$m \cdot s^{-1}$]	±0.48	±0.26	±0.26
GCT	193.7	199.3	190.0**
[ms]	±14.3	±13.9	±13.3
Asymmetry	2.57	2.47	2.65
[%]	±2.14	±1.79	±2.34

** $p < 0.01$ between gender.

Figure 7. A table of results from Ammann, et al.'s study regarding running asymmetries on a track[28]. Ground contact time asymmetry was measured at 2.57%.

In the same study investigating ankle kinematics, Hamill et al. discovered a significantly higher right side maximum vertical ground reaction force (vGRF) compared to the left while running a turn[19]. While overall increases in vGRF have been retrospectively correlated with higher rates of injury, the relationship between vGRF asymmetry and injury is not as clear[44]. Asymmetry in gait kinetics may be linked with overuse injuries[20]. While the validity of vGRF asymmetry as an injury predictor is unclear, retrospective studies have indicated significantly higher values of propulsive vGRF peaks between athletes with a history of tibial and femoral stress fractures compared with healthy controls[49]. Hamill et al.[19] assert that a higher right-side vGRF, coupled with a reduced eversion range of motion in the right ankle when running a track turn, indicates that the right leg may be less effective at absorbing shock and possibly more prone to developing stress fractures when consistently training and competing in the same counterclockwise direction.

Several different methods for reducing the magnitude of abnormal gait patterns during track turn running have been discovered. One of the most common ways of combatting these problems is by banking the turns of an indoor track (fig. 8). By banking the turns of a track at a precise angle, the athlete's net ground reaction force vector becomes perpendicular to the running surface[50]. The optimal angle for a banked track varies by height, weight, running speed, and other biomechanical factors. In newer facilities, hydraulic systems are used to change the angle of the running surface during a track meet to accommodate for different running speeds depending on which track event is taking place. For sprint events, the bank angle can become more extreme than for distance events.

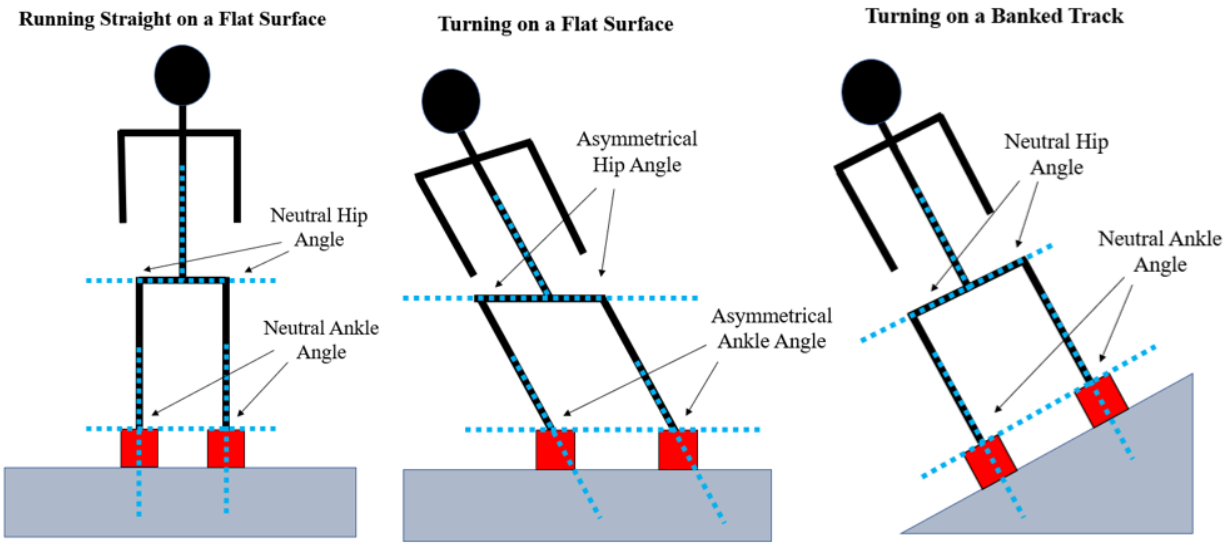

Figure 8. The difference between turning on a flat surface and turning on a banked surface in terms of joint angle positioning. Running straight on a flat surface and turning on a banked surface each produce relatively neutral levels of hip and ankle frontal plane angles.

Several studies have shown the various effects of banked tracks on running performance. Wannop et al. showed a significant decrease in joint loading in the transverse and frontal planes, right ankle inversion, and left ankle eversion on a 10˚ bank. Greene, et al.[51] showed that a banked

track greatly improves running speeds, while decreasing overall ground reaction force and ground reaction force asymmetry (fig. 9). White, et al.[52] similarly showed that overall ground contact time and ground contact time asymmetry can be reduced by running on banked turns. They also discovered that banked tracks allowed athletes to achieve a longer stride length while maintaining the same stride frequency, resulting in better performance. These studies indicate that gait asymmetries brought on by running a flat curve can be alleviated by banking the turns of an indoor track.

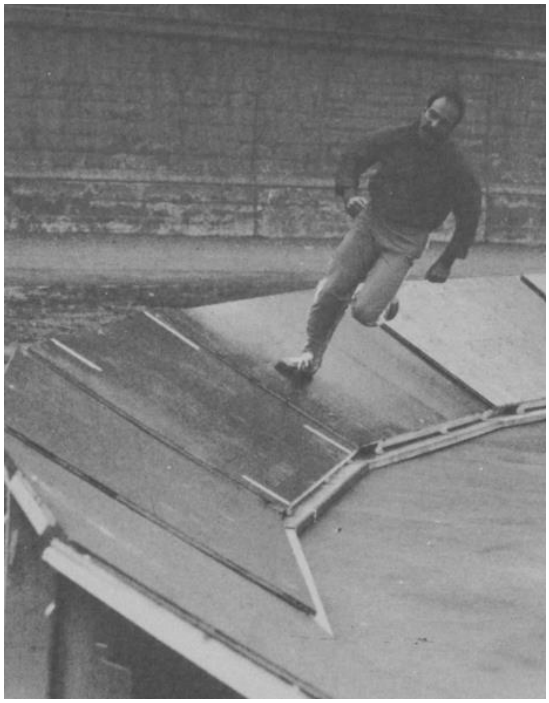

Figure 9. A photograph from one of the oldest studies regarding running on banked tracks. Greene[51] constructed a banked track out of plywood and sections of track surface to show the performance and biomechanical improvements caused by banking a track turn.

The difference in performance effects from banked tracks and flat tracks is highlighted in collegiate competition results. In the NCAA, conversion factors based on Greene's research exist during indoor track to compensate for the effects of banked track turns (Table 1). For a sprint

race like the 400m, a 200m flat track decreases performance by an estimated 1.57%. While the faster races experience a higher percentage adjustment due to the increased velocity term, the net performance reductions are exacerbated in a distance race due to a higher number of turn repetitions that take place during the race.

Table 1. Event-specific conversions used to compare banked track and flat track times by the NCAA[53]. For the US Men's Championship Qualifying Standard for a 3000m indoor race, the difference is 5.42 seconds.

Event	Multiplier	Men's 2023 US Championships Qualifying Standard	Equivalent Time on 200m flat track	Adjustment (seconds)
400m	0.9843	47.20	47.95	-0.75
800m	0.9859	1:47.75	1:49.34	-1.59
Mile	0.9874	3:54.00	3:56.99	-2.99
3000m	0.9885	7:46.00	7:51.42	-5.42

In addition to banked tracks, one study has shown that some benefits can be produced by banking an athlete's shoes using a wedge (fig. 10). Luo, et al.[27] found that with wedged shoes, an athlete is positioned in an advantageous way for use of the moment generation capacities of the ankle, thus increasing turn running performance. The angled shoes showed a positive effect on ankle moment generation, overall running speed, and total ground reaction force during turn running [27]. However, while angled shoes have shown positive effects on performance capabilities, their effect on biomechanics with relation to injury mechanisms remains unknown. Specifically, the effect of turn running shoes on kinematics, muscle activation, and ground reaction force and contact time asymmetry has not been investigated.

Figure 10. The control and wedged shoes from a study investigating the effects of corner running in wedged shoes[27]. These shoes were able to improve an athlete's ankle moment generation, ground reaction force, and overall turn running performance.

While banked shoes and banked tracks both increase running performance, modifying the angle of the effective running surface is not the only way to improve turn running performance and decrease gait asymmetries. Chang, et al. performed a study in which they compared the running speed and mechanics of athletes running along a curved path to athletes running along a curved path with a tether applying centripetal force to their center of mass[16]. Tethered athletes were able to run at much higher speeds than without a tether. In addition, they found that while vGRF was higher on the right side than the left side when running a turn while untethered, vGRF asymmetry disappeared when a tether applied centripetal force to the athlete's center of mass (fig. 11). This study indicates that if a runner is provided with a more effective way to meet centripetal force requirements, overall performance and gait symmetry can be improved.

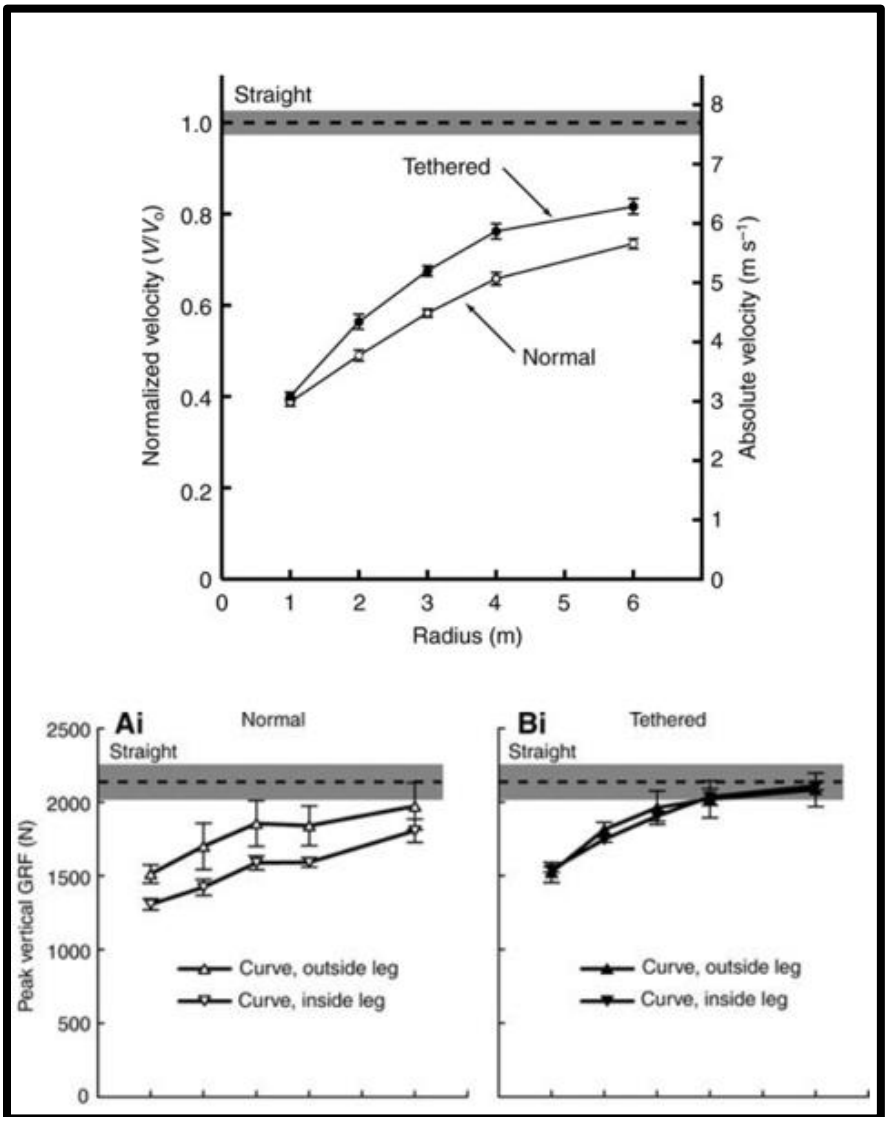

Figure 11. The difference found between velocity and vGRF asymmetry of runners when tethered and untethered to a stationary center point[16]. Providing athletes with an effective way of meeting centripetal force requirements improved overall running speed and vGRF asymmetry.

Synthesizing the findings from banked track studies, the banked shoe study, and the tether study, we concluded that an effective solution to mitigate negative effects of tight corner turn running is to provide a way for the athlete to more effectively generate lateral forces required when turn running. While the effects of a banked track and banked shoes indicate that an angular adjustment of the effective running surface may be necessary for the correction of

biomechanical asymmetries, the tether study suggests that introducing an external method of more effectively counteracting the lateral force requirements may be the primary mechanism that contributes to the ability of these interventions to decrease asymmetry. A lower cost and practical alternative to banked tracks turns and athlete tethering is needed to assist runners with lateral force generation. One newly popularized method of increasing the energy return of a running stride specifically for straight running is to increase the longitudinal bending stiffness of a running shoe. This is typically done by integrating a stiff plate into the midsole of the shoe[54–58]. However, there is a limit to the amount of longitudinal stiffness that still improves running energetics and optimal values exist[59]. Like bank angle, truly optimal values for longitudinal shoe bending stiffness vary by a variety of factors, including height, weight, and running speed[58]. Because of this, studies have produced varying "optimal" stiffness values. There is no clinical consensus on optimal shoe stiffness, but positive effects on running economy and biomechanics have been shown for a 3-point bending stiffness of 14-24 N/mm[54,57,60,61] (fig. 12). While other studies have shown improved running economy at much higher stiffness values (35-45 N/mm), these studies primarily focused on the reduction of EMG muscle activity during sprinting by restriction of the metatarsophalangeal (MTP) joint[62]. Further studies have indicated that submaximal running energetics are affected poorly by MTP joint restriction[59,62].

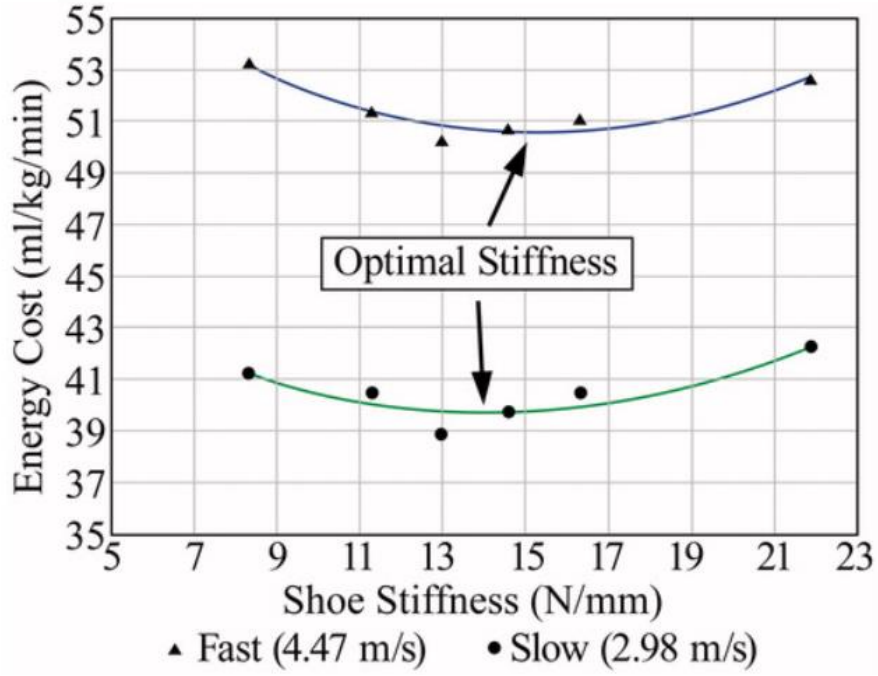

Figure 12. Energy cost vs. shoe stiffness. Optimal values varied between participants unpredictably, but typical values of shoe stiffness that influenced improvements were around 15-17 N/mm[57].

While the positive effects of increasing longitudinal shoe bending stiffness have only been observed for straight running conditions, we theorize that greater amount of lateral energy return could be provided to an athlete by angling the midsole plates in the direction an athlete is turning. Primary bending of the midsole plate will occur around the neutral axis of the plate. When an athlete runs a turn with a flat (non-angled) midsole plate, the only improved value of energy return is oriented in the vertical direction. By angling the plate, the primary direction of enhanced energy return would theoretically act at an angle oriented slightly towards the inside of the turn. For straight running, a component of this return would still be oriented vertically, but for turn running it would now also include a lateral component. Similarly, straight running in shoes that have a higher longitudinal bending stiffness increases the lever arm lever arm of the ankle and the average ankle moment[63]. By angling the plate, we theorize that a similar effect will

occur about the ankle axis during turn running, but oriented at an angle relative to the running surface, allowing for more effective force generation in the lateral direction.

In summary, every winter, injuries induced by short-turn flat-track indoor track and field competition and training create financial, emotional, and physical pain for athletes. Right now, the only widely used and feasible intervention for asymmetrical turn running mechanics is the high-cost method of banking the turns of an indoor track. While banked shoes and tethering a runner to a stationary center point have both shown positive effects on turn running mechanics, neither are feasible for prolonged training on an indoor flat track where straight running is also required. It is possible that other feasible and cost-effective solutions exist, but their effect on both straight and turn running mechanics must be investigated. To eliminate the burden caused by these injuries, it will be crucial to develop low-cost surface-based, footwear-based, or training-based solutions to combat the biomechanical changes induced by running fast around a turn.

To this end, we have designed and tested a prototype turn running insole (fig. 13). The design utilizes a rigid midsole plate embedded at an angle 10˚ relative to the ground, aiming to provide a response force angled towards the inside of the track turn. In addition, we have tested a physically angled “wedge” insole to use as a comparison. In previous studies, a wedge insole has demonstrated a performance enhancing effect, but its impact on turn running related biomechanics has not been well defined. We hypothesized that (1) athletes running a turn utilizing the angled plate insoles will experience lower values of left foot maximum eversion angle[17,19], right ankle inversion angle at initial contact[19], left hip maximum adduction angle[17], gastrocnemius medialis[26] and gluteus medius[11] muscle activation asymmetry, ground reaction

force asymmetry[12], and ground contact time asymmetry[28] than when running a turn in baseline, flat insoles and (2) an athlete running straight in the angled plate insoles will experience no change to the aforementioned measurements when compared to straight running mechanics in baseline, flat insoles.

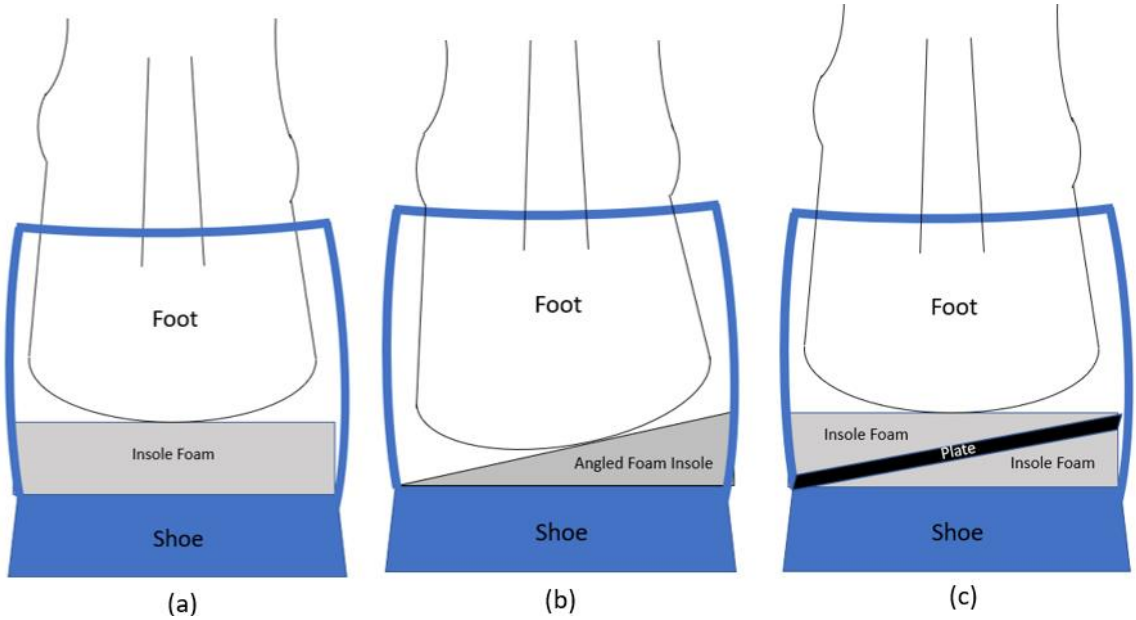

Figure 13. Rear view schematics for test 3 insoles: (a) baseline, (b) wedge, and (c) angled plate insoles. The wedge and angled plate insoles were each compared to the baseline insole.

CHAPTER TWO

METHODOLOGY

To test our hypotheses, 3 insoles were developed and tested on human participants. A flat insole and a physically angled insole were used as benchmarks for a third insole containing an angled stiff plate. Simplified analytical models were used to generate preliminary design specifications, followed by finite element analysis and physical testing for property verification. Participants then ran multiple running trials for each insole while kinematics, muscle activation, and plantar pressures were measured.

Prototype Design Criteria

Three insoles were developed for testing: a baseline flat insole containing no plate (baseline), an angled foam (wedge) insole that would physically position the athlete's ankles at an angle relative to the running surface, and a flat insole containing an embedded stiff plate that is angled relative to the running surface (angled plate). While straight running, energy storage and return can be enhanced by integrating a flat plate within a shoe[54,56,58,62–64]. By angling the plate, the primary direction of energy return would theoretically act at an angle oriented towards the inside of the turn. For straight running, a component of this energy return vector would still be oriented vertically, but for turn running it would now also include a lateral component to provide a more effective way to produce the lateral force required to run a track turn. While the angled plate may provide improved lateral energy return and force generation capacity during turn running, the flat interface between the insole and the foot should theoretically allow the plates to produce this lateral energy return only when an increased lateral force is present, like

when running a turn, and should not significantly alter straight running mechanics. While most running shoes utilize midsole plates to achieve a positive effect on running energetics and mechanics, insoles were utilized in this study to avoid manufacturing an entire shoe from scratch. Typical running shoe anatomy is detailed in Appendix A.

The design of each turn running insole aimed to emulate the effects of a banked track by providing a response force oriented parallel to each participant's body position while turning. Design criteria for the insoles focused on geometry, plate stiffness, plate range of motion and ultimate failure limit, foam material compressibility, and safety of the insole materials. The angled plate insole was designed with the following specifications:

Geometry

An insole designed to assist with turn running injury mechanics should provide a response force directed to the inside of the turn, allowing the athlete to more effectively counteract the centripetal motion encountered when running a turn[16,18,27]. The optimal value for this angle varies by turn radius, speed, height, weight, and running style, showing a direct relationship with the inverse Froude number. More information regarding this theory is detailed in Appendix B. However, the angle that accommodates the broadest spectrum of possibilities and is used by the NCAA for a standard fixed angle banked track is 10°[13,18]. In addition, while the plate should be imbedded at an angle in order to provide both lateral and vertical energy return, the contact area with the athlete's foot should remain neutral to minimize alteration to straight running ankle kinematics.

Plate Stiffness

A possible method for providing a directional force during turn running is by implementing a stiff mid-plate oriented at an angle within the insole. The optimal stiffness for this plate varies by participant[56]. There is no clinical consensus on optimal shoe stiffness, but positive effects on running economy and biomechanics have been shown for a 3-point bending (fig. 14) stiffness of 14-24 N/mm[54,57,60,61]. This range was generated by compiling the results of multiple studies regarding longitudinal bending stiffness of shoes. Positive results were found for several values within this range and each study included a baseline stiffness that was less than 14 N/mm. While a 3-point bending test does not accurately simulate realistic conditions a plate will experience during running, it is a simple and repeatable way of measuring longitudinal shoe stiffness.

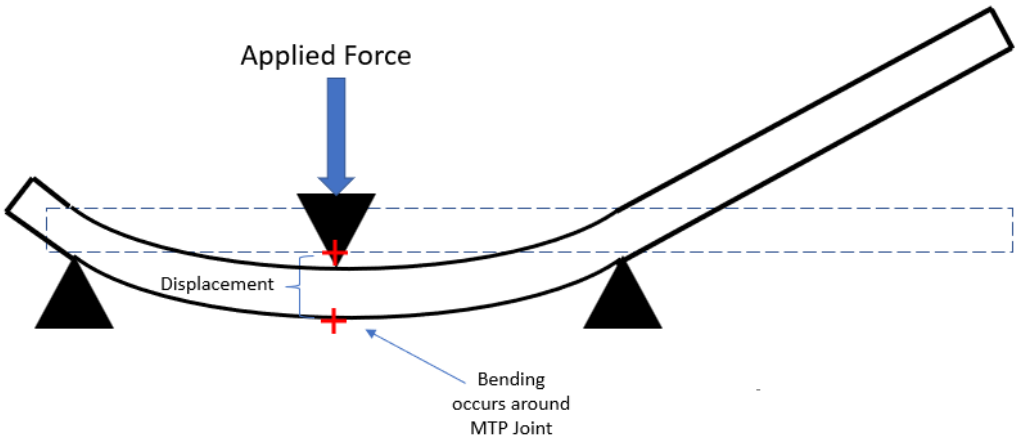

Figure 14. A 3-point bending test. The stiffness is found by dividing the maximum displacement by the force applied. The results of this test are dependent on the length of material tested. The stiffness range of 14-24 N/mm was found over a portion of the shoe centered around the bending of the metatarsophalangeal joint.

Plate stiffness is dependent on shoe geometry and for the purpose of material selection had to be converted to an appropriate Young's Modulus. For initial material selection, the plate geometry could be simplified to a rectangular plate that is the average width of the bending region[65]. To reduce manufacturing cost and time, all designs were based around a US size 11 insole (all male participants in this study). The average width of the bending region of a size 11 insole is approximately 101.6 mm. For isotropic materials, the flexural modulus is equal to the Young's Modulus of the material due to the second moment of inertia for a rectangular beam and the derivation of elastic beam theory[66]. The equation

$$E_F = E = \frac{L^3 m}{4bd^3} \tag{1}$$

where E_F is flexural modulus, E is Young's modulus, L is the pinned material length during the 3-point bending test, m is the 3-point bending stiffness, b is the material width, and d is the material thickness, was used to generate possible combinations of Modulus and thickness that would produce the desired 3-point bending stiffness. The pinned material length is 80 mm, which is the support distance used by many studies that have related longitudinal shoe bending stiffness with improved energy return[54–57,60,62,64]. To make direct stiffness comparisons to these studies, the support distance was set to 80 mm. However, because material thickness had not been defined and the plate was desired to be as thin as possible, material thickness is left as an unconstrained variable. Optimizing for lowest material thickness would be a complex process involving 3D optimization spaces. However, because of available manufacturing processes, we know that plate material will be purchased from a selection of material thicknesses that are commercially available. Because of this, our thickness variable can be simplified to the array

$$t = [0.0625;\ 0.125;\ 0.1875;\ 0.25;\ 0.3125 \ldots]in. \tag{2}$$

By plugging in equation 2 and other fixed variables (insole width, support distance, and desired stiffness) into equation 1, we used equation 3 to generate an appropriate range of Young's modulus for each option of thickness that would produce the desired stiffness of 14-24 N/mm, shown in table 2.

$$E = \frac{(80\ mm)^3(14 - 24\frac{N}{mm})}{4 \times (101.6\ mm)([1.59;\ 3.18;\ 4.76;\ 6.350;\ 7.94 \ldots]\ mm)^3} \quad (3)$$

Table 2. Combinations of material thickness and Young's modulus that would produce the desired bending stiffness of 14-24 N/mm.

Material Thickness (mm)	Corresponding Young's Modulus (GPa)
1.59 (1/16 in.)	17.64 – 30.24
3.18 (1/8 in.)	2.20 – 3.78
4.76 (3/16 in.)	0.65 – 1.12
6.35 (1/4 in.)	0.28 – 0.47
7.94 (5/16 in.)	0.14 – 0.24

The simple, 3-point bending model was used to initially identify the material and thickness that may be appropriate for the plate. Final estimation of plate bending properties utilized a finite element model (FEM) in ABAQUS 2023 (Dassault Systèmes SE, Vélizy-Villacoublay, France). A digital 3-point bending test of the plate utilizing 2nd order tetrahedral (C3D10M) solid continuum elements were simulated on a plate with the final shape for the insoles and verified that the stiffness fell within the range of 14-24 N/mm.

Plate Range of Motion and Ultimate Failure

Unrestricted motion of the metatarsophalangeal (MTP) joint requires 30˚ of bending[57]. For an insole containing a stiff mid-plate, restriction of the MTP joint becomes a concern[59]. For a

men's US 11 size foot (the only size of prototype developed for this study), the MTP joint is located approximately 6.35 cm from the most distal point of the foot[67] with a properly fitting shoe including an additional 1.27 cm of space between the foot and shoe front[68]. A simplified cantilever bending scenario was used to verify stresses in the material at this deflection. The front portion of the insole was considered fixed beneath the front portion of the foot, while the rear was unconstrained (fig. 15). A US size 11 insole is 29.21 cm long, overall, and the midsole plate (rear section) could be modeled as a cantilever beam of 21.59 cm unfixed length. To validate the ultimate bending limit, the prototype plate was fixed in a cantilever bending scenario and manually deformed beyond the required maximum bending limit.

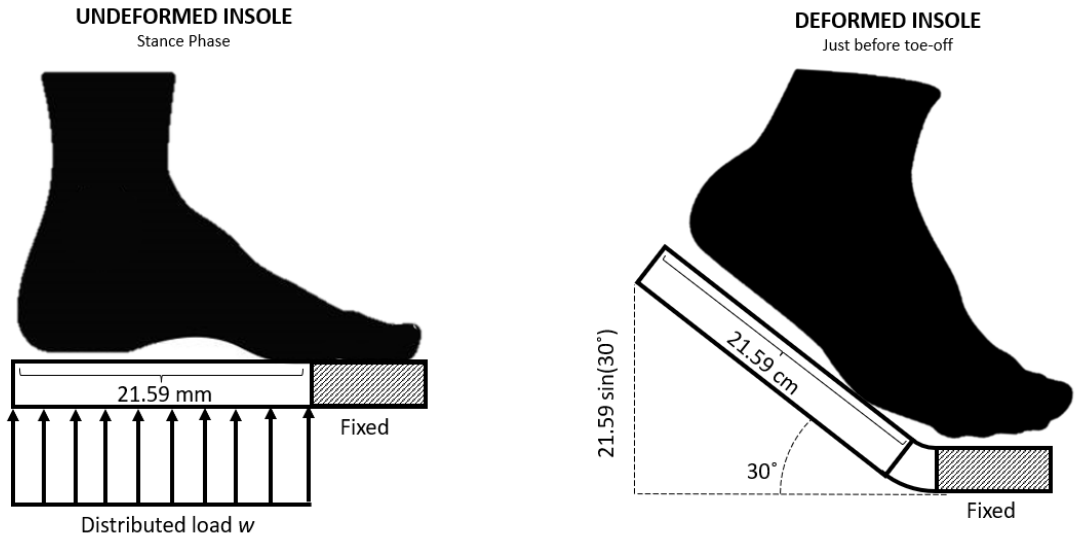

Figure 15. An undeformed plate and a plate bending around the MTP joint. Using this diagram, the maximum strain could be calculated, which is used to define the material requirements.

The maximum deflection of the end of a cantilever beam, the resulting maximum bending moment, and the maximum stress experienced by the beam at the point of fixture are expressed by equations 4, 5, and 6, respectively[69,70].

$$\partial_{max} = \frac{wL^4}{8EI} \tag{4}$$

$$M = \frac{wL^2}{2} \tag{5}$$

$$\sigma_{max} = \frac{My}{I} \tag{6}$$

In these equations, δ is deflection, w is the magnitude of the distributed load, L is cantilever beam length, E is Young's modulus, I is the area moment of inertia, σ is stress, and y is the distance away from the beam's neutral axis. Substituting equation 4 into equation 5 and the resulting equation into equation 6 gave:

$$\sigma_{max} = \frac{\partial_{max} 8Ey}{2L^2} \tag{7}$$

Note that once maximum stress was isolated, specific variables cancel out and maximum stress was no longer dependent on the area moment of inertia, distributed load magnitude, or bending moment, as all terms were simplified to be reflected in the deformation term. Using equation 7, we could iterate through the previously generated values of thickness and Young's modulus to generate an additional column for table 2, defining the required ultimate strength of the plate and producing table 3. Table 3 and fig. 16 define the boundaries of material properties that produced the appropriate 3-point bending stiffness of 14-24 N/mm.

Table 3. Viable options for material thickness, Young's Modulus, and yield stress. These values defined our boundaries for material selection.

Material Thickness (mm)	Corresponding Young's Modulus (GPa)	Required Yield Strength (MPa)
1.59 (1/16 in.)	17.64 – 30.24	129.69 – 222.33
3.18 (1/8 in.)	2.20 – 3.78	32.42 – 55.58
4.76 (3/16 in.)	0.65 – 1.12	14.41 – 24.70
6.35 (1/4 in.)	0.28 – 0.47	8.11 – 13.90
7.94 (5/16 in.)	0.14 – 0.24	5.19 – 8.89

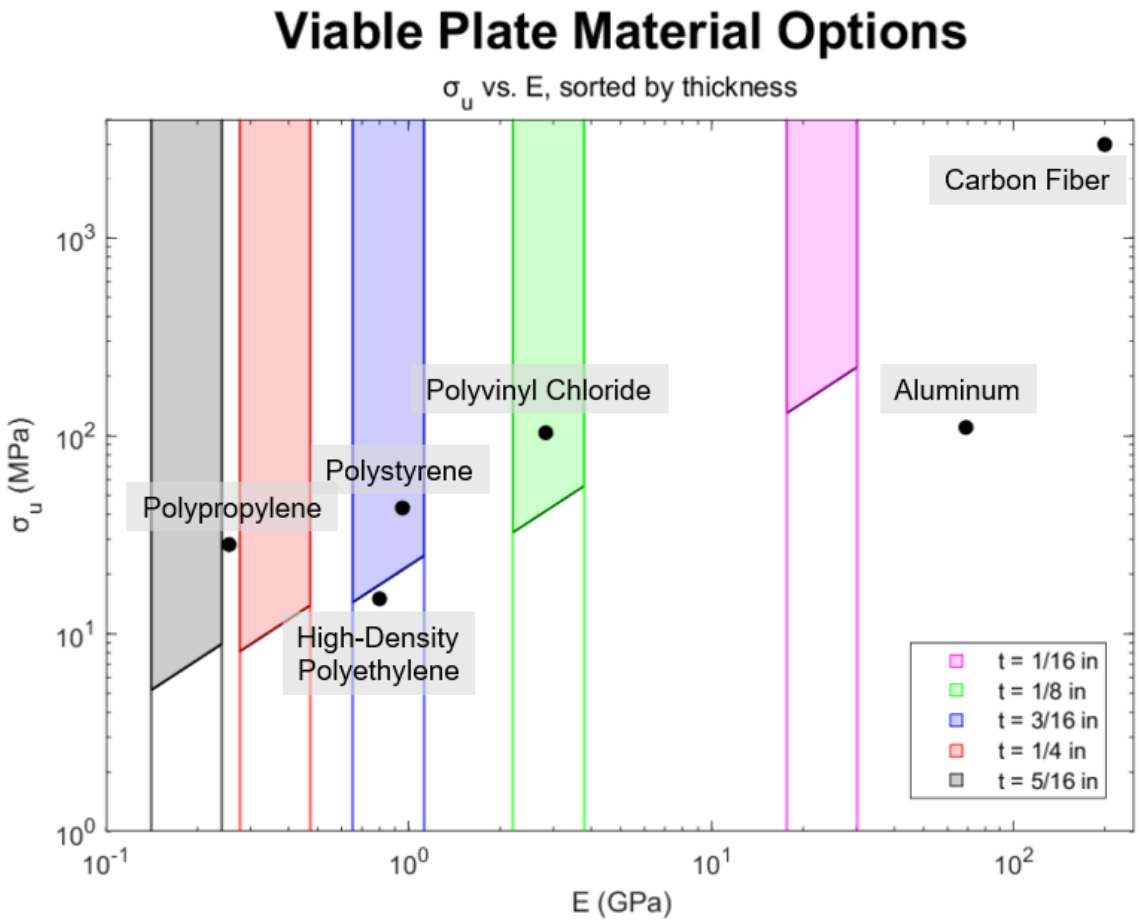

Figure 16. Viable options for plate material. Shaded regions represent material property combinations that would produce the appropriate 3-point bending stiffness of 14-24 N/mm. Varying material thicknesses that are readily available for purchase are differentiated by color.

Insole Foam Material Compressibility

In addition to the plate, the foam used in each insole must also be considered. Typical running shoe insole and midsole materials include ethylene-vinyl acetate (EVA) and polyurethane (PU) foam. These materials are favored by running shoe manufacturers for their combination of shock absorption and energy return[68,71]. While the compressibility and shock absorption properties of running shoes vary greatly by shoe and by training volume[72], our goal was to create an insole that closely mirrored the compressibility of the test specimen shoe to avoid impedance mismatch[73]. Using two foam materials of different compressibility would result in unfavorable behavior of energy return and shock absorption that would vary between different strides. The experimental shoe should be a standard (widely used, high-volume), low stiffness, lightweight running shoe to limit confounding variables.

Safety

The material selected had to fail plastically to avoid shattering. This excluded all brittle materials. Brittle materials typically have yield strength and ultimate strength values that are very near to each other, causing failure to occur at very low levels of flexion. Ideally, our plate would not fail under normal running loads. However, in the event that our plate did fail, it is important that the effects of the failure be mitigated. By restricting plate material to materials that fail plastically, we ensured that permanent, detectable deformation would occur well before ultimate failure, protecting the participants from being hurt by sharp fractured plate edges. Plate material was restricted to ductile materials, commonly defined as materials with an ultimate strength that is approximately 1.5 times higher than yield strength[69].

Material Definition

The initial plan for manufacturing was to select carbon fiber as the plate material. For commercial shoes containing a stiff midsole plate, carbon fiber is typically the primary material selection due to its superior stiffness, ultimate bending limit, and low density. In addition, the directional nature of carbon fiber allows material properties to be specifically tailored to longitudinal direction bending stiffness while ignoring all other unnecessary directions, lowering the necessary weight and material thickness to achieve the appropriate stiffness.

Early in the design process, it was assumed that a unidirectional carbon fiber plate would be best suited for our application. Literature that details the improved running energetics brought on by increased shoe bending stiffness only describes the benefit of longitudinal bending stiffness[56,57,62,64,74], so prioritizing stiffness in a single direction seemed to be the best decision. However, it was soon discovered that carbon fiber would not be feasible for production with the available facilities. Utilizing a wet lay-up carbon fiber method of production would make controlling material properties within allowable error levels extremely difficult. In addition, Montana State University does not currently possess facilities to safely cut cured or pre-impregnated carbon fiber. Cutting carbon fiber on the laser cutter would result in the expulsion of toxic gas and cutting carbon fiber on a CNC machine would result in carbon dust particles that can interfere with electronics.

A material other than carbon fiber would be required as a plate material. Our goal was to closely replicate the properties of carbon fiber, selecting a material that is stiff, flexible, and light. The classes of material that are similar to carbon fiber are stiff polymers and low-density metals (fig. 17).

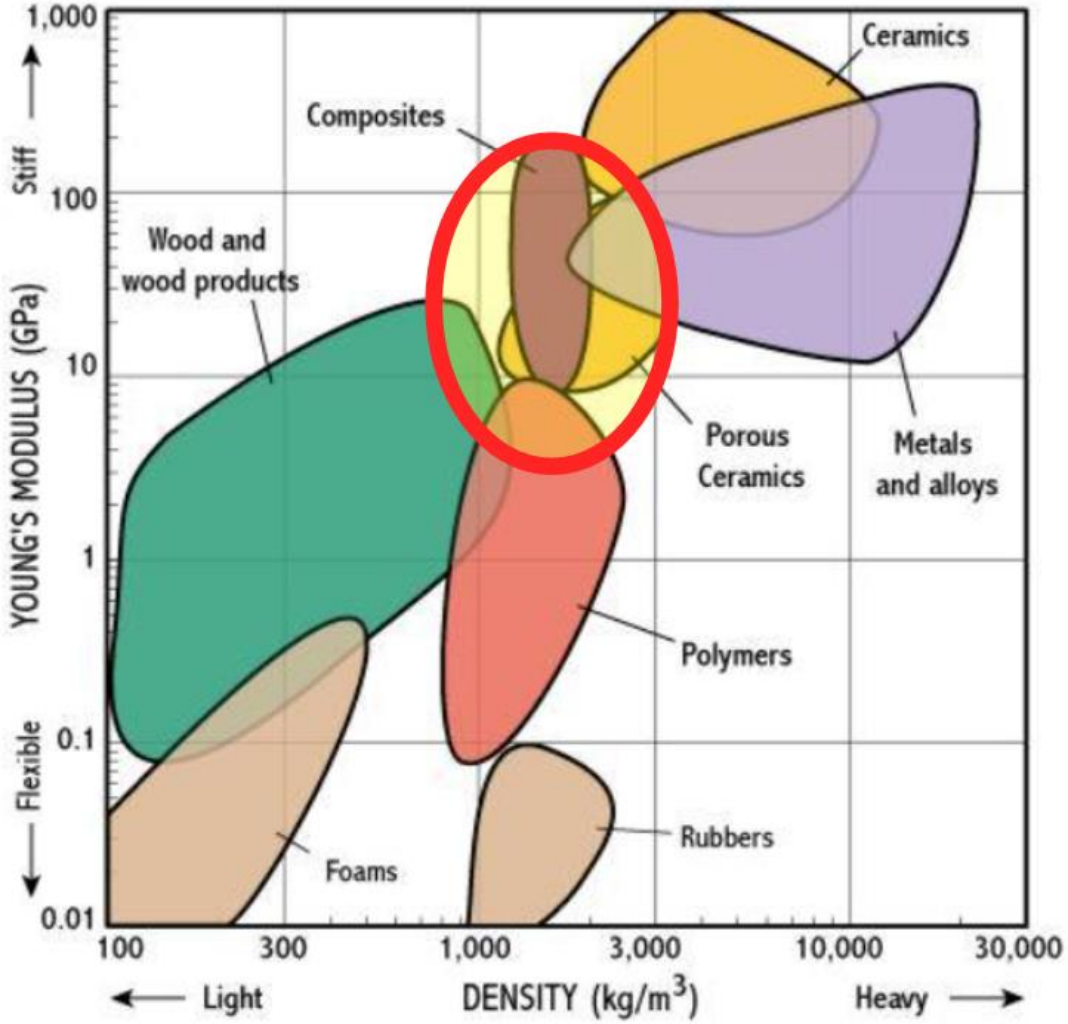

Figure 17. Materials plotted by Young's Modulus vs. Density. Materials that have a relatively high Young's modulus and low density are desirable for this application. The region of interest is circled in red.

Initial investigation of materials resulted in five material options: polystyrene (PS), high-density polyethylene (HDPE), polypropylene (PP), polyvinyl chloride (PVC), and aluminum (fig. 16). HDPE and PP were quickly excluded, as they were near matches but did not end up falling within a viable range for material property combinations that could produce the appropriate bending stiffness (fig. 16). Aluminum, while readily available for purchase in a wide range of thicknesses, did not possess a high enough ultimate strength to allow for full

metatarsophalangeal range of motion and was heavier than the other available choices. 4.76 mm (3/16 in.) PS and 3.18 mm (1/8 in.) PVC both fell within required ranges for both stiffness and ultimate strength, and both have an ultimate strength that is greater than 1.5 times its yield strength. Both materials are readily available for purchase at the required thicknesses.

To minimize material thickness and weight, PVC – Type 1, Young's modulus of 2.83 GPa and a yield strength of 50.33 MPa, was selected as the angled plate material, resulting in a plate that is 3.175 mm thick. The ultimate flexural strength is 103.42 MPa, meaning failure will occur at over twice the yield stress. These values fall well within our desired range (3.18 mm thickness, 2.20 – 3.78 GPa modulus, 32.42 – 55.58 MPa ultimate stress). At this thickness, PVC is estimated to have a 3-point bending stiffness of 17.97 N/mm from our simplified analytical solution.

Finite Element Analysis

To verify the stiffness of the plate, a finite element model (FEM) was created of a 3-point bending test in ABUQUS 2023. 3-point bending tests are a consistent method of classifying the bending stiffness of running shoes. By setting the supports at a fixed distance from each other (80 mm) and applying a known force to the center of the bending section and measuring the resulting deformation, a consistent stiffness value in the units of force/deformation distance can be extracted. Our goal was to reproduce the values attained by previous studies that demonstrated a positive effect on running energetics (14-24 N/mm) that used a support distance of 3.15 inches (80 mm).

Plate geometry was initially created in SolidWorks according to the drawings in Appendix C. The outer shape of the plate was then converted to a .inp file and imported to

ABAQUS. The part was then extruded to 0.125 inches. To accurately recreate a 3-point bending scenario, the part was partitioned in 3 locations: once at the location of the metatarsophalangeal (MTP) joint and at two locations 1.575 inches on either side of the MTP joint (fig. 18). The partitions do not physically break the geometry, they define regions that were meshed independently and ensure nodal placement along partition boundaries.

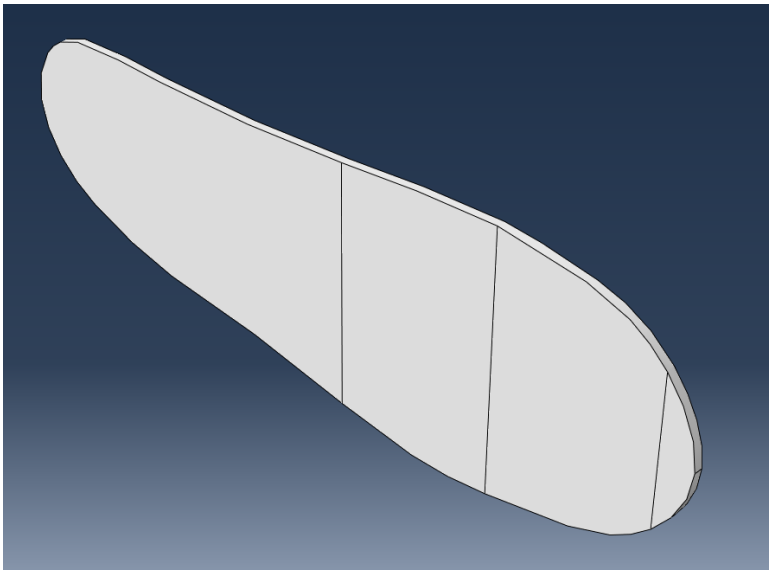

Figure 18. The original geometry of the plate in the finite element model. The geometry is partitioned in 3 locations to represent where the supports and force mechanism would contact the plate.

Next, supports and the force mechanism were added to the model (fig. 19). A typical 3-point bending test used steel or aluminum rounded contact points. Our FEM recreates these accurately by defining rounded contact regions as rigid contact points. Reference points were added along each point of contact to simplify the definition of boundary conditions.

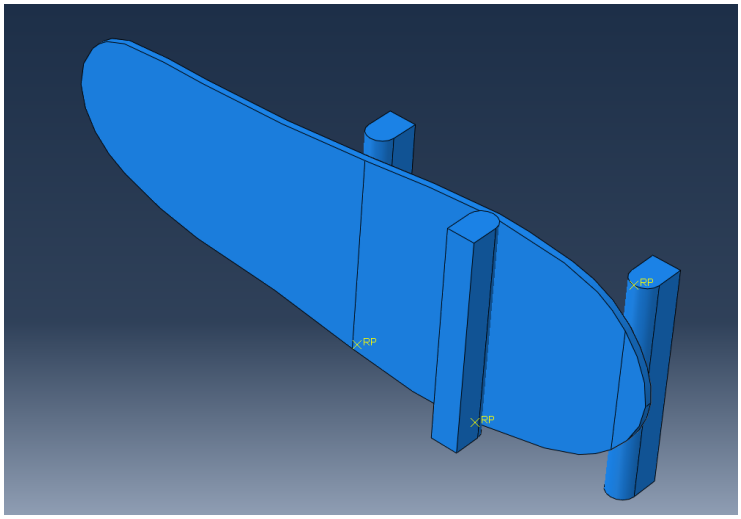

Figure 19. The initial geometry of the FEA with the supports added. The supports were designed to have rounded contact points with the plates and undergo rigid contact with the plate.

Boundary conditions were then added to each support part (fig. 20). All faces of each stationary support were fixed for rotation and translation in the x, y, and z directions. The force mechanism support was constrained similarly, but still allowed translation in the z direction. Each partition of the plate was constrained in the x, y, and z directions of translation and the x and z axes of rotation but allowed rotation about the y axis. The choice to add linear constraints on portions of the plate was made to ensure the model would not diverge to infinite displacement while closely replicating a physical 3-point bending test. In a physical bending test, the bending specimen would be pinned at each support, allowing rotation about a single axis. Lastly, the open face of each support was 4 inches long and 0.5 inches wide, resulting in a flat face of area 2 square inches. By applying a pressure of 0.5 psi to the 2 square-inch plate, a resulting net force of 1 pound is applied to the force mechanism. Doing so allows simplified bending stiffness calculation while avoiding stress concentration effects that would not be present in a physical 3-point bending test.

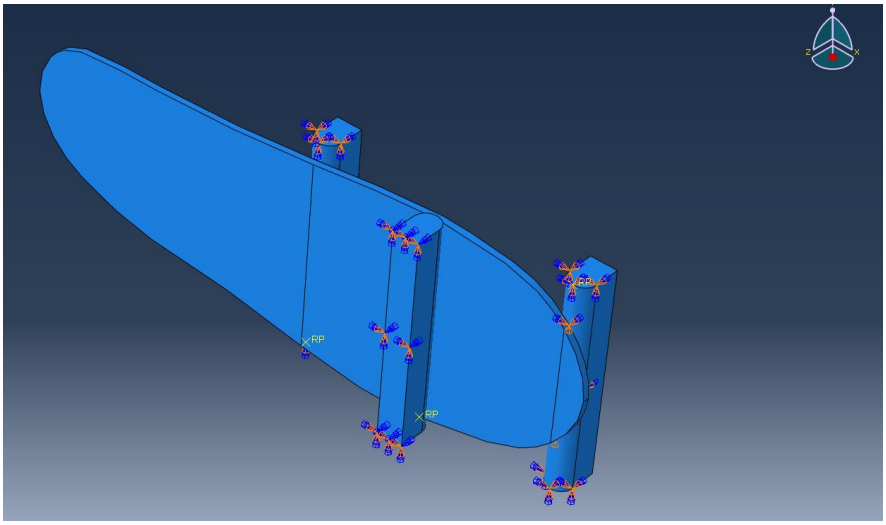

Figure 20. The initial geometry of the FEA with boundary conditions and loads applied to various points of the supports. The two outermost supports are fully fixed, a pressure resulting in a total load of 1 lb. is applied to the flat surface of the force mechanism support, and the partitions of the plate are constrained to only rotate about a single axis.

Finally, the plate could be meshed (fig. 21) and tested for convergence (fig. 22). 3-dimensional second-order tetrahedral (C3D10M) solid elements were selected for the final model. Second-order tetrahedral elements, or parabolic elements, have 10 nodes each (4 corner nodes and 6 edge midpoint nodes) and model second-order displacement in volume, along faces, and along edges[75]. These elements are favored for their ability to accurately represent curvature due to the ability of their edges and faces to curve before and after deformation[76]. While a plane stress assumption or the utilization of first-order elements may have simplified this problem and reduced required computational power, a 3-dimensional model with second-order elements produces the most accurate results[77].

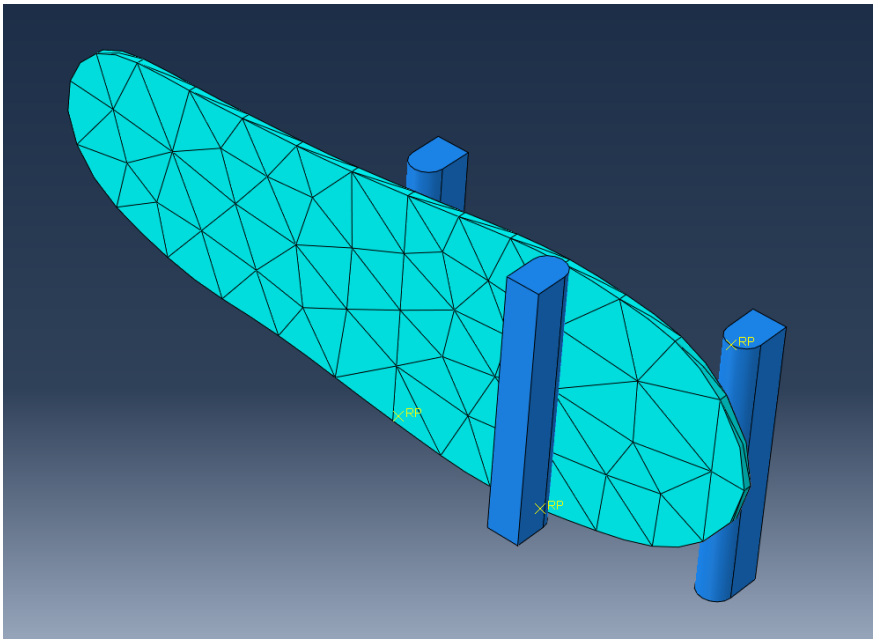

Figure 21. The plate with a mesh applied. The model utilized second-order tetrahedral (C3D10M) solid elements and a total of 624 nodes.

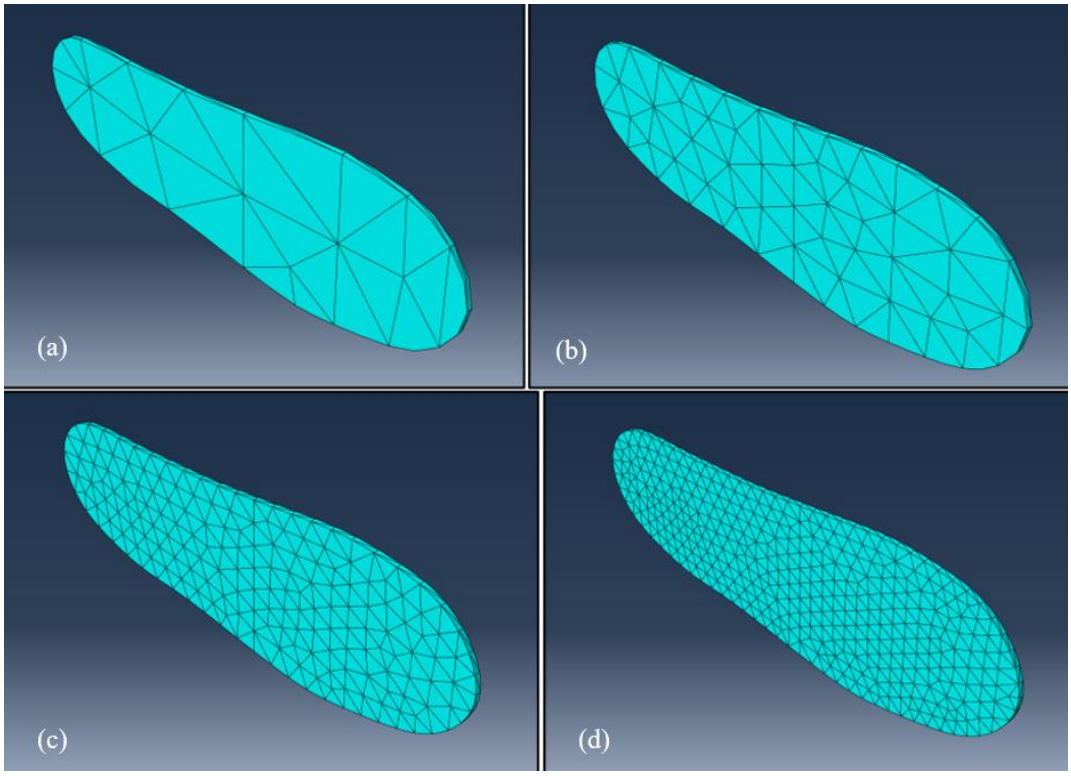

Figure 22. Varying levels of mesh refinement (a: 66 nodes, b: 278 nodes, c: 624 nodes, d: 2145 nodes). A finer mesh produces more accurate results but requires exponentially higher processing power.

The model was then tested for convergence (fig. 23, table 4). A finite element model is considered to converge when a successive refinement of the mesh produces negligible change in output. The goal stiffness was 14-24 N/mm, meaning that acceptable values would be 19 ± 26.3%. With such a wide acceptable range of stiffness values, convergence criteria would not be limited by processing power. Convergence was defined as <1% change between iterations. From the third iteration (624 nodes) to the fourth iteration (2145 nodes), the total beam displacement decreased by only 0.51%. A fifth iteration (4383 nodes) was tested, and another negligible level of change was observed.

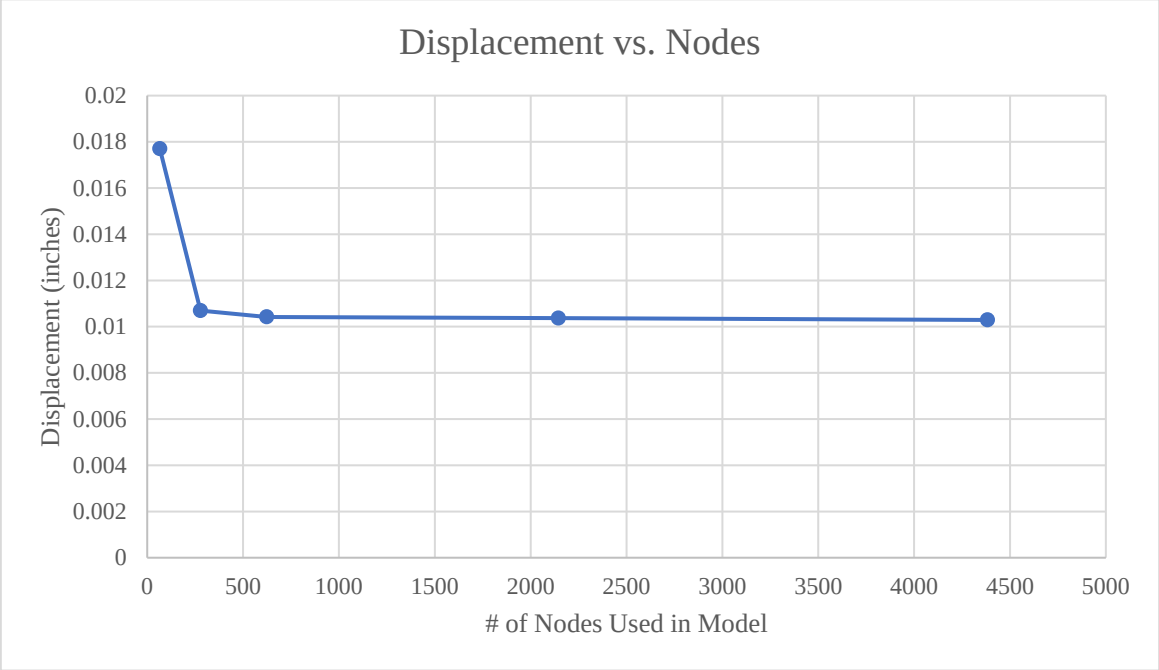

Figure 23. Plate deflection vs. number of nodes in the model. Convergence occurred at 624 nodes.

Table 4. Displacement by the number of nodes in each successive mesh refinement. Beyond 624 nodes, successive mesh refinement produced negligible change.

Nodes Used in Model	Displacement (in.)	% Change From Previous Iteration	% Error from Analytical Model
66	0.017698	-	81.53%
278	0.010695	65.48%	9.70%
624	0.010420	2.64%	6.88%
2145	0.010367	0.51%	6.33%
4383	0.010290	0.75%	5.54%

The final model contained 624 nodes and calculated midline bending displacement to be 0.0104 inches under 1 pound of force (fig. 24). Converting units, this is equivalent to 0.265 mm of displacement under 4.45 N of force. Dividing applied force by displacement yields our FEM predicted bending stiffness of 16.81 N/mm. This is 6.88% lower than the analytical solution found when simplifying the cross section of the plate to a rectangle. Both values fall within the desired range of 14-24 N/mm.

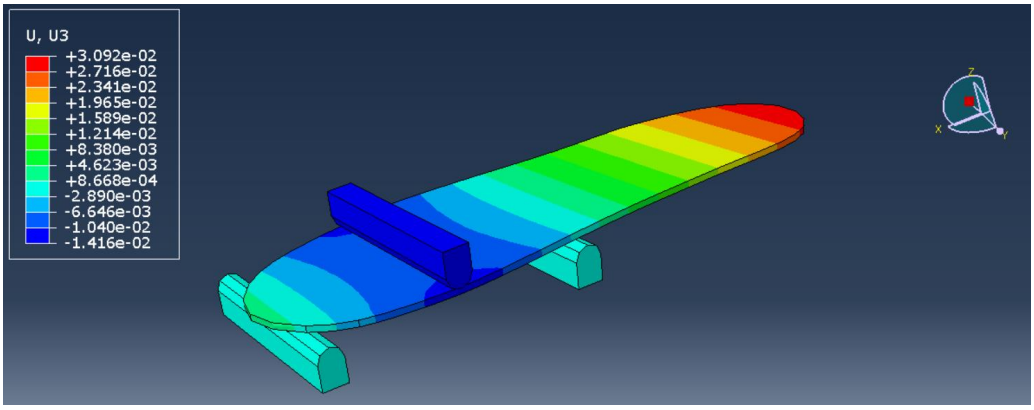

Figure 24. The finite element model of a 3-point bending loading scenario for the midsole plate. Under 4.45 N of force, the middle portion of the plate had a maximum deformation of 0.26 mm. This corresponds to a 3-point bending stiffness of 16.81 N/mm.

Prototype Production

The outer geometry of the plate was modeled in SolidWorks (Dassault Systèmes SE, Vélizy-Villacoublay, France). The geometry was obtained from the test specimen shoe by taking careful measurements along the centerline and recreating the shape with splines (fig. 25).

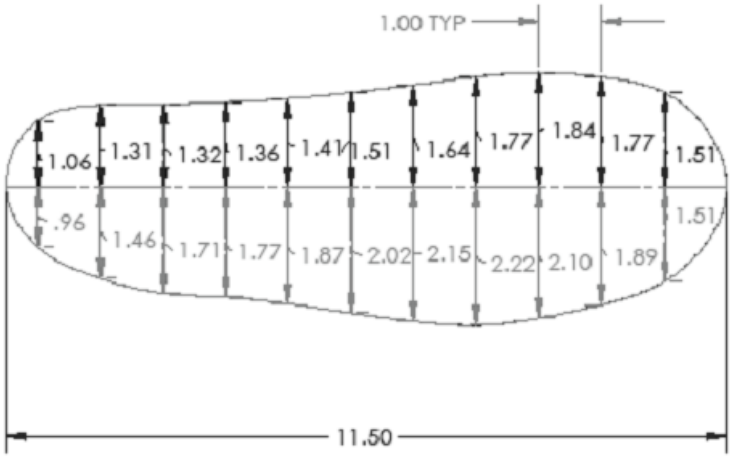

Figure 25. The outer geometry of the plate, modeled in SolidWorks. The shape is modeled to match the inside of the test specimen shoe.

The exact dimensions of each piece of each insole are described in Appendix C. This geometry was converted to a .dxf file and imported to a CNC control laptop. The plate was cut from a large sheet of PVC plastic on a ShopBot (Durham, NC, USA) Desktop CNC Router (fig. 26)

Figure 26. A ShopBot Desktop CNC Router that was used to accurately cut the outer geometry of the foam insole material and plate.

The insole foam material of each insole was selected to be ethylene-vinyl acetate (EVA) foam. EVA foam is closed-cell and crosslinked, making it an effective shock absorber and load distributor[78]. The properties of EVA foam are detailed in Table 5. Most importantly, the Hyperion Tempo (Brooks, Seattle, WA, USA), which has an EVA midsole, would be used as the base test shoe. Utilizing the same foam material for the insole and shoe midsole avoids an impedance mismatch. The outer geometry of the foam insole material was cut on a ShopBot (Durham, NC, USA) Desktop CNC Router (fig. 26). The EVA foam was then cut to 10˚ on a bandsaw using a handmade platform attachment that would orient the foam at the correct angle (fig. 27).

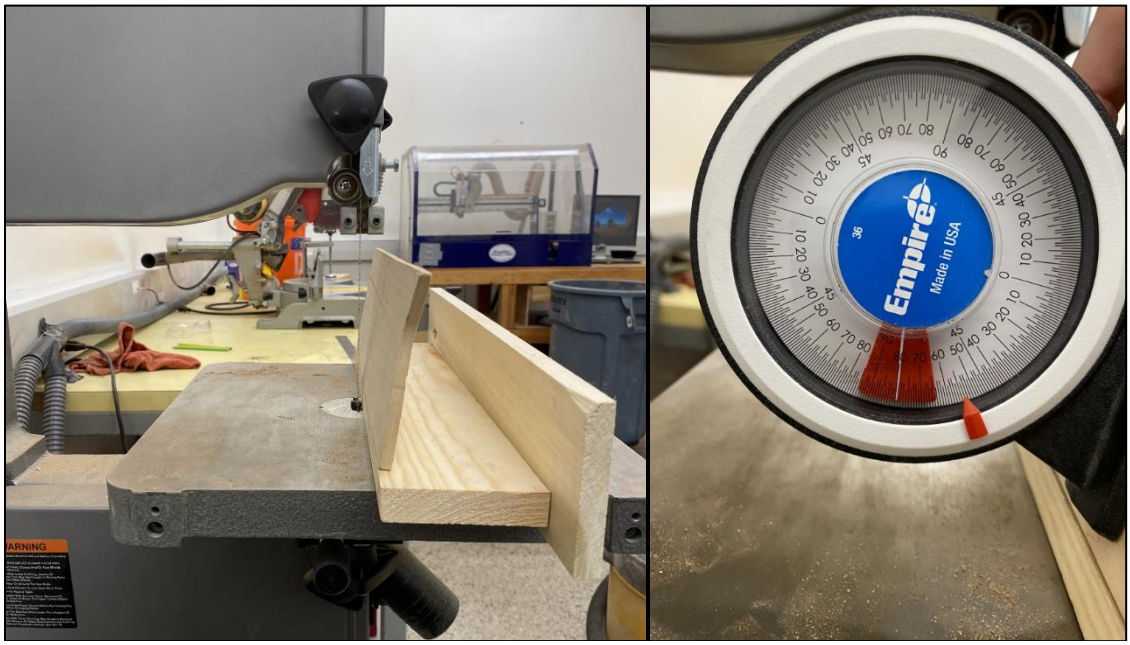

Figure 27. The platform (left) used to hold the EVA foam at a 10˚ angle while being cut on the bandsaw with angle verification (right)

Table 5. Final material selection and specifications. PVC – Type 1 was selected as the plate material and EVA was selected for the bulk foam material.

Final Material Selection and Design Specifications	
Insole Foam: Material	EVA Foam
Insole Foam: Density	0.032 g/cc
Insole Foam: Pressure to compress 25%	0.0275 MPa
Plate: Material	Thermoformable PVC – Type 1
Plate: Thickness	3.175 mm
Plate: Young's Modulus	2.83 GPa
Plate: Estimated 3-point bending stiffness	17.97 N/mm
Plate: FEA 3-point bending stiffness	16.81 N/mm
Plate: Max. Stress Experienced at 30˚	41.62 MPa
Plate: Yield Strength	50.33 MPa
Plate: Ultimate Flexural Strength	103.42 MPa
Plate: Yield/Ultimate Strength	2.05

The final prototypes consisted of 1 control insole and 2 experimental insoles: a flat foam (baseline) insole that was constructed to match the foam material properties and thickness of the other 2 test insoles, a physically angled (wedge) insole, and an insole that is flat on the top and

sits parallel to the shoe sole but contains an angled stiff plate (angled plate) (fig. 28). All three insoles are 19.05 mm thick and fit within a modified Hyperion Tempo (Brooks, Seattle, WA, USA), running shoe. To accommodate the height of the insoles, the upper portion of the shoe was cut open and the shoe was "laced" to the participant's foot with athletic tape. When the shoes had been fully taped to the participants' feet, each participant was instructed to run a short distance to test the comfort and fit of the shoe. Based on participant verbal feedback, tape was either added or removed until the participant reported that the shoe felt comfortable and secure for running. Throughout testing, there were no instances of a shoe becoming loose or of tape breaking, and participants reported that the taped shoes felt similar to a regular running shoe. While this workaround was imperfect and may have caused additional motion artifacts in the data, we hoped that by constructing each insole of the same material, of a similar stack height, and by taping each shoe in every trial, we would make variation consistent across the board and comparisons between trials within the study would remain valid. The baseline insole was flat and served as a control (fig. 30). The angled plate insole contains a stiff mid-plate that is angled at 10˚ (fig. 28). The angled foam insole is cut longitudinally at 10˚ relative to the ground (fig. 29).

Figure 28. Left to right: front and top view of the angled plate insole prototype.

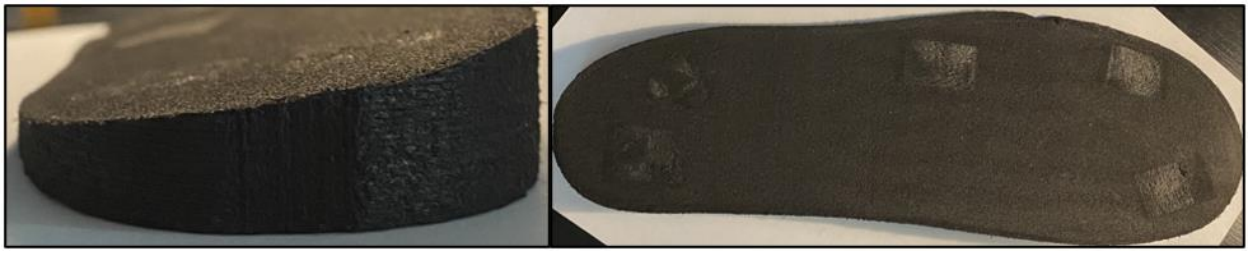

Figure 29. Left to right: front and top view of the wedge insole prototype.

Figure 30. Front view cross-sections of all 3 insoles for the right shoe. From left to right: baseline, wedge, and angled plate insoles. The wedge and angled plate insoles were each compared to the baseline insole.

Bending Limit Verification

The plate was bench tested to ensure that it met required bending limit specifications (fig. 31). Normal motion of the metatarsophalangeal (MTP) joint during running is 30°[59]. The maximum passive bending limit of the MTP joint is approximately 62°[67,79]. While the shoes were primarily used during running, it was also important for the plate to allow additional flexion if a participant forces them into extreme position by stretching or intentionally bending them to an extreme amount. To mimic the motion of the MTP joint, the first 3-inch section of the plate was secured to a flat surface. The free end of the plate was then manually bent to approximately 62° and photographed. The photograph was then imported to AutoCAD (Autodesk, San Francisco,

CA, USA) and measured with an angle measurement tool. The plate achieved a bending angle of 65˚ and returned to its original position with no apparent signs of damage or permanent deformation.

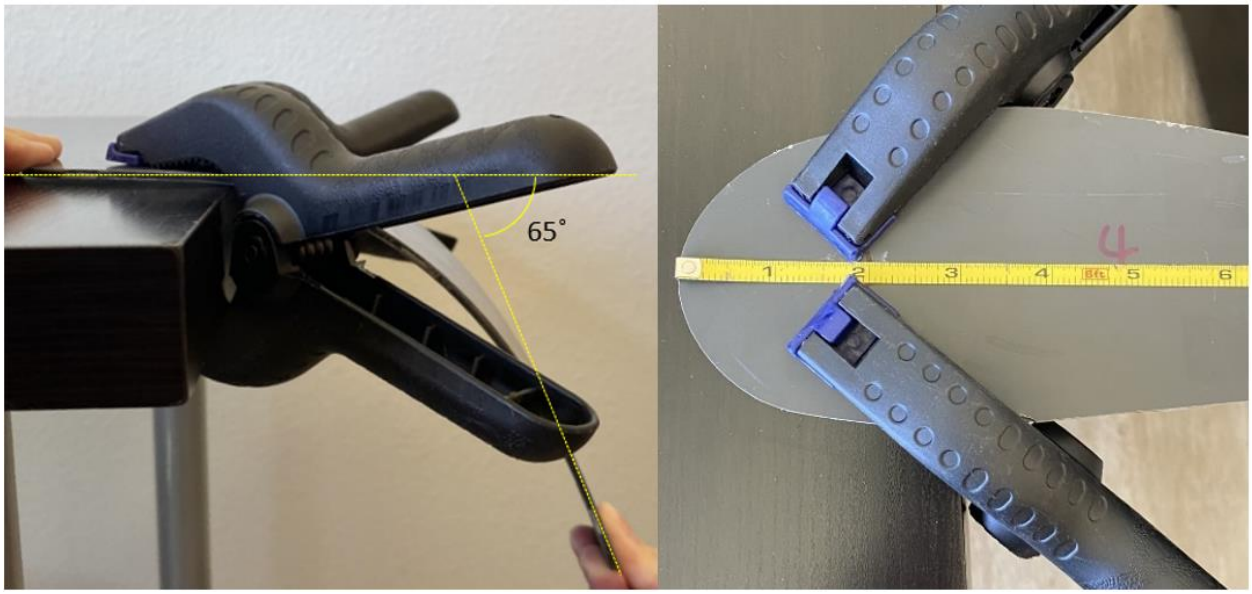

Figure 31. A bench test of a cantilever bending scenario showing that the plate is capable of, at a minimum, 65˚ of flexion.

Experimental Design

Power Analysis

An a priori power analysis was conducted using G*Power[80] version 3.1.9.7 for sample size estimation. For our study, we would investigate the effects of different test conditions within the same sample of individuals, meaning that our results would be analyzed with a single sample matched pairs t-test with dependent groups. In order to ensure that significant differences would be detectable in all metrics, the sample size was selected to accommodate the lowest existing effect size among the metrics being measured, based on data from previous studies.[12,19,26,27,46,51,52,81,82] The metric with the lowest effect size was determined to be right ankle

inversion at contact with an effect size of 3.60. With a significance of $\alpha = 0.05$ and a power of 0.80, the minimum required sample size was found to be N = 4. Because this analysis was based on assumptions regarding the magnitude of insole effect, the actual sample size was set at N = 6 to allow room for additional error.

Experimental Procedure

The effects of each insole on indoor flat track running mechanics were tested with human participant running trials. Participants were recruited via an announcement provided to a collegiate level track and field coach. Interested participants that fit recruitment criteria were instructed to directly contact the study coordinator. Twelve National Collegiate Athletic Association (NCAA) Division 1 track and field athletes (6 male, 6 female, age: 21 ± 2 years, mass: 61.4 ± 11.4 kg, height: 1.77 ± 0.17 m) who specialize in distance and mid-distance (800m to 5000m) provided informed consent to participate in this Institutional Review Board-approved protocol (Appendix D). All participants were free of any musculoskeletal injury that resulted in surgery or more than 2 weeks away from training over the last 12 months by self-report. Participants were selected in a convenience sample from the Montana State University Track and Field team. All participants were right hand and right leg dominant.

Because the angled plate insoles required specific geometry-dependent material property selection to achieve appropriate bending stiffness, only one size of angled plate insole could be developed due to time and budget constraints. All male participants were required to have a US men's size 10.5-11.5 foot to fit this prototype. Female participants only completed trials with the baseline and wedge insoles, and thus were not subject to a shoe size restriction. All trials were completed at the Montana State University outdoor track facility where a semicircular path with

the turn radius of a standard indoor track lane 1 (17.2 m) was drawn on the interior of the outdoor track area. When participants arrived at the MSU outdoor track and field complex, they were provided with the consent form (Appendix E). Participants reported their gender, age, weight, height, and training volume in miles per week.

Participants were then equipped with an Xsens (Movella, Henderson, NV, USA) MVN Link Inertial Measurement Unit (IMU) Suit (Wi-Fi, 240 Hz) for kinematic data collection, 2 Trigno (Delsys, Natick, MA, USA) Avanti (single-channel, 1926 Hz sampling frequency) sensors and 2 Trigno Maize (16-channels, 1000 Hz sampling frequency) surface electromyography (EMG) sensors for muscle activation data collection, and XSensor (XSensor, Calgary, AB, Canada) Pro Intelligent Insoles (150 Hz, 1-128 psi range) for plantar pressure data collection. Specifics of these data collection devices and procedures are detailed in the following subsection.

Participants were instructed to begin with a 10-minute warm up at a self-selected pace. Participants were allowed to walk, jog, run, or perform dynamic stretches during this time. When the participant indicated they were ready to begin, the test procedure was explained in detail. Five possible conditions existed for testing: straight running with baseline insoles, corner running with baseline insoles, straight running with the angled plate insoles, corner running with the angled plate insoles, and corner running with physically angled foam insoles. The primary purpose of the wedge insoles was to provide the most extreme version of angled footwear that would provide an upper bound of benefit for an angled insole while turning and provide the ability to compare outcomes with previous angled shoe data. Straight running with the wedge insoles was not tested out of precaution from injury such as sprained ankles or falls, particularly

due to the high speed and effort that was required from the individuals (see pace in next paragraph), as 10˚ is a common inversion angle used to simulate ankle inversion sprains in a lab[83–85]. Participants performed three trials with each possible test scheme for a total of fifteen trials per male participant and nine trials per female participant. The difference in total trial count is because the angled plate insoles were not tested on the female participants due to shoe size limitations.

The order of tests was determined by uniform random number generation[86] using the "rand()" command in MATLAB R2023a (MathWorks, Natick, MA, USA) to avoid any effects from ordering. Participants were instructed to run within 5% of the speed that matches their personal record pace in whichever event they have the highest public ranking from World Athletics[87]. Running speed was verified by live center of mass velocity monitoring as calculated by the Xsens IMU suit. See the following subsection for a description of this process. Trials were repeated if a participant deviated more than 5% from their target pace during the window of interest. At the beginning of each trial, participants executed a maximum effort vertical jump to assist with a manual synchronization of kinematic, muscle activation, and plantar pressure data. This was not a true frame-by-frame synchronization of data, as we only wanted to verify that all data was being collected from the same set of stride cycles within each trial.

For each trial, the data collection software would be initialized, and the participant was instructed to walk to the proper starting line (fig. 32). The participant would then complete one maximum effort vertical jump and begin running along the specified path, eventually reaching their prescribed race pace for a period of a few seconds. When reaching the end of the path, the participant would slow down, and the data collection software would be ended. The participant

would then walk or jog back to the starting area. When all trials were completed, the participant performed a 5-minute cool down jog and was permitted to leave.

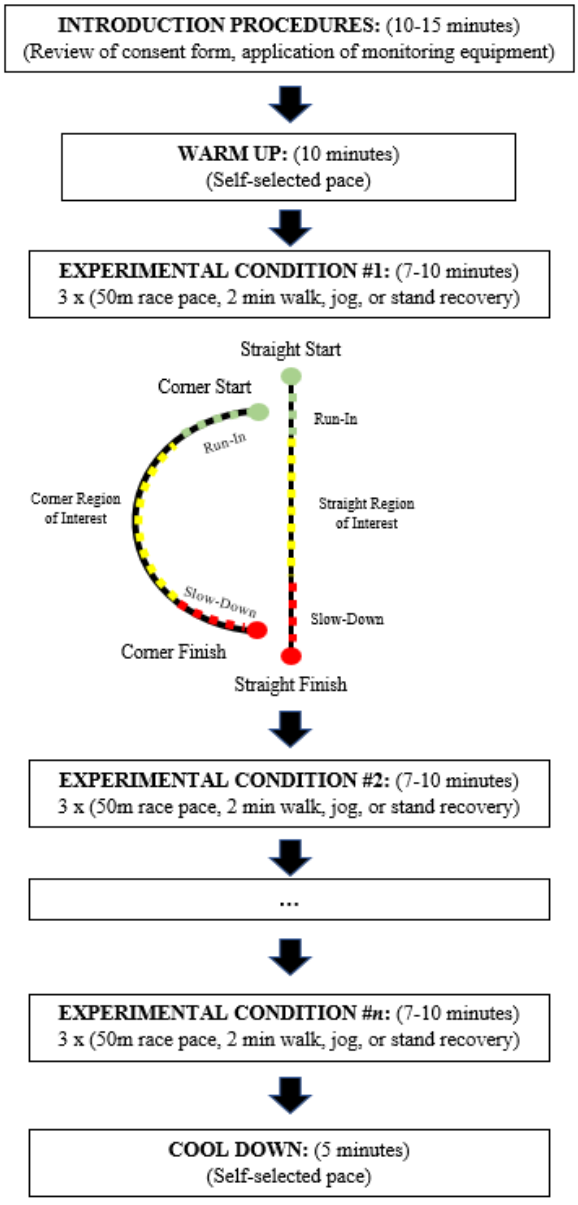

Figure 32. Testing procedure for the study. Participants performed 3 trials for each test condition (varying shoe inserts) over a period of approximately 1 hour. Straight and turn running were tested at the individual's self-identified race pace.

Data Collection Equipment

Kinematic Data Collection Equipment and Procedure

Joint angles and center of mass velocity were collected using a Movella (Delft, Zuid-Holland, Netherlands)) Xsens MVN Link Inertial Measurement Unit (IMU) Suit [88,89]. The IMU suit consists of a tight-fitting shirt and pants, 17 MTx IMU sensors, a battery pack, and a data logger. The data logger was wirelessly connected to a WiFi router that was wired to a data collection computer, allowing for real time monitoring of the device. IMU sensors were placed on each participant's head, shoulders, upper arms, forearms, hands, pelvis, upper leg, lower leg, and feet according to Movella's recommendations that may assist with data acquisition accuracy, prevention of early sensor dysfunction, and ergonomic commodity[90]. Elastic Velcro straps were used to hold each sensor in place as the study progressed.

Each IMU sensor contains 3D gyroscopes, 3D accelerometers, and 3D magnetometers (38 x 53 x 21 mm, 30 g) to provide 3D angular velocity, acceleration, and earth magnetic field at a sampling rate of 240 Hz[91]. When attaching the sensors to a body, the initial orientation between the sensors and body segments is unknown. To define this relationship, the subject stands in 2 known positions: N-pose (arms neutral and beside the body) and T-pose (upright with arms horizontally and thumbs forward) to perform the system calibration. The rotation from sensor to body segment is determined by coupling the orientation of the sensor in the global frame with the orientation of each segment in these known positions[88]. The Xsens suit tracks the motion of the body with a biomechanical model consisting of 23 segments (pelvis, L5, L3, T12, T8, neck, head, shoulders, upper arms, lower arms, hands, upper legs, lower legs, and feet). For each segment (B), kinematic quantities are expressed in a local right-handed Cartesian coordinate

system (L) with X oriented to the front of the body, Y pointing laterally and orthogonal to X and Z, and Z oriented in the upwards vertical direction (fig. 33).

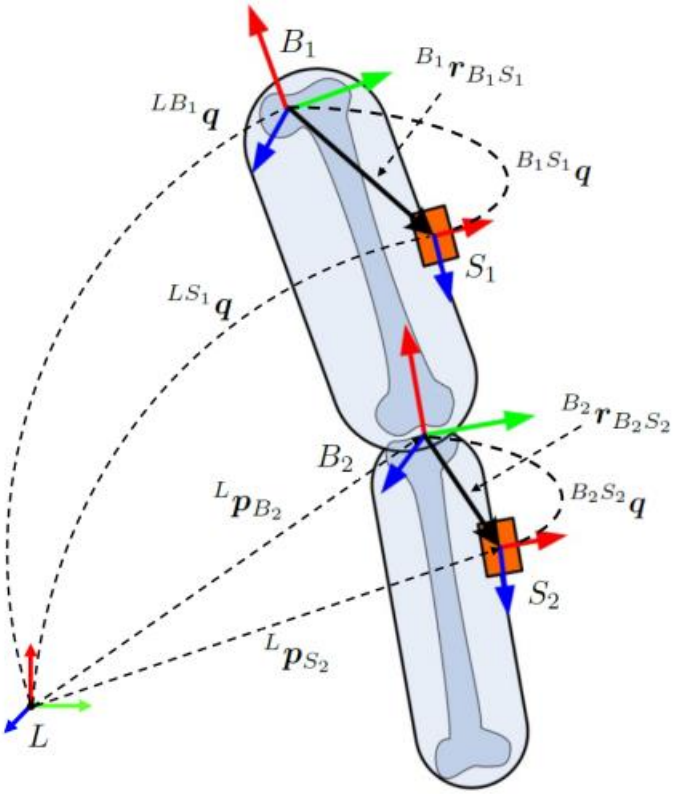

Figure 33. Sensor (S), segment (B), and local (L) coordinate frames used to calculate joint angles[91].

The MTx sensor gyroscopes measure angular velocity that, when integrated over time, provide the change in orientation of each body segment over each time step[88]. Linear accelerometers measure the acceleration vector and gravitational acceleration that, when excluding gravity and integrating twice over time, provide the change in position for each body segment. With position and orientation established, the joint angles are calculated using the difference between the orientation of the distal segment and the proximal segment using

quaternion multiplication. This quaternion is then converted to Euler angles following the ISB and Grood and Suntay recommendations[92]. All Xsens MVN joint angles follow the extraction sequence ZXY (Z, flexion and extension; X, abduction and adduction; Y, internal and external rotation)[88].

Xsens uses the ISB biomechanical model[93] to estimate center of mass (COM) position, velocity, and acceleration. The software uses approximate segmental analysis by first calculating the position and orientation of each body segment and approximating the mass fractions and COM positions of each body segment using previously defined anthropometric tables. To assist with this calculation, the user must enter the participant's body height, shoulder height, shoulder width, arm span, wrist span, elbow span, hip height, hip width, knee height, ankle height, foot length, and extra shoe sole thickness.

The kinematic data that was exported from the MVN software (fig. 34) included both eversion and inversion data for the right and left ankle, abduction and adduction data for the right and left hips, and COM velocity.

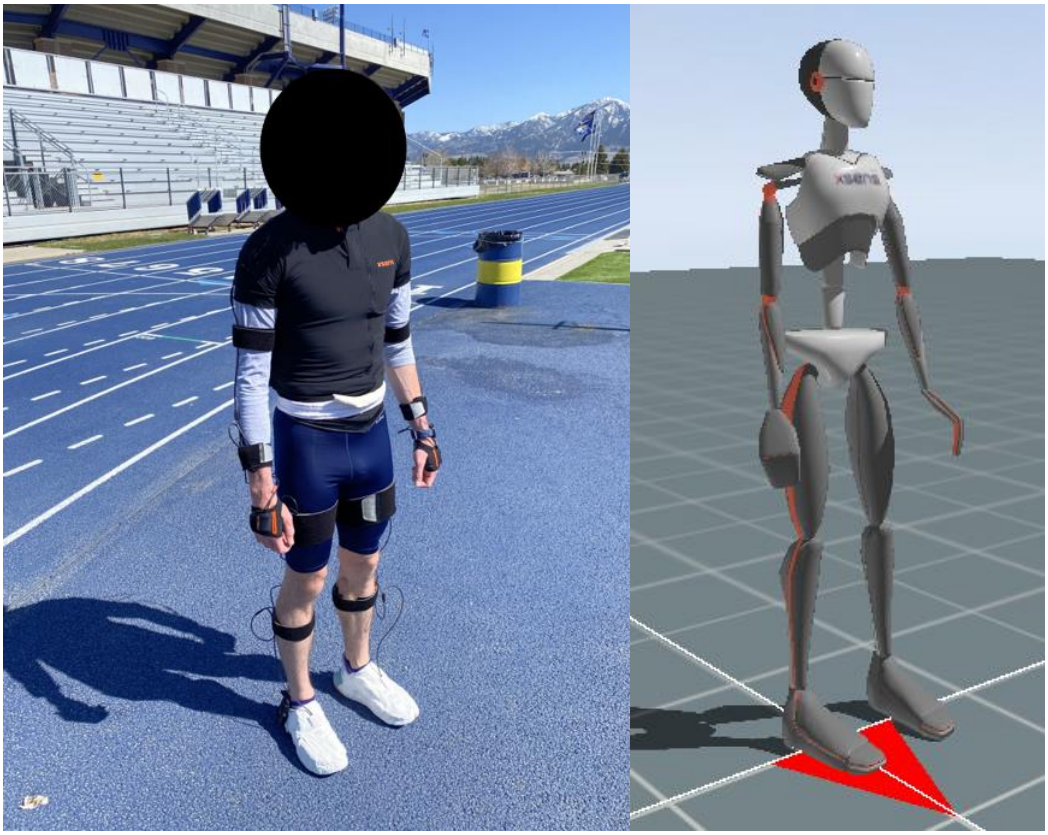

Figure 34. An example of the IMU suit interpreting a participant's body position in real time in the a priori N-pose. From this model, all required joint angle data could be directly exported from the software.

Muscle Activation Data Collection Devices and Procedure

Surface electromyography (EMG) signals were collected using 2 Trigno (DELSYS, Natick, MA, USA) Avanti (single-channel, 1926 Hz sampling frequency, 10 mm inner-electrode distance) sensors and 2 Trigno Maize (16-channels, 1000 Hz sampling frequency, 10 mm inner-electrode distance) sensors (fig. 35). The use of two different types of sensors was necessitated by lab availability. Comparisons were only made between sensors of the same type. The Avanti sensors were placed according to the SENIAM guidelines[94] on each participant's left and right gluteus medius muscles and the Maize sensors were placed on each participant's left and right medial gastrocnemius muscles. As each muscle was being compared to its opposite side

counterpart, it was important to use the same type of sensor on each paired muscle (single channel on gluteus medius, multi-channel on gastrocnemius lateralis).

Figure 35. Trigno Maize sensor (left, multi-channel) and Trigno Avanti sensor (right, single channel). The Maize sensors were used on the gastrocnemius medialis, and the Avanti sensors were used on the gluteus medius.

The skin of each sensor placement location was shaved and cleaned with an alcohol wipe before attaching the sensors to reduce impedance and to improve electrode adherence. For gluteus medius sensor placement, participants laid on their side while a research coordinator applied downward pressure to the outside ankle. Participants were then instructed to abduct their upper leg, resisting the applied downward force. The trochanter and crista iliaca were then identified and the electrodes were placed halfway between each (fig. 37). For gastrocnemius medialis sensor placement, participants laid face down and a foam roller was placed underneath their ankle. Participants were instructed to plantarflex and slightly internally rotate their ankle to further define the muscle. The electrodes were then placed, per SENIAM guidelines, on the most prominent bulge of the muscle (fig. 36).

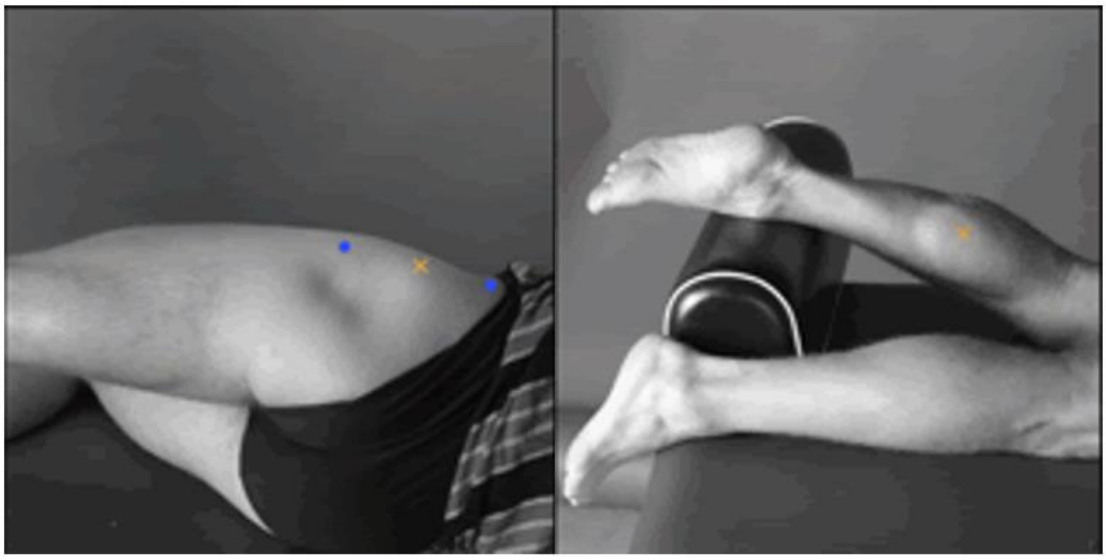

Figure 36. Images from SENIAM showing the ideal placement location for EMG sensors on the gluteus medius (left) and gastrocnemius medialis (right).

Electrodes were secured to the skin with double sided tape and then wrapped with an elastic Velcro strap (fig. 37). The EMG sensors wirelessly connect to the main charging hub that was connected to a different data collection computer, again allowing live monitoring of these devices.

Figure 37. An EMG sensor fixed securely to a gastrocnemius medialis muscle. The sensor was first secured to the skin with double sided tape and then wrapped with an elastic Velcro strap.

Plantar Pressure Data Collection Equipment and Procedure

Pressure data was collected using two XSensor (Calgary, AB, Canada) Pro Intelligent Insoles (100 Hz, 1-128 psi range). The insoles contain 235 individual pressure sensors each, producing a resolution of 7-9.4 mm, depending on insole size. They are capable of measuring a pressure range of 0.7-88.3 N/cm^2. The pressure insoles were used to estimate vertical ground reaction force and ground contact time. While the XSensor insoles (fig. 38) measured only pressure and contact area, an estimated ground reaction force is automatically generated by the analysis software within error levels of ± 5%[95–97].

Figure 38. The XSensor Pro Intelligent Insoles used to measure ground contact time and ground reaction force.

The pressure insoles are placed directly into each participant's shoe. The insoles have a thickness of only 2 mm, meaning they are almost undetectable by the user. The insoles connect to a data transmitter that clips onto the outside of the participant's shoe (fig. 39). This transmitter

connects wirelessly to a third data collection computer, allowing all three devices to be monitored in real time. The pressure sensors directly report pressure and contact area of each foot and automatically generate estimates for vertical ground reaction force.

Figure 39. The XSensor pressure insole in an athlete's shoe. The data transmitter and battery clip onto the outside of the shoe.

Data Processing

All data processing and statistical analyses were completed in MATLAB R2023a (MathWorks, Natick, MA, USA). Each set of data was manually synchronized by identifying the frame on which each participant landed from the initial vertical jump. This procedure was not a true synchronization, but rather ensured that the data from each trial was extracted from the same set of stride cycles. Small time-shifting may have occurred when synchronizing data with different sample rates, however, data was analyzed on a stride-by-stride basis from heel strike to heel strike via time index, allowing side-by-side comparison of the data. The landing of this jump appeared as a sharp positive spike in center of mass acceleration in the IMU suit data, a sharp spike in positive acceleration for the built-in inertial measurement of the EMG signals, and a sharp spike in overall estimated load in the pressure insole data. Center of mass (COM) velocity data, as reported by the IMU suit, was used to determine when each participant reached within 5% their predefined goal pace, which signified the beginning of the window of interest. The first 4 stride cycles within the window of interest were analyzed from each trial. While some trials produced more than 4 viable stride cycles, the same number of strides was analyzed for each trial to ensure consistent data collection.

IMU Data Processing

For each joint, the specific metric of interest was a joint angle peak at a specific point in the stance phase. Using COM velocity data, the point at which each participant met their target speed was documented as the beginning of the window of interest. From this point, the next four complete stride cycles were isolated and plotted versus time. By comparing this data with the Xsens software running model, the specific frames on which initial contact and toe-off occurred

could be identified. Then, within these time spans, a MATLAB code would select and export each metric of interest (left ankle maximum eversion during midstance, left hip maximum adduction during midstance, and right ankle inversion at initial contact) along with their corresponding timestamp. These metrics were selected due to their historical correlation with injury[32,33,39,41,98–100] In addition, COM velocity data for every trial was individually verified to ensure each participant met and maintained within 5% of their target velocity during the full four stride cycles. Average velocity over the four analyzed stride cycles was extracted from the data and recorded for each trial to be analyzed as a possible covariate within the data.

EMG Data Processing

Raw EMG signals were first bandpass filtered at 20-450 Hz with Trigno's onboard signal processing filter[101]. In MATLAB, each signal was then digitally high-pass filtered at 20 Hz[102], fully rectified[103], and then low-pass filtered using a 50 ms sliding-window RMS average[104]. Full rectification of an EMG signal takes the absolute value of every data point, allowing for analysis of signal amplitude[105]. Without this step, the mean of each signal would be zero. Finally, a moving window low-pass filter calculates the RMS of all data points within a fixed window length, smoothing the data and allowing a clear amplitude peak to be identified[104].

The EMG sensors contain an internal IMU unit which was used to identify when each participant landed from their initial vertical jump, matching the stride cycles of interest between the EMG data and IMU suit data. Within each window of interest, EMG Data was normalized to the mean value of the control condition and then compared between muscles in terms of asymmetry index (ASI), shown in fig. 40[106].

Left Calf	***Right Calf***
$Baseline\ straight\ mean = 20\ mV$	$Baseline\ straight\ mean = 40\ mV$
$Baseline\ turn\ reading = 30\ mV$	$Baseline\ turn\ reading = 30\ mV$
$\%\ increase = \left(\frac{30\ mV}{20\ mV}\right) \times 100\% = 150\%$	$\%\ increase = \left(\frac{30\ mV}{40\ mV}\right) \times 100\% = 75\%$
$calf\ activation\ ASI = \left(\frac{150\% - 75\%}{150\% + 75\%}\right) = 33.3\%$	
Interpretation: "The left calf accounted for 33.3% more of total calf activation than the right calf did. If left and right calf activation was equal in the baseline straight condition, out of the total amount of calf activation experienced over a complete stride cycle, the left calf accounted for 33.3% more of the activation than the right calf did."	

Figure 40. A sample calculation showing the method in which EMG data was normalized to compare activation between muscles.

Pressure Insole Data Processing

The pressure insole data processing was very similar to the IMU suit data processing. When the jump landing had been identified and the window of interest was defined, maximum load estimates were extracted from the peak of each dataset. To measure ground contact time, the time between the onset and end of ground reaction force was calculated. These metrics were also evaluated in terms of ASI using the formula[107]:

$$ASI = \left(\frac{X_R - X_L}{X_R + X_L}\right) \times 100\% \quad (8)$$

where X_R is the right-side measurement and X_L is the left-side measurement.

As a discussion topic, vertical average loading rate (VALR) was also considered. VALR can be calculated in several different ways, one of which is the slope between the initial contact point and the impact peak on the force vs. time graph. To estimate VALR, the time stamps of each ground reaction force onset and each ground reaction force peak were documented. By dividing the peak vGRF by the time required to achieve peak vGRF, average rate of force development for each stride cycle can be obtained (fig. 41). While this differs from the more commonly measured instantaneous vertical loading rate[108], this value has also been, while controversial, loosely associated with various injuries[21,35,109].

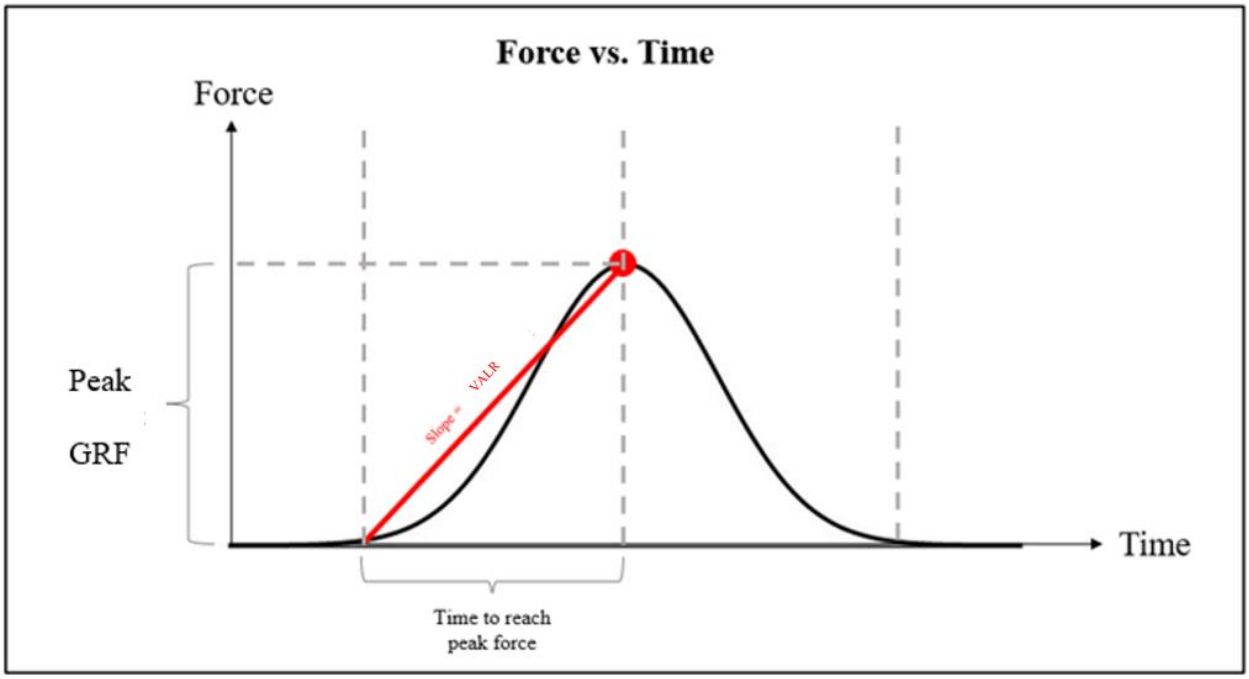

Figure 41. The method used to estimate the vertical average loading rate for a given stride. While instantaneous rate of force development was not extracted, this value provides a qualitative measure of which limb experiences higher rates of force development.

Statistical Analyses

Analysis of Variance

A repeated measures analysis of variance (ANOVA) was conducted to determine the presence and significance of main effects. Data was grouped by participant and by trial. A repeated measures ANOVA is useful when each data point may be dependent on other data points, such as data produced by the same participant or data collected from different strides within the same trial. The alpha value of this test was set at 0.05.

Linear Mixed Effects Model

Initially, the ANOVA was used to indicate if an overall significant difference existed between test conditions. If an overall difference was found, a linear mixed effects model (LME) was used to generate estimates of each independent variable and determine whether the effects of each insole were dependent on various possible covariates. The data processing resulted in a 576 by *n* table, with each row including data relating to personal identifiers relating to possible compounding effects (fig. 42). An LME analysis with a statistical significance value of $p = 0.05$ was performed with test condition ("scheme", in fig. 43) considered as the primary fixed effect. Sex, height, weight, training volume, race pace, and velocity were each evaluated both as possible dependent and independent covariates (fixed effects). By creating models that include every possible combination of these metrics as covariates and then comparing each model with an equivalent model where one metric was removed, each possible covariant could be evaluated using MATLAB's "compare" function[110]. If a model was not significantly changed ($p > 0.05$) by removing an effect, that specific effect was not considered a significant part of the model, and the differences seen in the independent variable did not depend on the removed effect. For

example, to evaluate if participant weight significantly improved the fit of the LME model, the two models:

$$Left\ Hip\ Adduction \sim Scheme + Weight + (1|Participant) \quad (9)$$

$$Left\ Hip\ Adduction \sim Scheme + (1|Participant) \quad (10)$$

were created. Using the "compare" function in MATLAB on these two models generated comparison metrics based on change in AIC, BIC, loglikelihood, and p-value. Comparison p-values of less than 0.05 indicated when a model was significantly better fit based on the inclusion or exclusion of covariates.

	1 FileName	2 Sex	3 Height_	4 Weight_	5 MilesPerWeek	6 Speed_	7 Scheme	8 R_Average	9 R_Peak	10 R_EstimatedLoa	11 R_HeelEstimate
1	"P01"	"M"	74	160	90	266	"SF"	143.5700	428.4400	1.7765e+03	94.9500
2	"P01"	"M"	74	160	90	266	"SF"	140.3400	421.2800	1.7417e+03	121.4400
3	"P01"	"M"	74	160	90	266	"SF"	147.0700	435.6600	1.7377e+03	290.8200
4	"P01"	"M"	74	160	90	266	"SF"	143.9700	411.6700	1.8214e+03	112.6800
5	"P01"	"M"	74	160	90	266	"SF"	145.7000	426.3400	1.7890e+03	81.6500
6	"P01"	"M"	74	160	90	266	"SF"	143.7200	411.7200	1.8494e+03	121.3600
7	"P01"	"M"	74	160	90	266	"SF"	146.1100	411.7200	1.8664e+03	89.8000
8	"P01"	"M"	74	160	90	266	"SF"	141.2800	390.0400	1.8295e+03	93.5700
9	"P01"	"M"	74	160	90	266	"SF"	146.6500	456.2700	1.7858e+03	143.5600
10	"P01"	"M"	74	160	90	266	"SF"	153.1300	482.4400	1.8254e+03	211.6400
11	"P01"	"M"	74	160	90	266	"SF"	149.8600	440.9700	1.8719e+03	NaN
12	"P01"	"M"	74	160	90	266	"SF"	154.4200	433.6700	1.9666e+03	NaN
13	"P01"	"M"	74	160	90	266	"CF"	126.5600	378.1300	1.5440e+03	185.0300
14	"P01"	"M"	74	160	90	266	"CF"	124.3200	361.0300	1.6037e+03	236.0900

Figure 42. A sample of the data table generated from our data processing procedures. Each column represents either a personal identifier or a dependent variable.

Tukey's Honestly Significant Difference Test

Post hoc pairwise comparisons were completed using Tukey's Honestly Significant Difference (HSD) with a family wise confidence level of 95%. This analysis evaluates the differences of means between two populations and is similar to a paired t-test but uses a different

range distribution[111]. This studentized range distribution allows Tukey's test to correct for type 1 error and was performed following an analysis of variance, meaning that any estimates created by this test would be statistically conservative. Tukey's HSD also corrects for multiple comparisons.

CHAPTER THREE

RESULTS

Engineering Results

Geometry

Three experimental insoles were developed: a flat foam (baseline) insole, a physically angled (wedge) insole, and an insole containing an angled stiff plate (angled plate) (fig. 43). All three insoles are 19.05 mm thick and fit within a modified Hyperion Tempo (Brooks, Seattle, WA, USA), running shoe. The Hyperion Tempo is a neutral, lightweight, and low stiffness running shoe[112]. This shoe does not contain a midsole plate and was selected for its solid EVA midsole in order to limit uncontrolled running shoe variables related that may impact results. To accommodate the height of the insoles, the upper portion of the shoe was cut open and the shoe was "laced" to the participant's foot with athletic tape. This procedure was completed for every test condition to ensure that comparisons between trials remained consistent. The baseline insole was flat and served as a control. The angled foam insole is cut longitudinally at 10˚ relative to the ground and served as an additional comparison for the angled plate insoles. The angled plate insole contains a stiff mid-plate that is angled at 10˚.

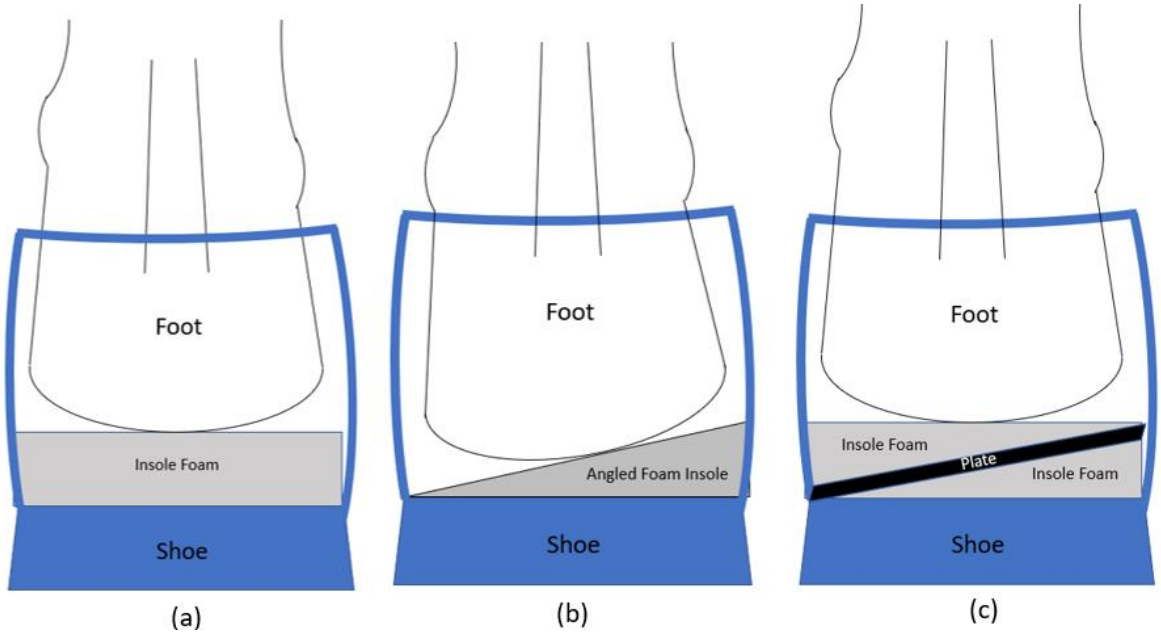

Figure 43. Rear view schematics of all 3 insoles for the right shoe: (a) baseline, (b) wedge, and (c) angled plate insoles. The wedge and angled plate insoles were each compared to the baseline insole.

Plate Stiffness

PVC – Type 1 (table 6), Young's modulus of 2.83 GPa and a yield strength of 50.33 MPa, was selected as the angled plate material, resulting in a plate that is 3.175 mm thick. These values fall well within our desired range (3.18 mm thickness, 2.20 – 3.78 GPa modulus, 32.42 – 55.58 MPa ultimate stress). At this thickness, PVC is estimated to have a 3-point bending stiffness of 17.97 N/mm from our simplified analytical solution.

The 3-dimensional finite element model utilized 855 2nd order tetrahedral (C3D10M) solid continuum elements (fig. 44). The model simulated a 4.45 N load applied at the location of the MTP joint and yielded a maximum deflection of 0.26 mm, corresponding to a 3-point bending stiffness of 16.81 N/mm. This is 6.90% lower than the analytical solution found when

simplifying the cross section of the plate to a rectangle. Both values fall within the desired range of 14-24 N/mm.

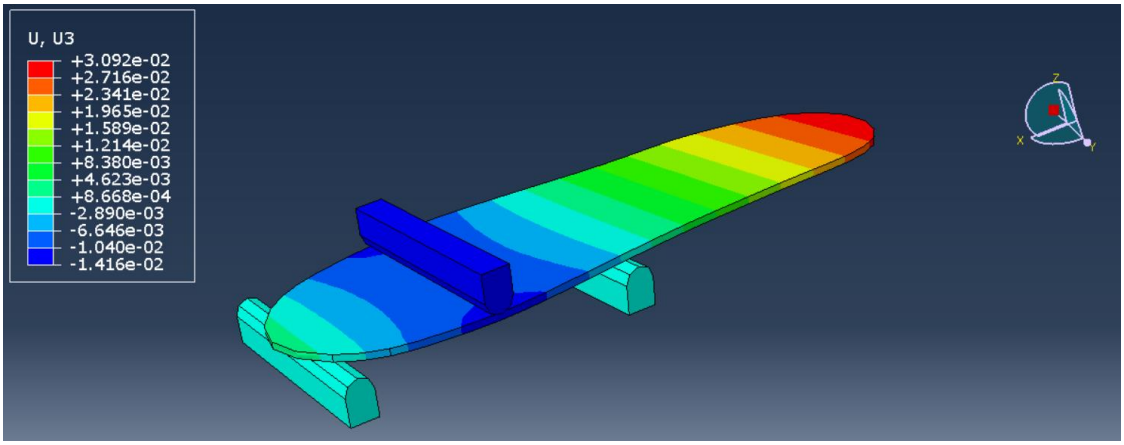

Figure 44. A finite element model of a 3-point bending loading scenario for the midsole plate. Under 4.45 N of force, the middle portion of the plate had a maximum deformation of 0.26 mm. This corresponds to a 3-point bending stiffness of 16.81 N/mm.

Plate Range of Motion and Ultimate Failure

The range of motion of the plate was bench tested to ensure that it would be able to accommodate the MTP joint's 30° of bending while running and 62˚ of maximum passive flexion[59,67,79]. By securely clamping the front 7.62 cm of the plate to a flat surface, a cantilever bending scenario was created to simulate the bending that occurs during running. The plate was capable of bending to over 65° of flexion, over double the required range for running and further than the maximum passive range of motion of the MTP joint, without failure or permanent deformation. This verified that the plate would not fail under normal MTP joint flexion and would not inhibit natural MTP joint motion.

Insole Foam Material Compressibility

The insole foam material of each insole is ethylene-vinyl acetate (EVA) foam (table 6). EVA foam is closed-cell and crosslinked, making it a common selection for commercial shoe material due to its shock absorbing and load distributing properties[78]. Most importantly, the Hyperion Tempo (Brooks, Seattle, WA, USA), which has an EVA midsole, would be used as the base test shoe. Utilizing the same foam material for the insole and shoe midsole avoids impedance mismatch that may lead to additional sources of variance within the shoe[73].

Safety

The ultimate flexural strength of PVC – Type 1 is 103.42 MPa and the yield strength is 50.33 MPa, meaning failure will occur at over twice the yield stress. This ensures that before ultimate failure, permanent plastic deformation of the insole plate would occur that would be detectable to the user.

Table 6. Final material selection and specifications

Final Material Selection and Design Specifications	
Insole Foam: Material	EVA Foam
Insole Foam: Density	0.032 g/cc
Insole Foam: Pressure to compress 25%	0.0275 MPa
Plate: Material	Thermoformable PVC – Type 1
Plate: Thickness	3.175 mm
Plate: Young's Modulus	2.83 GPa
Plate: Estimated 3-point bending stiffness	17.97 N/mm
Plate: FEA 3-point bending stiffness	16.81 N/mm
Plate: Max. Stress Experienced at 30˚	41.62 MPa
Plate: Yield Strength	50.33 MPa
Plate: Ultimate Flexural Strength	103.42 MPa
Plate: Yield/Ultimate Strength	2.05

Human Participant Testing Results

Kinematics

The repeated measures ANOVA showed that significant differences existed between test conditions for left hip adduction ($p = 0.004$), left ankle maximum eversion ($p < 0.001$), right ankle inversion at initial contact ($p < 0.001$), and right ankle eversion at midstance ($p = 0.027$) as a function of 'Scheme'. In the linear mixed effects model, the inclusion of sex, height, weight, training volume, or running speed as additional fixed effects or covariates did not significantly ($p > 0.05$) improve the fit of the model and were thus excluded from the final analysis. In the baseline turn condition, left hip maximum adduction during the stance phase and left ankle maximum eversion during stance phase both significantly ($p \leq 0.007$) increased compared to the baseline straight condition (fig. 45). Plot markers with different letters indicate where significant differences were detected. If two conditions display any of the same letters, no significant difference was detected. If two conditions do not display any of the same letters, a significant difference was detected.

For left hip adduction (fig. 45), no significant difference was observed between either of the straight conditions or between any of the turn conditions ($p > 0.05$). The angled plate turn condition displayed a significantly higher hip adduction angle than the baseline straight condition ($14.97 \pm 0.77°$ for angled plate turn vs. $12.30 \pm 0.66°$ for baseline straight, $p = 0.015$). In the baseline turn, angled plate turn, and wedge turn conditions, the peak value of left hip adduction was significantly ($p < 0.05$) higher than the baseline straight and angled plate straight condition. Peak hip adduction occurred between 40% and 50% of midstance (fig. 46).

The left ankle maximum eversion angle during midstance (fig. 45) was significantly higher in the angled plate turn condition compared to the baseline straight condition (31.06 ± 1.47° vs. for angle plate turn, 15.44 ± 1.29° for baseline straight, $p < 0.001$). However, no significant difference was observed between the baseline straight condition and the angled plate straight condition (15.44 ± 1.29° for baseline straight vs. 16.89 ± 1.49° for angled plate straight, $p = 0.069$). The wedge insole condition did not display a significantly different value of left ankle eversion than the baseline straight condition (18.80 ± 1.33° for wedge turn vs. 15.44 ± 1.29° for baseline straight, $p = 0.466$) and a significantly lower value than the baseline turn condition (18.80 ± 1.33° for wedge turn vs. 26.74 ± 1.29° for baseline turn, $p < 0.001$). Peak ankle eversion also occurred between 40% and 50% of midstance (fig. 47).

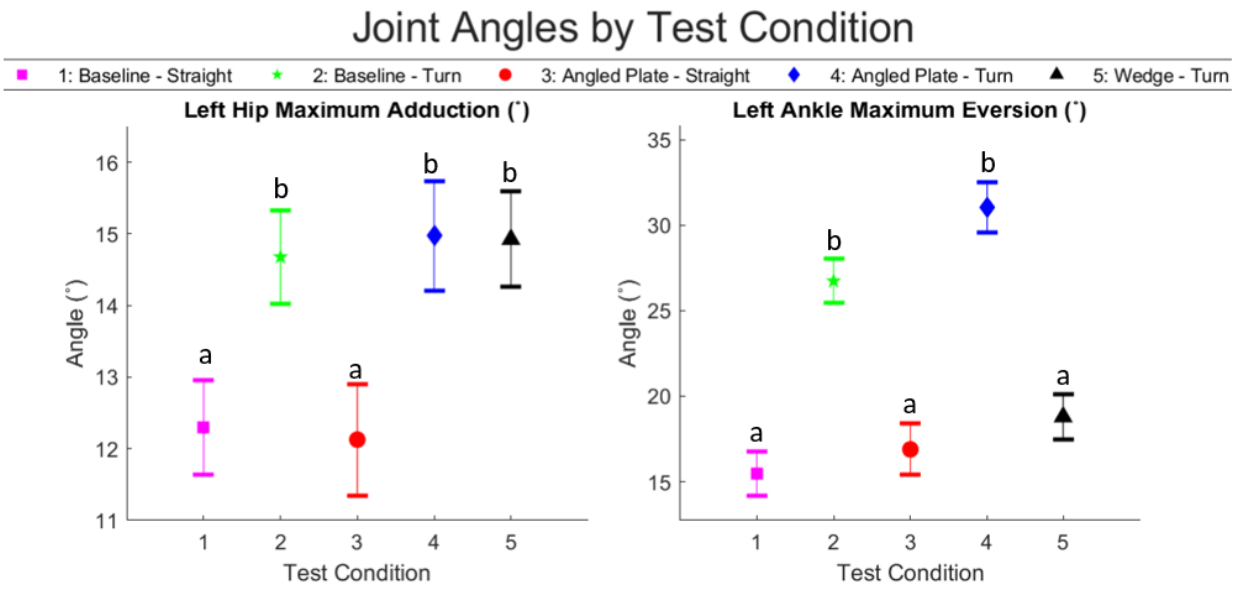

Figure 45. Left hip adduction and left ankle eversion by test condition. Different letters indicate where significant differences were detected (left hip adduction: a < b, $p \leq 0.015$; left ankle eversion: a < b, $p < 0.001$).

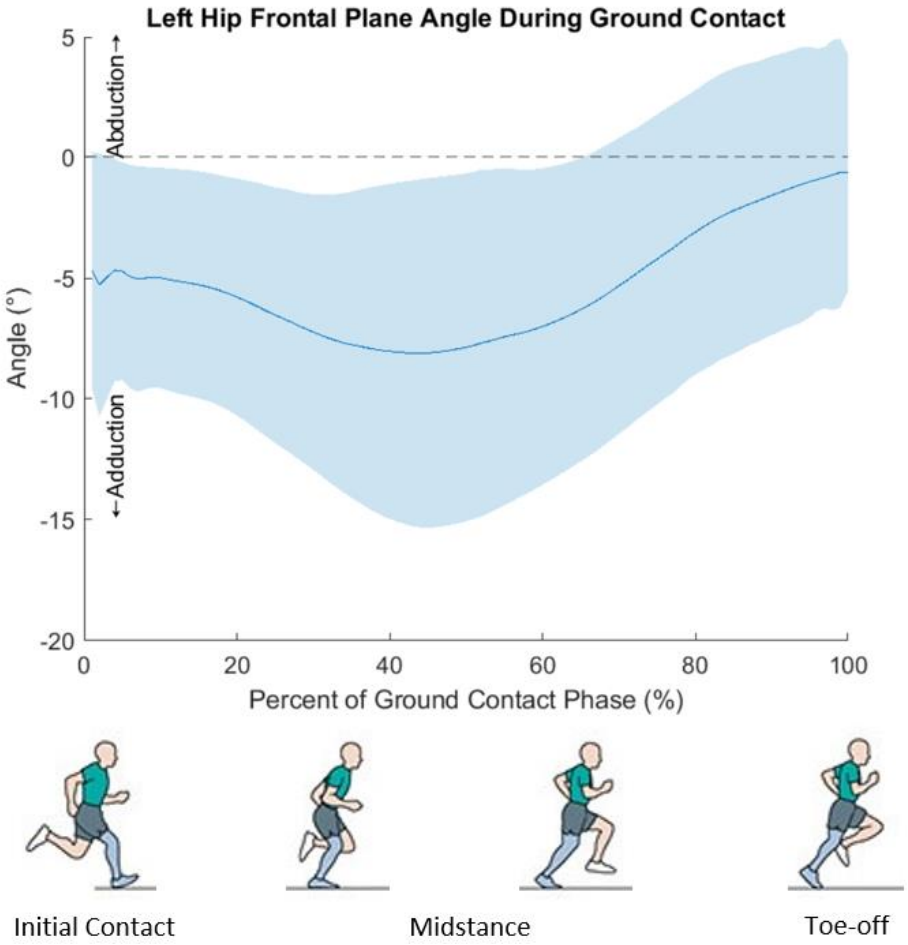

Figure 46. Left hip abduction/adduction during the stance phase. Peak left hip adduction occurred between 40% and 50% of the stance phase.

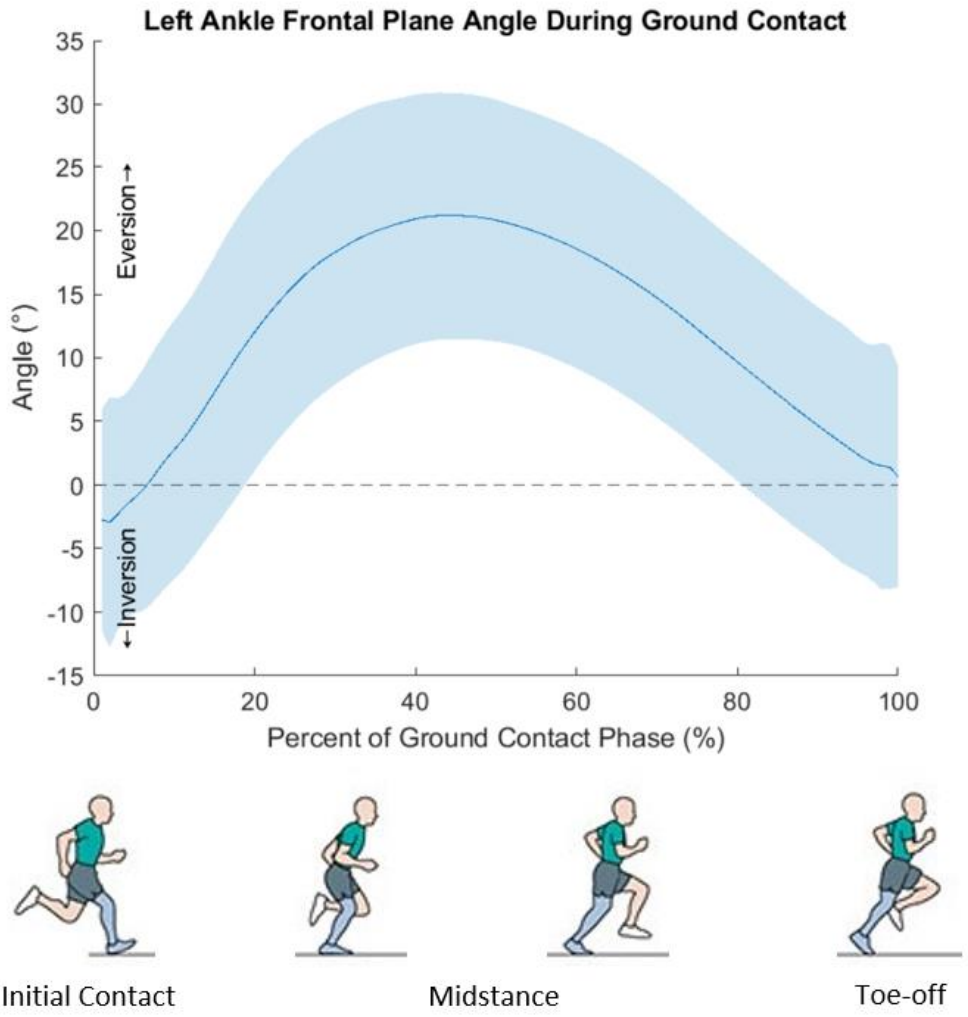

Figure 47. Left ankle inversion/eversion during the stance phase. Peak left ankle eversion occurred between 40% and 50% of the stance phase.

For right ankle inversion angle at initial contact (fig. 48, fig. 49), no significant difference was found between the angled plate turn condition and the baseline straight condition (8.22 ± 1.75° for angled plate turn vs. 10.55 ± 1.26° for baseline straight, $p = 0.034$). In addition, a significant decrease was found when comparing the baseline turn and angled plate turn condition (14.32 ± 1.26° for baseline turn vs. 8.22 ± 1.75° for angled plated turn, $p = 0.025$). The wedge turn condition and angled plate straight condition also exhibited significant decreases when compared to the baseline turn condition ($p \leq 0.006$).

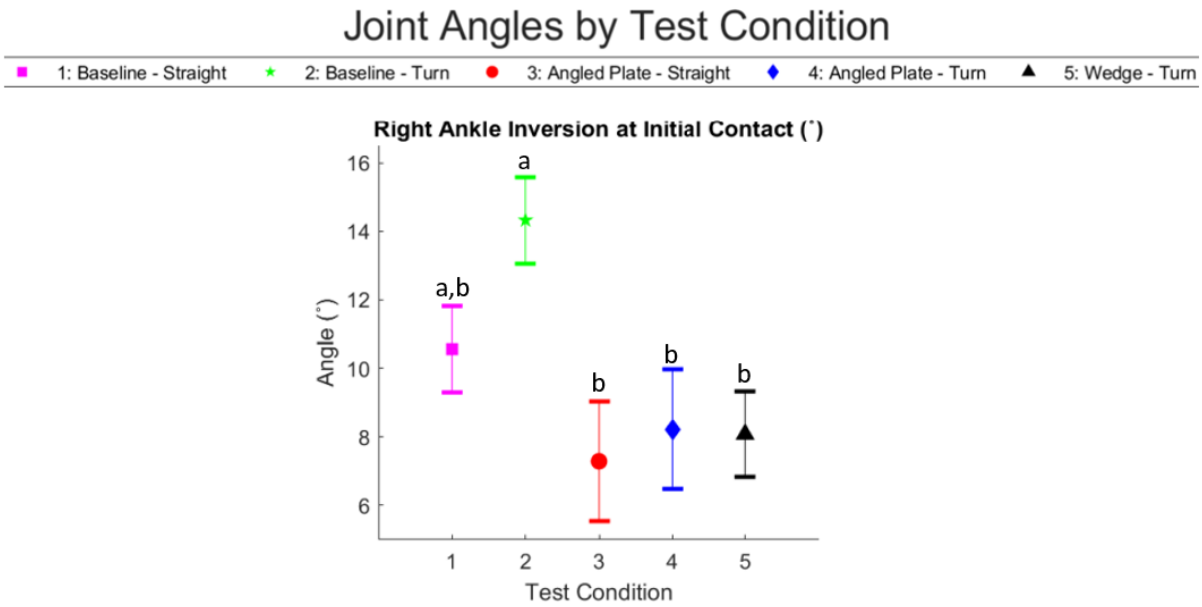

Figure 48. Right ankle inversion at initial contact by test condition. Different letters indicate where significant differences were detected ($a > b$, $p \leq 0.025$).

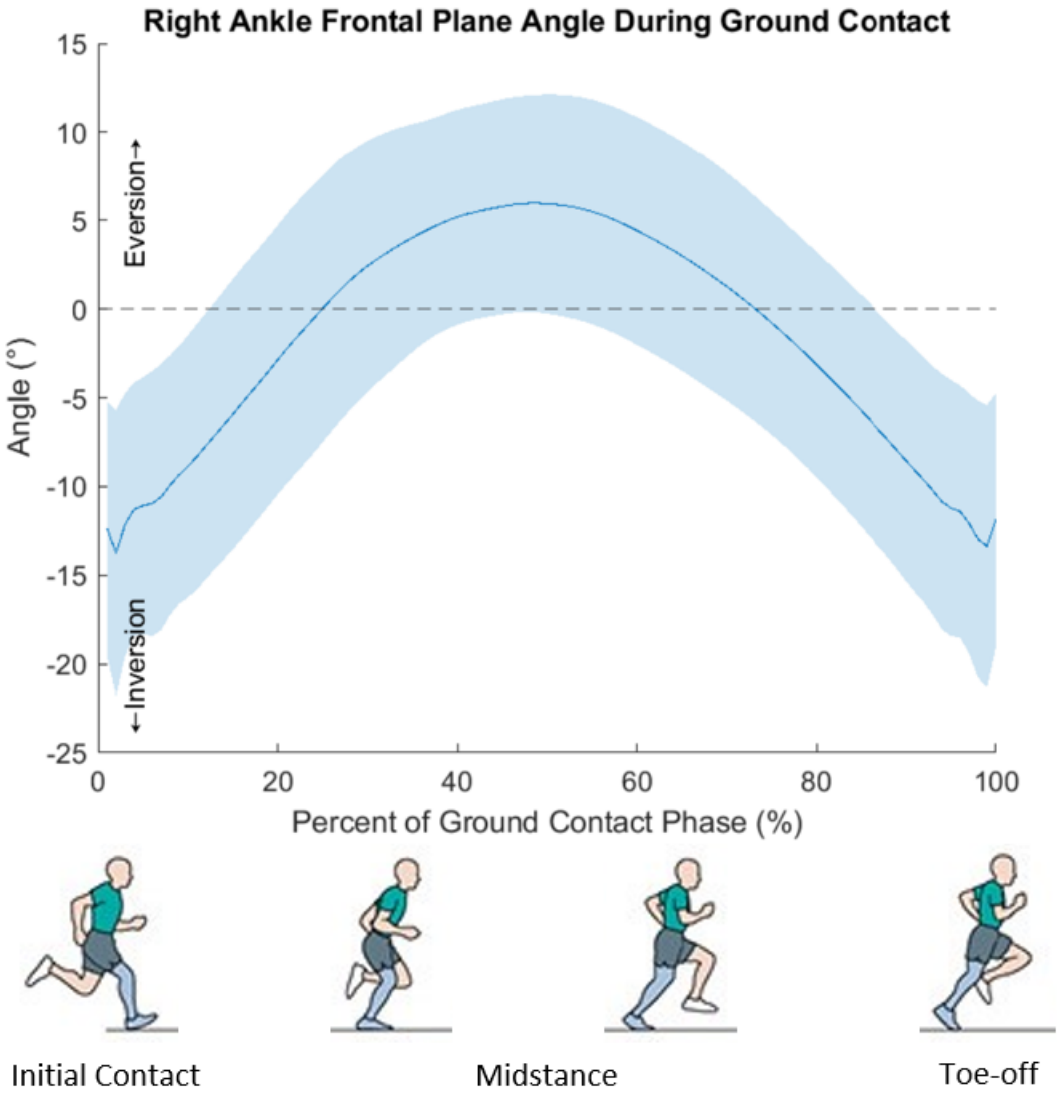

Figure 49. Right ankle inversion/eversion during the stance phase. Right ankle inversion was inspected at initial contact while peak right ankle eversion occurred between 40% and 50% of the stance phase.

Muscle Activation

Due to a gluteus medius EMG sensor becoming displaced for 3 participants (2 male, 1 female) and a gastrocnemius medialis EMG sensor becoming displaced for 1 male participant, the sample sizes were decreased for the EMG analysis (gluteus medius: 9 wedge and 4 angled plate, gastrocnemius medialis: 11 wedge and 5 angled plate). With this reduced sample size, the error ranges of the data became much larger, particularly within the gluteus medius data. The repeated measure ANOVA showed no significant difference between gluteus medius muscle activation asymmetry by test condition ($p = 0.986$), but significant effects were still observable in the gastrocnemius medialis results by test condition ($p = 0.027$). Like the kinematics results, the fit of linear mixed effects model was not significantly ($p > 0.05$) improved by the inclusion of sex, height, weight, training volume, or running speed as fixed effects or covariates, so the model was evaluated without consideration of these effects.

For gastrocnemius medialis activation ASI (fig. 50), in the baseline turn condition, no significant difference was detectable over the baseline straight condition ($0.17 \pm 3.06\%$ vs. $4.52 \pm 3.13\%$, $p = 0.628$). The angled plate straight, angled plate turn, and wedge turn conditions all demonstrated higher gastrocnemius medialis activation asymmetry compared to the baseline straight condition ($0.17 \pm 3.06\%$ for baseline straight vs. $10.31 \pm 4.40\%$ for angled plate straight, $p = 0.019$; $0.17 \pm 3.06\%$ for baseline straight vs. $13.87 \pm 4.39\%$ for angled plate turn, $p = 0.029$; $0.17 \pm 3.06\%$ for baseline straight vs. $16.86 \pm 3.28\%$ $p < 0.001$).

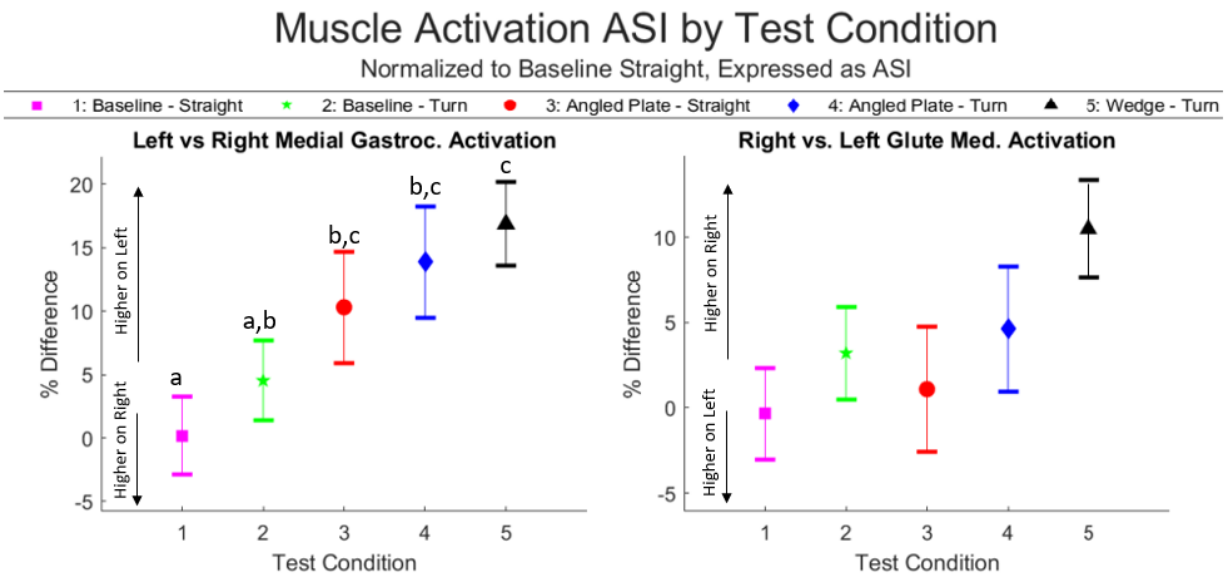

Figure 50. Muscle activation asymmetry index by test condition. Gastrocnemius (calf) activation asymmetry is measured as left/right while gluteus medius (glute) activation is measured as right/left. Different letters indicate where significant differences were detected (gastrocnemius medialis activation asymmetry: a < b, $p \leq 0.029$, b < c, $p \leq 0.026$; gluteus medius activation asymmetry: no significant difference detected by ANOVA).

Ground Reaction Force and Contact Time Asymmetry

The repeated measures ANOVA detected significant differences in both vertical ground reaction force (vGRF) asymmetry ($p < 0.001$) and ground contact time (GCT) asymmetry ($p = 0.037$) by test condition. Again, the inclusion of sex, height, weight, training volume, and running speed as additional fixed effects or covariates in the model did not result in a significantly ($p > 0.05$) better fit, resulting in the exclusion of these variables from the model.

In the baseline straight condition, the right foot had a 2.15 ± 0.52% higher GCT than the left foot. In the baseline turn condition and the angled plate turn condition, there was a significantly lower amount of GCT asymmetry than in the baseline straight condition (2.15 ± 0.52% for baseline straight vs. 0.14 ± 0.49% for baseline turn, $p = 0.016$). The angled plate turn condition also produced a significantly lower amount of GCT asymmetry than the baseline

straight condition (2.15 ± 0.52% for baseline straight vs. -0.50 ± 0.60% for angled plate turn, p = 0.034). The angled plate straight condition and the wedge turn condition were each not significantly different from the straight baseline ground contact time asymmetry (2.15 ± 0.52% for baseline straight vs. 1.93 ± 0.66% for angled plate straight, p = 0.997 and 2.15 ± 0.52% for baseline straight vs. 1.44 ± 0.50% for wedge turn, p = 0.906).

The vertical ground reaction force (vGRF) asymmetry (fig. 51) displayed a similar trend. When running straight, the ground reaction force on each side was approximately equal (-0.93 ± 2.09%). The angled plate straight condition and the wedge insole turn condition showed no significant difference from the baseline straight condition (p ≥ 0.989). However, in the angled plate turn condition, the vGRF asymmetry became significantly higher than the baseline straight condition (-0.93 ± 2.09% for baseline straight vs. 6.33 ± 2.31% for angled plate turn, p = 0.025) A complete collection of all results is shown in Table 7 and Table 8.

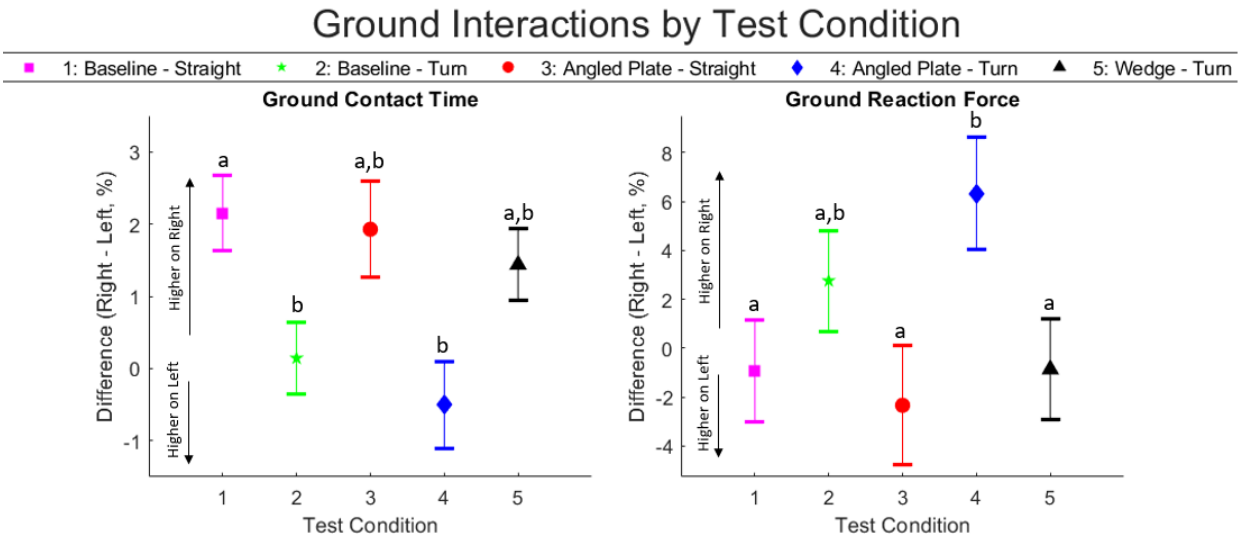

Figure 51. Ground interaction variable asymmetry by test condition. Different letters indicate where significant differences were detected (GCT asymmetry: a > b, p ≤ 0.034; GRF asymmetry: a < b, p < 0.048)

Table 7. Results for all measured metrics across all test conditions. Between conditions, different letters indicate where significant differences were detected. (**) indicates that the metric was not used to evaluate hypotheses and was only evaluated for the sake of discussion.

	Baseline – Straight	Baseline – Turn	Angled Plate – Straight	Angled Plate – Turn	Wedge – Turn
Left Hip Max Adduction	12.30 ± 0.66° a	14.68 ± 0.65° b	12.13 ± 0.78° a	14.97 ± 0.77° b	14.92 ± 0.66° b
Left Ankle Max Eversion	15.44 ± 1.29° a	26.74 ± 1.29° b	16.89 ± 1.49° a	31.06 ± 1.47° b	18.80 ± 1.33° a
Right Ankle Inversion at Initial Contact	10.55 ± 1.26° a, b	14.32 ± 1.26° a	7.29 ± 1.75° b	8.22 ± 1.75° b	8.08 ± 1.26° b
Left vs. Right Gastrocnemius Medialis Activation ASI	0.17 ± 3.06% a	4.52 ± 3.13% a, b	10.31 ± 4.40% b, c	13.87 ± 4.39% b, c	16.86 ± 3.28% c
Right vs. Left Gluteus Medius Activation ASI	-0.33 ± 2.70% a	3.22 ± 2.73% a, b	1.10 ± 3.66% a, b	4.62 ± 3.67% a, b	10.51 ± 2.87% b
Ground Contact Time Asymmetry (Right – Left, %)	2.15 ± 0.52% a	0.14 ± 0.49% b	1.93 ± 0.66% a, b	-0.50 ± 0.60% b	1.44± 0.50% a, b
Ground Reaction Force Asymmetry (Right – Left, %)	-0.93 ± 2.09% a	2.76 ± 2.06% a, b	-2.33 ± 2.45% a	6.33 ± 2.31% b	-0.86 ± 2.06% a
**Right Ankle Max Eversion	11.52 ± 1.19° a, c	4.02 ± 1.18° b	15.68 ± 1.39° a	9.38 ± 1.39° c	14.63 ± 1.21° a
**VALR Asymmetry (Right – Left, %)	-5.21 ± 2.50% a	2.91 ± 2.44% b	-4.84 ± 3.23% a	6.90 ± 2.84% b	-3.16 ± 2.44% a

Table 8. Post-hoc p-values from Tukey's HSD for each possible comparison between conditions. The family-wise confidence level was set at 95%. (*) indicates where significant differences were detected and (**) indicates that the metric was not used to evaluate hypotheses and was only evaluated for the sake of discussion.

	Baseline Straight vs. Baseline Turn	Baseline Straight vs. Angled Plate Straight	Baseline Straight vs. Angled Plate Turn	Baseline Straight vs. Wedge Turn	Baseline Turn vs. Angled Plate Straight	Baseline Turn vs. Angled Plate Turn	Baseline Turn vs. Wedge Turn	Angled Plate Straight vs. Angled Plate Turn	Angled Plate Straight vs. Wedge Turn	Angled Plate Turn vs. Wedge Turn
Left Hip Adduction	0.007*	0.762	0.015*	0.003*	0.001*	0.516	0.995	0.001*	< 0.001*	0.340
Left Ankle Eversion	< 0.001*	0.998	< 0.001*	0.466	< 0.001*	0.832	< 0.001*	< 0.001*	0.508	< 0.001*
Right Ankle Inversion at Contact	0.400	0.184	0.509	0.469	0.004*	0.025*	0.006*	0.977	0.874	0.998
Gastroc. Med. Activation Asymmetry	0.628	0.019*	0.029*	< 0.001*	0.209	0.300	0.026*	0.999	0.999	0.995
Glute. Med. Activation Asymmetry	0.938	0.990	0.843	0.038*	0.999	0.993	0.208	0.990	0.372	0.714
GRF Asymmetry	0.157	0.999	0.025*	0.989	0.382	0.748	0.334	0.048*	0.992	0.037*
GCT Asymmetry	0.016*	0.997	0.034*	0.906	0.264	0.998	0.113	0.257	0.998	0.160
**Right Ankle Maximum Eversion	< 0.001*	0.537	0.411	0.065	< 0.001*	0.016*	< 0.001*	0.046*	0.985	0.001*
**VALR Asymmetry	0.012*	0.999	0.035*	0.974	0.048*	0.999	0.044*	0.036*	0.989	0.038*

CHAPTER FOUR

DISCUSSION

Engineering Process

We designed and tested a prototype insole with the aim of reducing the incidence of certain turn-running related and injury-correlated biomechanics in track turn running. The insole utilized an angled plate embedded at a 10˚ angle relative to the running surface (angled plate) and aimed to allow athletes to more effectively produce the lateral force required to run a track turn. Two additional insoles were developed for comparison: a flat foam insole (baseline) and a physically angled wedge insole that provided a 10˚ adjustment to the effective running surface (wedge). In previous studies, a wedge insole has demonstrated a performance enhancing effect, but its impact on turn running related biomechanics has not been well defined. The wedge insole was intended to provide a depiction of the maximum possible benefit achievable by an insole-based intervention for comparison to the effects of the angled plate insole. We hypothesized that (1) athletes running a turn utilizing the angled plate insoles will experience lower values of left hip maximum adduction angle, left ankle maximum eversion angle, right ankle inversion angle at initial contact, gastrocnemius medialis and gluteus medius muscle activation asymmetry, ground reaction force asymmetry, and ground contact time asymmetry than when running a turn in the baseline insoles and (2) an athlete running straight in the angled plate insoles will experience no change to the aforementioned measurements when compared to straight running mechanics in baseline, flat insoles.

Prototype Design

The design of the insoles was able to meet or exceed all specified objectives. In reference to these objectives:

Design 1: Foam Wedge Insoles

1. The insoles were physically angled at 10˚ relative to the running surface, changing the effective angle of the contact surface.
2. The wedge insoles did not provide a response force via an energy returning plate and thus were not required to possess a specific 3-point bending stiffness.
3. The wedge insoles were capable of 180˚ of flexion without failure and did not inhibit metatarsophalangeal (MTP) joint motion, exceeding the 30° requirement.
4. The wedge insoles were constructed from a bulk foam material of EVA, matching the properties of the test shoe and preventing impedance mismatch.
5. The wedge insoles were constructed with a material that is not brittle and will not injure a participant.

Design 2: Angled Plate Insoles

1. The angled plate insoles contain a stiff mid-plate angled at 10˚ relative to the running surface, providing a response force in the same direction.
2. The plate was constructed of PVC – Type I and possesses a 3-point bending stiffness of 16.81 – 17.97 N/mm, falling within our desired range of 14-24 N/mm.
3. The plate was capable of at least 65˚ of flexion in a cantilever bending scenario, exceeding the 30° requirement.

4. The insoles in which the plate was embedded were constructed from a bulk foam material of EVA, matching the properties of the test shoe and preventing impedance mismatch.
5. The plate material (PVC – Type I) failed plastically at a load that is 2.08 times lower than its ultimate failure load, exceeding the 1.5 minimum definition, indicating safe usage for human participants.

Discussion of Human Participant Testing

Overall, few significant changes were detected that contributed to the evaluation of our hypotheses. The angled plate insoles demonstrated a significant reduction in right ankle inversion angle at heel contact over the baseline turn condition, but no significant impact on any other metric. Compared to the baseline straight condition, the angled plate insoles only influenced a significant difference in gastrocnemius medialis activation. The wedge insoles were intended to demonstrate the greatest possible effect achievable by an insole on turn running but only influenced a significant reduction in left ankle eversion at midstance and right ankle inversion at initial contact. A summary of each insole's effect on each metric is shown in Table 9, Table 10, and Table 11.

Table 9. Evaluation of hypothesis 1 based on the comparison between the baseline turn condition and the angled plate turn condition. Green/check indicates evidence in favor of hypothesis 1, grey/dash indicates evidence neither for nor against hypothesis 1, and red/x indicates evidence directly against hypothesis 1.

Hypothesis 1: The ***angled plate insoles*** will ***decrease*** left hip adduction, left ankle eversion, right ankle inversion at contact, gastrocnemius medialis activation asymmetry, gluteus medius activation asymmetry, ground reaction force asymmetry, and ground contact time asymmetry ***compared to the baseline turn condition.***		
Metric		**Comparison**
Left Hip Adduction	-	No significant difference
Left Ankle Eversion	-	No significant difference
Right Ankle Inversion at Contact	✓	Significant Reduction ($p = 0.025$)
Gastrocnemius Medialis Activation Asymmetry	-	No significant difference
Gluteus Medius Activation Asymmetry	-	No significant difference
GRF Asymmetry	-	No significant difference
GCT Asymmetry	-	No significant difference

Table 10. Evaluation of hypothesis 2 based on the comparison between the baseline straight condition and the angled plate straight condition. Green/check indicates evidence in favor of hypothesis 2, grey/dash indicates evidence neither for nor against hypothesis 2, and red/x indicates evidence directly against hypothesis 2.

Hypothesis 2: The ***angled plate insoles*** will ***not significantly change*** left hip adduction, left ankle eversion, right ankle inversion at contact, gastrocnemius medialis activation asymmetry, gluteus medius activation asymmetry, ground reaction force asymmetry, and ground contact time asymmetry ***compared to the baseline straight condition.***		
Metric		**Comparison**
Left Hip Adduction	✓	No significant difference
Left Ankle Eversion	✓	No significant difference
Right Ankle Inversion at Contact	✓	No significant difference
Gastrocnemius Medialis Activation Asymmetry	×	Significant Increase ($p = 0.019$)
Gluteus Medius Activation Asymmetry	✓	No significant difference
GRF Asymmetry	✓	No significant difference
GCT Asymmetry	✓	No significant difference

Table 11. Evaluation of wedge insole function based on the comparison between the wedge turn condition and the baseline turn condition. The wedge insoles were not evaluated for straight running.

Wedge Insole Comparison to Baseline Turn:		
Metric		**Comparison**
Left Hip Adduction	-	No significant difference
Left Ankle Eversion	✓	Significant Reduction ($p < 0.001$)
Right Ankle Inversion at Contact	✓	Significant Reduction ($p = 0.006$)
Gastrocnemius Medialis Activation Asymmetry	×	Significant Increase ($p = 0.026$)
Gluteus Medius Activation Asymmetry	-	No significant difference
GRF Asymmetry	-	No significant difference
GCT Asymmetry	-	No significant difference

<u>Kinematics</u>

No significant reduction of left hip maximum adduction was caused by either insole in the turning conditions, providing evidence against our first hypothesis. However, the straight angled plate condition and the baseline straight condition did not demonstrate any significant difference, providing evidence in favor of our second hypothesis.

For left ankle eversion angle, the angled plate turn condition did not provide any reduction in magnitude relative to the baseline turn condition, providing evidence against our first hypothesis. In fact, the angled plate turn condition influenced the greatest magnitude of left ankle eversion out of all conditions, reaching a near maximal value of 31.06 ± 1.26°. In another study[19], the left ankle reached a maximum eversion angle of 22.56˚ when running a track turn. While that study was conducted on a 400m track and we would expect a shorter turn radius to influence higher levels of ankle eversion[12,16,17,27], 31.06° borders on physiologically impossible without sustaining acute ankle injury[83,84]. A possible explanation of this is that the increased stack height of the angled plate insole allowed for additional eversion of the foot within the shoe and exaggerated the magnitude of the joint angle. If this study is to be repeated, it will be important to embed the plate within the midsole of the shoe to limit variance caused by additional movement.

For the wedge insoles, the reduction of left ankle eversion and the absence of a significant difference for left hip adduction may be explained by the effective leg length introduced by an angled body position[19,51]. For both feet to contact the ground when turning, the pelvis must rotate in the frontal plane, causing the left leg to be effectively “longer” (fig. 52b). Each ankle must then rotate opposite to the pelvis for both feet to be flat on the ground. By positioning the athlete’s ankles at 10˚, the left and right ankle angles can be returned to neutral (fig. 52c), but the left hip angle remains unaffected because the wedge insoles did not address the issue of altered effective leg length. This differs from a banked track, on which an angled pelvis is not required to maintain symmetrical effective leg length[51].

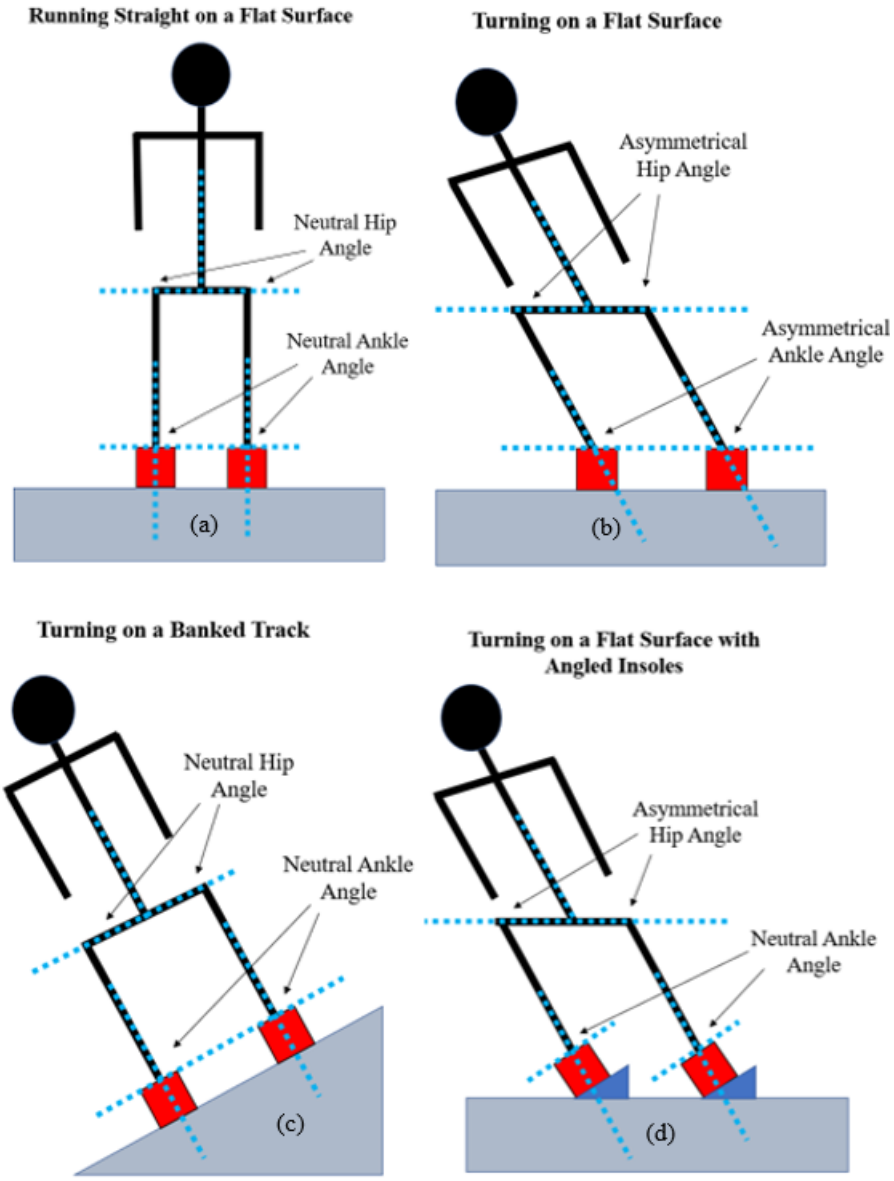

Figure 52. Running straight on a flat surface, turning on a banked track, turning on a flat surface, and turning on a flat surface with the wedge insoles shown from behind the runner. A banked track can correct for both hip angle asymmetry and ankle angle asymmetry, but the wedge insoles can only assist with ankle angle asymmetry.

While ankle eversion's independent contribution to injury is highly debated, the combination of an increase in ankle eversion and hip adduction seen in track running may be indicative of medial limb collapse and function as a predictor for tibial stress fractures[35]. The wedge insole demonstrated the ability to reduce the magnitude of left ankle maximum eversion

and right ankle inversion angle at initial contact, but no effect on the left hip adduction angle. Because the wedge insole did not decrease both left hip adduction and left ankle eversion simultaneously, the wedge insole may have no correlation with the reduction of injury potential.

The angled plate insoles were able to reduce right ankle inversion at initial contact but had no effect on left ankle eversion or left hip adduction. Differing effective leg length may also play a role here, but the difference between the left and right legs indicates that the left leg may be the limiting factor in this regard (i.e., the left leg must shorten until the right leg can reach the ground, but the right leg does not lengthen). Another possible cause is the difference in force requirements between each leg when running a turn. When running a turn, the right leg produced higher vertical ground reaction forces than the left. While we only measured vertical ground reaction force, other studies have indicated that the difference in lateral ground reaction force produced by the right and left limbs may be even higher than the difference in vertical ground reaction force[17,19]. To produce this force, the right ankle will invert more at initial contact and at toe-off, and the right hip will abduct and externally rotate[19]. By increasing the energy return in the direction the athlete is turning, the right leg may have been able to meet the higher demand of lateral force without the need to additionally invert the right ankle. While the same improved energy return was provided to the left leg, the excessive frontal plane motion of the left side may have been primarily caused by the shortening of the left leg, not increased force demand, and was thus not alleviated by the angled plate.

To provide a more comprehensive view of the right ankle frontal plane motion, right ankle eversion angle at midstance was also investigated. Our hypotheses were not evaluated based on right ankle eversion at midstance because it has not been demonstrated to significantly

change during turn running, whereas left ankle eversion at midstance increases significantly when turning left[17,19]. While preliminary literature review indicated that these may be useful metrics in determining injury likelihood[33,113,114], further review has shown that the correlation between absolute ankle eversion and inversion angle and injury is weak[115–117]. While the topic is now highly debated, it was originally thought that a "hyper-supinated" foot, a term that is not well defined, may limit the shock absorbing ability of the limb and lead to injuries like tibialis posterior tendonitis[33,99,113,118]. Right ankle inversion angle at initial contact was initially investigated in an attempt to depict whether the right ankle was in a more "hyper-supinated" position during turn running than in straight running. However, because ankle eversion is a mechanism of shock absorption[119], we believe that investigating the restriction of right ankle eversion may provide a more complete view of reduced shock absorption by the right limb than looking at the right ankle inversion angle at contact alone.

In our investigation, maximum right ankle eversion occurred at 40-50% of the stance phase (fig. 50). Right ankle maximum eversion was significantly decreased in the baseline turn condition when compared to the baseline straight condition ($4.02 \pm 1.18°$ for baseline turn vs. $11.52 \pm 1.19°$ for baseline straight, $p < 0.001$). A small but significant decrease was observed in the angled plate turn condition when compared to the baseline straight condition ($11.52 \pm 1.19°$ vs. $9.38 \pm 1.39°$, $p = 0.010$). Conversely, the angled plate straight condition showed a slight increase over the baseline straight condition ($15.68 \pm 1.19°$ vs. $11.52 \pm 1.19°$, $p < 0.001$).

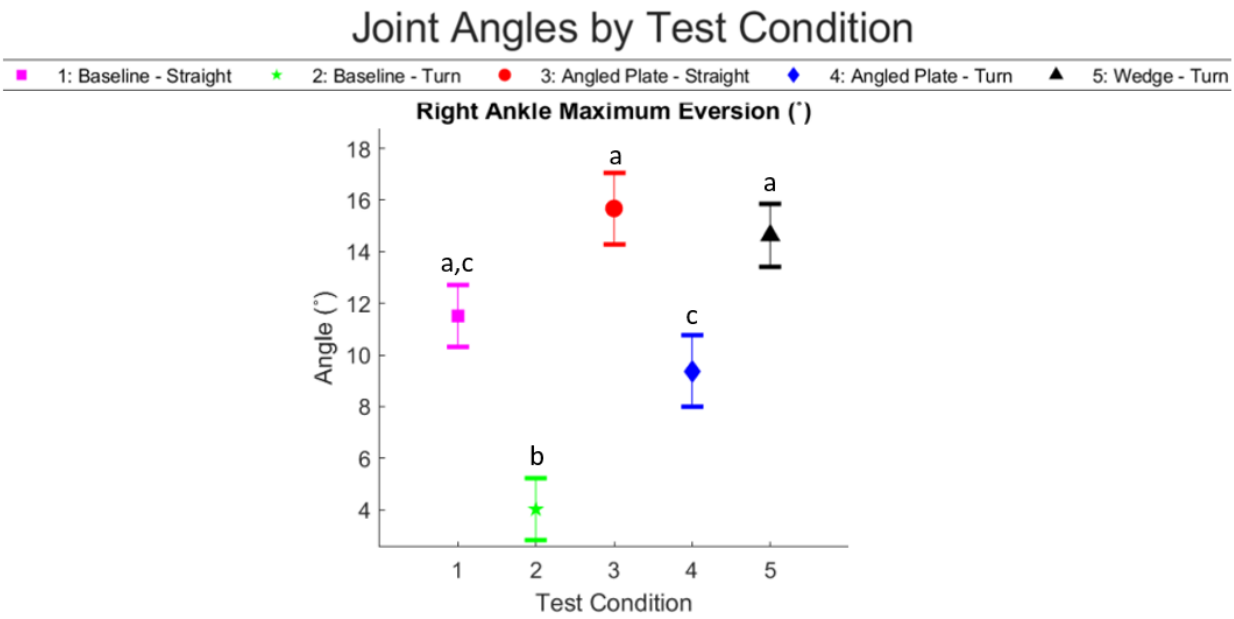

Figure 53. Right ankle maximum eversion by test condition. Different letters indicate where significant differences were detected (a > c, $p \leq 0.046$; c > b, $p \leq 0.016$)

These results indicate that the angled plate straight, angled plate turn, and wedge turn conditions all restricted right ankle eversion less than the baseline turn condition. While restricted ankle eversion has not been directly tied to injury, ankle eversion functions as a natural mechanism of shock attenuation and a restriction of this natural motion may indicate decreased shock absorption of the limb[119].

While maximum ankle eversion, ankle inversion at initial contact, and hip adduction all have weak correlations to injury[34,41,99,118], it may have been more productive to evaluate each complete stride in a time series analysis to investigate differences based on the region of the stride phase rather than maximum joint angle[120]. For example, one study has indicated that the duration of eversion during the stance phase may be a more useful injury (Achilles tendinopathy and medial tibial stress syndrome) predictor than a discrete measure of frontal plane joint angle[36]. The only temporal analysis completed thus far has been a combination of all trials,

separated between the left and right side. Revisiting those plots (fig. 54), it is noticeable that, in general, the left ankle is spending a much higher proportion of the stance phase in eversion than the right. This observation indicates a possible increased incidence of medial tibial stress syndrome and Achilles tendinopathy for the left limb[36], though direct conclusions cannot be made until each limb has been stratified by test condition. Overall, the relationship between any discrete or continuous kinematic variable and injury likelihood is inconsistent and largely dependent on both the population and specific injuries[121]. To relate the use of these insoles to injury potential in any way, a long-term study would need to be conducted that evaluates the insoles' effects on injury prevalence between a control group and a test group.

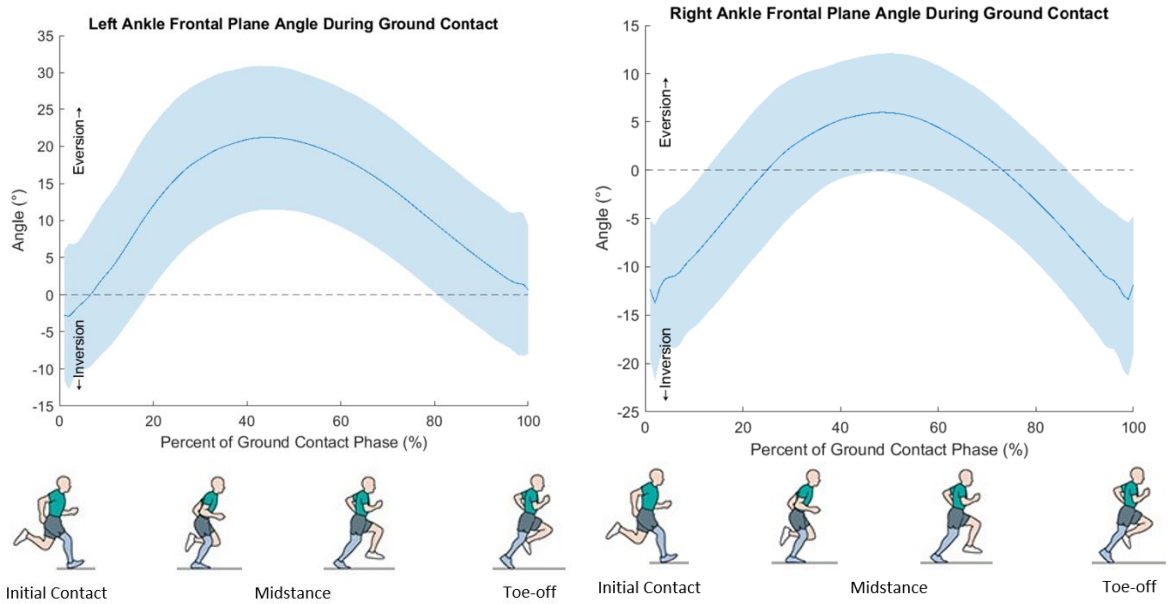

Figure 54. Left vs right ankle angles during the stance phase. These plots were initially used to highlight where certain values were occurring during the stride cycle, but they can also provide a lens into a possible difference in the duration of time each limb spends everted in the stance phase.

Muscle Activation

Due to a gluteus medius EMG sensor becoming displaced for 3 participants (2 male, 1 female) and a gastrocnemius medialis EMG sensor becoming displaced for 1 male participant, the EMG normalization process was rendered invalid for these trials. As a result, the sample sizes were decreased for the EMG analysis (gluteus medius: 9 baseline/wedge and 4 angled plate, gastrocnemius medialis: 11 baseline/wedge and 5 angled plate). While the repeated measures ANOVA, linear mixed effects model, and Tukey's HSD all remain accurate with differing sample sizes and no explicit statistical errors were introduced because of the collection errors, the limited sample size was reduced even further when omitting the erroneous data. With this reduced sample size, the error ranges of the data became much larger, particularly within the gluteus medius data. Because of this reduction, all data relating to muscle activation will be omitted from any published report of this study.

The gastrocnemius medialis (MG) EMG measurements yielded surprising results. It was hypothesized that by integrating an enhanced energy return directed towards the inside of the turn that the requirement for muscle activation asymmetry would be reduced. However, when running in both the angled plate and wedge insoles, participants experienced more MG muscle activation asymmetry than in the baseline insoles while turning. In addition, the angled plate insoles showed a significant increase in MG muscle activation asymmetry during straight running, indicating that both our first and second hypotheses were incorrect.

While neither insole was able to decrease muscle activation asymmetry, the EMG readings may provide insight into necessary mechanical changes related to adjusting running trajectory. While joint angles were positively affected by the wedge insoles, this corrected joint orientation may have allowed muscles to act more effectively against the lateral force

requirement encountered when running a turn. The MG is one of the two major muscles in the calf that contributes to ankle plantarflexion. When running a track turn, the left ankle must plantarflex and invert in order to propel the athlete forward and push the athlete leftwards[17]. While many different muscles contribute to ankle inversion (tibialis anterior, tibialis posterior, flexor digitorum, flexor hallucis, and extensor hallucis[122]), the MG also has a slight inversion moment arm under the right conditions[44]. During turn running, a higher overall ankle inversion moment is required[27], resulting in MG activation asymmetry. During turn running in the angled plate insoles, a greater amount of lateral energy return may have been produced, causing the overall inversion moment requirement to increase and in turn, higher left side MG activation. In an everted position, like the left ankle in the baseline turn condition, the MG will have a shorter inversion moment arm on the ankle, causing it to act poorly as an invertor (fig. 55). In a neutral or slightly inverted position, the MG has a longer inversion moment arm on the ankle and can act more effectively as an invertor. When the wedge insoles reduced left ankle eversion and right ankle inversion, the MG may have functioned more effectively as an invertor with the ankle joint in a more neutral position, and in turn contributed more to the overall increase of ankle inversion moment. This would result in increased muscle activation asymmetry between the left and right MG. It has been seen that over the course of a track and field season, left side invertor groups, including the MG, and right side evertor groups develop significant strength improvements, while the left side evertor groups and right-side invertor groups do not[9]. For ankle invertor muscles like the MG, this can lead to the development strength asymmetries and a higher possibility of injury[9,47].

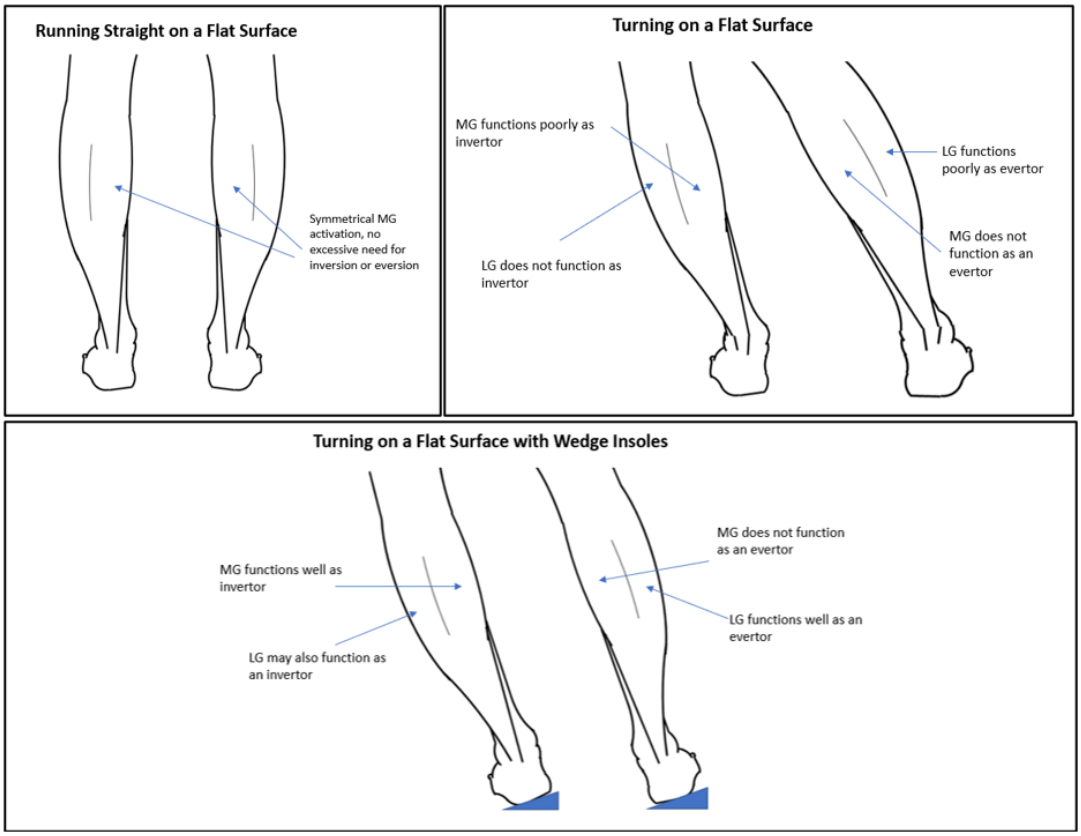

Figure 55. The possible cause for the difference in gastrocnemius medialis activation asymmetry. Because the ankle joint was placed in a neutral position with the wedge insoles, the gastrocnemius medialis was able to function more effectively as an ankle invertor.

Asymmetrical muscle activation can lead to strength asymmetries[47], indicating that neither insole would effectively decrease the development of strength asymmetries. However, our study reveals that asymmetrical muscle activation may be required to redirect an athlete's trajectory, and that asymmetrical muscle activation may occur regardless of intervention method. In addition, while our study controlled for speed, it is possible that our insoles may improve turn running performance by allowing athletes to activate turn-running specific muscles to a higher degree. When running at higher speeds, higher levels of muscle activation are required[123], so insoles that allow higher levels of turn-specific muscle activation may increase turn running performance. Alternatively, it may also be possible that a higher level of activation during the

same task indicates that the muscle was acting less efficiently. To more definitively draw this conclusion, a comprehensive view of muscle activation would need to be provided by including investigation of overall ankle inversion and eversion moment, as well as EMG analysis for other ankle evertor and invertor muscles. It may also be productive to investigate the left- and right-side muscle activations independently of each other to determine whether the activation asymmetry was caused by an increase in left side activation or a decrease in right side activation.

Ground Interaction

For ground contact time (GCT) asymmetry and ground reaction force (GRF) asymmetry, a positive percentage of asymmetry indicates the GCT or GRF was higher on the right side. Conversely, a negative percentage of asymmetry indicates that the GCT or GRF was higher on the left side. The most surprising result of the ground contact time analysis was an existing asymmetry detected in the straight baseline condition (2.15 ± 0.52%) that was significantly ($p = 0.016$) reduced in the baseline turn condition (0.14 ± 0.49%). While the wedge insoles induced a ground contact time asymmetry of 1.43± 0.47%, this value was not significantly different ($p = 0.906$) than the asymmetry detected in the baseline straight condition. In addition, while the angled plate turn condition displayed a significantly ($p = 0.034$) lower ground contact time asymmetry than the baseline straight condition (-0.50 ± 0.60% for angled plate turn vs. 2.15 ± 0.52% for baseline straight), this is not necessarily a positive result, as the angled plate turn condition was not significantly ($p = 0.998$) different from the value achieved in the baseline turn condition. No amount of GCT asymmetry is necessarily positive[48], but because an existing training effect existed within our sample in the baseline straight condition, the intervention insoles should aim to mirror natural straight running biomechanics regardless of baseline value.

Ground contact time asymmetry of just 1% can impair running economy, leading to increased fatigue and maladaptive compensatory patterns[82,124]. A pre-existing asymmetry (greater on the right) of was observed in the GCT data in the baseline straight condition, indicating that our sample had an existing compensatory pattern. In one study, GCT asymmetry in professional orienteers was monitored during a time trial on a 400m track and found an asymmetry of 2.57 ± 2.14%, with the left side having a longer GCT[28]. While these findings differ from ours, their research sample was 25 professional orienteers who typically train and compete on varied terrain and are likely free of any training effects relating to the repetitive left turns encountered during track running. Our research was conducted near the end of an outdoor track and field season, meaning participants had been competing with strictly left turns for 5 months leading up to when the research was conducted and likely had training effects present. If the orienteer sample is assumed to have had no GCT asymmetry present when running straight, then our study aligns with this one. In both studies, turning left influenced a shift in GCT asymmetry towards the left side[35].

No vertical ground reaction force asymmetry was detected for the baseline straight, angled plate straight, or wedge turn conditions, indicating that the angled plate insoles did not impede straight running mechanics, supporting our second hypothesis. However, the angled plate turn condition did not exhibit a statistically significant difference from the baseline turn condition, indicating that they were not able to alleviate any of the turn running mechanics relating to ground interaction, again disproving our first hypothesis.

While overall increases in vGRF have been retrospectively correlated with higher rates of injury, the relationship between vGRF asymmetry and injury is not as clear[44]. Asymmetry in gait

kinetics may be linked with overuse injuries[20], but vGRF asymmetry specifically has not been identified as a direct predictor of injury. While the validity of vGRF asymmetry as an injury predictor is unclear, retrospective studies have indicated significantly higher values of propulsive vGRF peaks between athletes with a history of tibial and femoral stress fractures compared with healthy controls[49]. While the wedge insoles displayed a statistically significant decrease of ground reaction force asymmetry, it is not clear if this decrease would provide any clinically significant reduction in injury potential.

The cause of the vGRF asymmetry in the angled plate turn condition may have been a compounding effect brought on by the already present vGRF asymmetry in the baseline turn condition. Because the right side vGRF is typically higher than the left side during turn running[17,19], increasing the energy return capabilities of each shoe may have exacerbated this difference in the angled plate turn condition. In this case, it likely would have been useful to compare with an insole containing a plate that was not angled to investigate whether enhanced shoe energy return, regardless of angle, would have made vGRF more asymmetrical.

It may have been more pertinent to evaluate the peak passive impact load rather than maximum vGRF. For rearfoot strikers, two peaks generally appear in vGRF force data[125]. The first peak is considered the passive impact load and correlated with impact related injuries, like tibial stress fractures[21,22,126,127]. The second peak occurs during the toe-off phase of the stride and is the active force peak associated with propulsion of the athlete and shows a slight correlation with tibial and femoral stress fractures[49]. However, most of the vGRF data collected in our study did not display two apparently separate peaks. For midfoot and forefoot strikers, the passive impact typically is not viewable in the time domain of the vGRF data[125]. Alternatively, it is

possible to measure the passive impact loads in the frequency domain using Fourier transforms[128]. For further investigations, new insight may be found by analyzing the vGRF data in this way, but time constraints did not allow for this additional analysis in our study.

The similarity of the trends observed in the ground contact time and ground reaction force sparked an additional analysis regarding vertical average loading rate (VALR)[108]. In our results, the trends of the GCT and vGRF plots were inverses of each other, meaning the magnitude of the differences would be exaggerated by dividing vGRF by GCT. The resulting quantity (vGRF/GCT) is not a commonly reported metric and has not been investigated with regards to injury. With additional research, it was then discovered that one method of calculating VALR includes dividing the peak of vGRF by the time from initial contact to the impact peak, a value that would be roughly proportional to vGRF/GCT. While clinically significant ranges of VALR asymmetry are not well documented, our VALR analysis showed significant differences between conditions that were not detected in the vGRF or GCT analyses. (fig. 56). Specifically, while no difference was detected between the baseline straight and baseline turn conditions for GRF asymmetry (-0.93 ± 2.09% for baseline straight vs. 2.76 ± 2.06% for baseline turn, $p = 0.157$) a significant difference was detected for VALR asymmetry (-5.21 ± 2.50% for baseline straight vs. 2.91 ± 2.44% for baseline turn, $p = 0.012$). Additionally, no significant difference was detected between the baseline turn and angled plate straight conditions for GCT asymmetry (0.14 ± 0.49% for baseline turn vs. 1.93 ± 0.66% for angled plate straight, $p = 0.264$), but a significant difference was detected between these conditions for VALR asymmetry (2.91 ± 2.44% for baseline turn vs. -4.84 ± 3.23% for angled plate straight, $p = 0.048$).

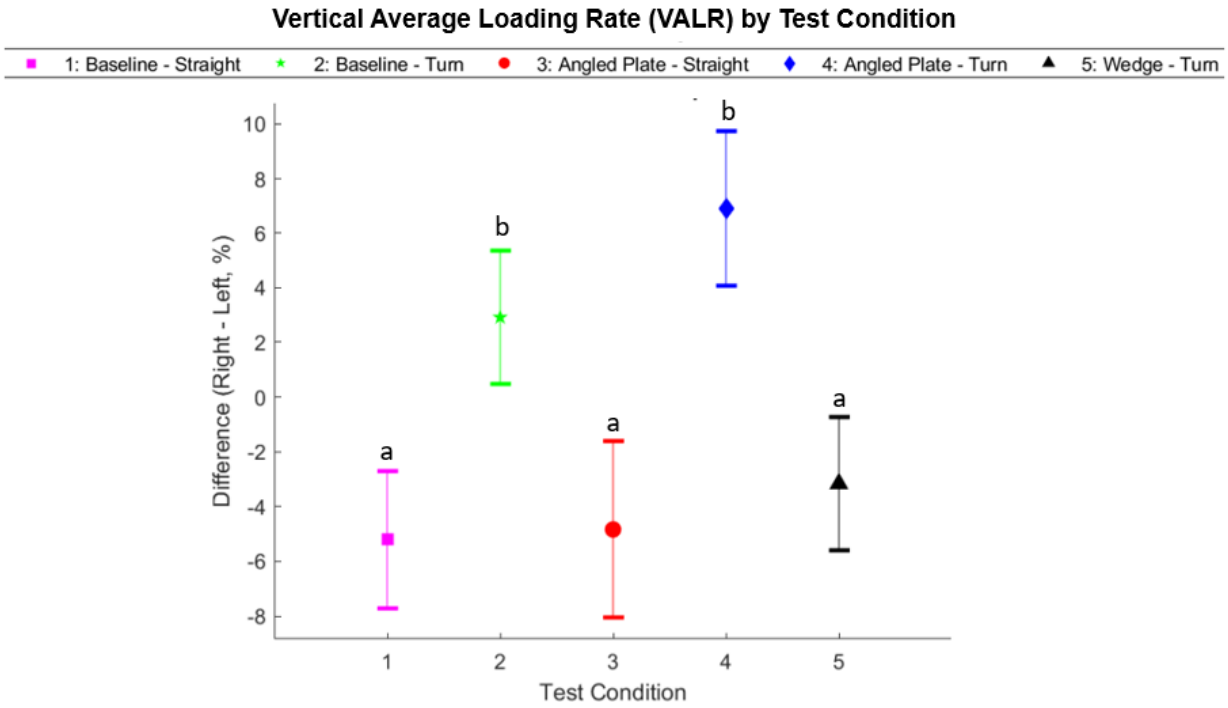

Figure 56. VALR by test condition. VALR was calculated by dividing the peak vGRF by the time between initial contact and peak vGRF. Different letters indicate where significant differences were detected ($a < b$, $p \leq 0.044$).

While GCT and vGRF have each historically been correlated to various injury mechanisms, VALR may provide a more comprehensive view of how vGRF and GCT interact. Like many other injury mechanisms, the relationship between VALR and injury is highly debated. Some studies claim a strong correlation between VALR and injury incidence for injuries like plantar fasciitis and patellofemoral pain[108,126], while others claim that no such relationship exists, regardless of calculation method[129]. However, few studies exist relating VALR asymmetry to injury potential. With our observations of VALR asymmetry, a prospective study that attempts to relate VALR asymmetry with injury incidence may be beneficial for further research.

Limitations and Sources of Error

In addition to the errors encountered with the EMG data collection, overall insufficient sample size likely decreased the ability to detect significant differences. The a priori power analysis was based on the ability to detect significant differences between the baseline straight and baseline turn conditions based on existing literature. While most metrics demonstrated significant differences between the baseline straight and baseline turn conditions, smaller reductions influenced by either insole over the baseline turn condition were not significantly detected. For example, when looking at ground contact asymmetry, a significant difference was detected between the baseline straight and baseline turn condition (2.15 ± 0.52% for baseline straight vs. 0.14 ± 0.49% for baseline turn, $p = 0.016$). However, while the wedge turn condition was not significantly different from the baseline straight condition (2.15 ± 0.52% for baseline straight vs. 1.44 ± 0.50% for wedge turn, $p = 0.906$), the difference between the wedge turn condition and the baseline turn condition was too small to be significantly detected (1.44 ± 0.50% for wedge turn vs. 0.14 ± 0.49% for baseline turn, $p = 0.113$).

Because the material properties of the angled plate prototype were governed by insole size and geometry, different sizes of insole would require different materials to have comparable stiffnesses. To ensure comparisons were kept consistent, only one size of angled plate insole was created. PVC was discovered to have the ideal material specifications for a US men's size 11 insole. Because of this, the testing of the angled plate prototype was restricted to individuals with a US men's size 10.5-11.5 shoe, all of whom were men. As a result, the baseline and wedge conditions had 12 participants each and the angled plate conditions had 6. With well-documented differences between male and female running mechanics, including hip adduction, knee

adduction, and frontal plane negative work, the sample population and resulting analyses should have either included both sexes or exclusively focused on one sex. These differences are observable between males and females on a large scale, but limited sample size may have caused any fixed effects from sex to be encompassed by the random effect of individual in the model. Even though no covariation was discovered for sex, the male and female results will need to be analyzed separately for conclusions to be effectively made from this work.

To accommodate the height of the insoles, the upper portion of each test shoe was cut and resecured to the participant's foot with athletic tape. The combination of excess stack height and decreased comfort likely impacted natural running mechanics[68] and may have allowed for additional foot motion within the shoe. However, this process was used for each test condition to allow equivalent comparison. While consistent methods were used for each test condition, the magnitude of observed effects may have been exaggerated or limited by this process due to the possibility of excess motion. By adding additional foam material to the shoe, additional motion may have been introduced to the system. Increasing the foam stack height of the shoe likely provided additional room for net compression of the foam, allowing the foot to rotate within the shoe. While this likely does not affect the direction of the observed trends, the magnitude of certain measurements, like ankle eversion, may have been exaggerated by this effect.

In addition to possibly exaggerating the kinematics, the extra deformation caused by increased foam stack height may have caused the "vertical" ground reaction force measurements to not be truly vertical. Because the pressure insoles were placed between the participant's feet and the insoles, the orientation of the pressure insole itself may have been affected by insole deformation, meaning the pressure was measured in the direction normal to the top face of the

insole. These pressure measurements may still provide an idea of how load was being distributed between the left and right limbs, but the term “normal” ground reaction force may have been more appropriate than “vertical” ground reaction force. For flat running, vertical and normal ground reaction force are interchangeable, as the foot is typically oriented normal to the running surface. However, most literature specifically investigates the vertical ground reaction force[38,97,108] and does not distinguish if the significance of this investigation is the vertical direction or the normal orientation to the foot. While the primary language used in the literature is “vertical,” it may be possible that in a case where the foot is not oriented normal to the running surface, the normal ground reaction force may be a more important metric to consider. While it is unclear if this distinction is impactful, it must be addressed due to the limitations brought on by estimating ground reaction force with pressure insoles[96,97]. Instead of the pressure insoles, a force plate, or series of force plates, should have been used to measure the ground reaction forces, which would have allowed the measurement of vertical, horizontal, and normal ground reaction forces. If this study is to be repeated, it is recommended that ground reaction force data be collected with force plates rather than plantar pressure insoles.

This research was conducted on NCAA Division 1 Track and Field athletes at the end of a 5-month long competition season. While the sample matched our population of interest, it is possible that some existing training effects existed within our sample. This was observable in the ground contact time data in which participants displayed an existing asymmetry of 2% when running straight that disappeared when running a turn. Although no other existing asymmetries were detected, it is possible that a sample of athletes that are inexperienced in track turn running would produce different results.

Data collection for this experiment did not occur on an actual indoor track. Due to a scheduling conflict, data collection had to be relocated to the outdoor track and field facility. To accommodate this change, a semicircular path with a radius of 17.2 m, emulating lane 1 of a standard indoor track, was drawn on the interior of the track area with tape. The testing area running surface and track surface are made of the same Benyon Sports BS 1000 polyurethane material. While it is not expected that this influenced any significant variation in the data, it should be noted that the collection did not take place on an actual indoor track.

While most joint angle data followed values existing in literature, the IMU suit displayed several distinct instances of error. Inexplicably, several trials (5/144) produced joint angles that are physiologically impossible (over 50˚ of ankle inversion, 90˚ of hip adduction). These errors were likely due to poor calibration and were individually removed from results. However, it is unknown if similar errors occurred on a smaller level and went undetected in our analysis. Because new calibrations were required every 3-4 trials, calibration error has a chance of inducing random effects in data.

Application

The effect of each insole on performance was not evaluated. The use of these insoles is not intended to increase performance, but if significant improvement and additional development allows the insoles to emulate the effects of a banked track, increased turn running performance may be un unintended effect[51]. In addition, even if refined versions of turn running shoes are developed that are shown to increase performance or decrease injury potential, they would likely not be allowed for competition. Professional organizations have already begun to ban shoes that provide too much of a mechanical advantage and the use of an insole to sidestep the negative

effects of a short radius flat track would likely be discouraged, especially considering the flat-track conversions that are currently built into the NCAA's ranking system.

If further development results in a shoe that can reduce gait asymmetry or injury potential, their use may be limited. Strength asymmetries and various other training effects brought on by repeated track turn running may be adaptations to high performance demand. While training effects related to consistently running on a short-radius indoor flat track are shown to exist[9], whether these effects are necessary for competitive racing has not been investigated. For this reason, prolonged use of insoles that decrease running form asymmetry when training may not be feasible for a competitive athlete and the application of a turn running insole may be limited to short-term use for the temporary alleviation of repetitive motion effects.

CHAPTER FIVE

CONCLUSION

This work outlined the design and testing of an insole designed to assist with turn running. The insole aimed to emulate the effects of a banked track by providing a more effective way to counteract the centripetal force required to run along a curved path by incorporating a stiff plate embedded at an angle. To define a baseline outcome and a positive outcome, a flat, baseline insole and a physically angled wedge insole were also designed and tested. The baseline insole showed increases in left ankle eversion during midstance, right ankle inversion at initial contact, left hip adduction during midstance, gastrocnemius medialis activation asymmetry, and ground contact time asymmetry during turn running. The wedge insole significantly reduced left ankle maximum eversion angle and right ankle inversion angle at initial contact but was deemed infeasible for straight running due to the direct alteration of ankle joint frontal plane angle. An insole containing an angled stiff plate reduced right-side ankle inversion at initial contact and did not significantly impact straight running mechanics. Both the angled plate insole and the wedge insole produced a higher level of muscle activation asymmetry, indicating that this may be a required effect of turn running regardless of joint angle positioning and ground interaction.

To effectively reduce gait asymmetry, each insole would require significant modification. Even then, the relationship between any specific biomechanics variable and injury likelihood is inconsistent and largely dependent on both the population and the specific injuries[121]. To relate the use of these insoles to injury potential in any way, a long-term study would need to be conducted that evaluates the insoles' effects on injury prevalence between a control group and a test group.

Recommendations for Future Work

While many aspects of gait mechanics were analyzed in this study, there are several remaining analyses that may prove useful. In general, maximum joint angles and muscle activation may not have been the best metric for evaluation of insole function. In general, using statistical parameter mapping to investigate when kinematic and kinetic variables differed over the stride phase may have provided a more comprehensive analysis of the changes caused by each insole[130]. In addition, the duration of time that an ankle is everted during the stance phase is more strongly correlated with injury potential (specifically Achilles tendinopathy and medial tibial stress syndrome) than any of the joint angle extremes discussed in this paper[36]. By performing this type of analysis, a more meaningful link between the intervention insoles and injury likelihood may be able to be established. Second, additional locations for EMG analysis may assist in explaining the trends observed in the gastrocnemius medialis activation data. To attain a full depiction of the biomechanics at play, it would have been useful to also monitor other ankle invertor muscles, like the tibialis anterior, tibialis posterior, flexor digitorum, flexor hallucis, and extensor hallucis[122]. It is possible that these muscles may have been varying in activation in conjunction with the gastrocnemius medialis[43,122]. Lastly, looking into hip internal and external rotation may have been helpful in explaining gluteus medius activation trends, as the gluteus medius functions as both an abductor and external rotator[131].

While this study controlled for stack height, plate geometry, and plate distance from the foot, each of these factors has been shown to impact running mechanics differently[55,68]. Specifically, curved midsole plates are more effective than flat insole plates[62,64,74,132]. To assess the applicability of the angled plate design isolated from these factors, it is recommended that a

prototype containing an angled curved midsole plate (as opposed to a flat plated insole) be developed.

The wedge insoles displayed a higher level of success in this study than the angle plate insoles but are likely not feasible for straight running. A solution to this would involve the development of an insole that replicates the geometry of the wedge insole only when running turns. This design would utilize either a pneumatic or hydraulic system to change the shoe angle when turning is detected and could effectively act as a temporary training intervention for athletes experiencing suspected turn running-related injuries.

Lastly, angling a stiff insole mid-plate is not the only way to achieve asymmetrical energy return within a shoe and several additional prototype possibilities have been ideated. First, it is possible that a flat plate with a laterally varied stiffness profile would also be effective at reducing certain turn related running mechanics with lower impact on straight running mechanics. By making the right side of each shoe stiffer than the left, bending about the neutral axis of the shoe would not vary, but a slightly angled applied force may induce an angled force response. A similar effect may be achieved by implementing half-width plates only on the right side of each shoe. Second, utilizing a multiple ply carbon fiber plate, with select layer of fibers oriented in the direction of straight running and other layers with fibers oriented diagonally, may assist athletes in producing the centripetal force required to run a turn. This concept has not been verified mathematically. Finally, recent research has shown that an increase in longitudinal bending stiffness may not be the primary cause of improved running energetics in certain plated shoes[74,132]. Plated shoes typically also utilize foam that has superior energy return properties compared to typical running shoe material, which may be the true cause of these shoes' increased

performance. Creating insoles or midsoles from foam with laterally varying energy return properties may prove to be more successful than an insole with an angled stiffness profile.

REFERENCES CITED

1. National Federation of State High School Associations. Track and field are still dominating the field. SportsEvents Media Group.

2. Becton S. 2023 indoor college track championships: Schedule, selections, how to watch. NCAA.com.

3. Hopkins C, Williams J, Rauh MJ, Zhang L. Epidemiology of NCAA Track and Field Injuries From 2010 to 2014. *Orthop J Sports Med*. 2022;10(1). doi:10.1177/23259671211068079

4. Parisien RL, Pontillo M, Farooqi AS, Trofa DP, Sennett BJ. Implementation of an Injury Prevention Program in NCAA Division I Athletics Reduces Injury-Related Health Care Costs. *Orthop J Sports Med*. 2021;9(9). doi:10.1177/23259671211029898

5. Sleeswijk Visser TSO, van Middelkoop M, Fokkema T, de Vos RJ. The socio-economic impact of running-related injuries: A large prospective cohort study. *Scand J Med Sci Sports*. 2021;31(10):2002-2009. doi:10.1111/sms.14016

6. Clement DB, Taunton JE, Smart GW, McNicol KL. A Survey of Overuse Running Injuries. *Phys Sportsmed*. 1981;9(5):47-58. doi:10.1080/00913847.1981.11711077

7. Castellani JW. Running in Cold Weather: Exercise Performance and Cold Injury Risk. *Strength Cond J*. 2020;42(1):83-89. doi:10.1519/SSC.0000000000000502

8. Farrokhyar F, Tabasinejad R, Dao D, et al. Prevalence of Vitamin D Inadequacy in Athletes: A Systematic-Review and Meta-Analysis. *Sports Medicine*. 2015;45(3):365-378. doi:10.1007/s40279-014-0267-6

9. Beukeboom C, Birmingham TB, Forwell L, Ohrling D. Asymmetrical Strength Changes and Injuries in Athletes Training on a Small Radius Curve Indoor Track. *Clinical Journal of Sport Medicine*. 2000;10(4):245-250. doi:10.1097/00042752-200010000-00004

10. Ryan GJ, Harrison AJ. Technical adaptations of competitive sprinters induced by bend running. *New Studies in Athletics*. 2003;18(4):57-70.

11. Nevison SE, Jun Y, Dickey JP. The Gluteus Medius Activation in Female Indoor Track Runners is Asymmetrical and May be Related to Injury Risk. *Sports and Exercise Medicine - Open Journal*. 2015;1(1):27-34. doi:10.17140/SEMOJ-1-105

12. Greene PR. *Running on Flat Turns: Experiments, Theory, and Applications*.; 1985. https://biomechanical.asmedigitalcollection.asme.org

13. *IAAF Requirements for Planning, Constructing, Equipping and Maintaining IAAF Track and Field Facilities Manual*.; 2008.

14. Picerno P, Padulo J. Acute kinematic adaptations to running on a centrifugal track: A pilot study. *Proc Inst Mech Eng P J Sport Eng Technol*. 2018;232(3). doi:10.1177/1754337117749515

15. McMahon TA, Greene PR. Fast running tracks. *Sci Am*. 1978;239(6):148-163. doi:10.1038/scientificamerican1278-148

16. Chang YH, Kram R. Limitations to maximum running speed on flat curves. *Journal of Experimental Biology*. 2007;210(6):971-982. doi:10.1242/jeb.02728

17. Alt T, Heinrich K, Funken J, Potthast W. Lower extremity kinematics of athletics curve sprinting. *J Sports Sci*. 2015;33(6):552-560. doi:10.1080/02640414.2014.960881

18. Greene PR. *SPRINTING WITH BANKED TURNS*.

19. Hamill J, Murphy M, Sussman D. The Effects of Track Turns on Lower Extremity Function. *International Journal of Sport Biomechanics*. 1987;3(3):276-286. doi:10.1123/ijsb.3.3.276

20. Carpes FP, Mota CB, Faria IE. On the bilateral asymmetry during running and cycling – A review considering leg preference. *Physical Therapy in Sport*. 2010;11(4):136-142. doi:10.1016/j.ptsp.2010.06.005

21. MILNER CE, FERBER R, POLLARD CD, HAMILL J, DAVIS IS. Biomechanical Factors Associated with Tibial Stress Fracture in Female Runners. *Med Sci Sports Exerc*. 2006;38(2):323-328. doi:10.1249/01.mss.0000183477.75808.92

22. Zifchock RA, Davis I, Hamill J. Kinetic asymmetry in female runners with and without retrospective tibial stress fractures. *J Biomech*. 2006;39(15):2792-2797. doi:10.1016/j.jbiomech.2005.10.003

23. Bredeweg SW, Buist I, Kluitenberg B. Differences in kinetic asymmetry between injured and noninjured novice runners: A prospective cohort study. *Gait Posture*. 2013;38(4):847-852. doi:10.1016/j.gaitpost.2013.04.014

24. Greene PR. *Running on Flat Turns: Experiments, Theory, and Applications*.; 1985. https://biomechanical.asmedigitalcollection.asme.org

25. Gilgen-Ammann R, Taube W, Wyss T. Gait asymmetry during 400-to 1000-m high-intensity track running in relation to injury history. *Int J Sports Physiol Perform*. 2017;12:157-160. doi:10.1123/ijspp.2016-0379

26. Pietraszewski P, Gołaś A, Krzysztofik M, Śrutwa M, Zając A. Evaluation of lower limb muscle electromyographic activity during 400 m indoor sprinting among elite female athletes: A cross-sectional study. *Int J Environ Res Public Health*. 2021;18(24). doi:10.3390/ijerph182413177

27. Luo G, Stefanyshyn D. Ankle moment generation and maximum-effort curved sprinting performance. *J Biomech*. 2012;45(16):2763-2768. doi:10.1016/j.jbiomech.2012.09.010

28. Ammann R, Wyss T. Running Asymmetries during a 5-Km Time Trial and their Changes over Time. In: *Proceedings of the 3rd International Congress on Sport Sciences Research and Technology Support*. SCITEPRESS - Science and and Technology Publications; 2015:161-164. doi:10.5220/0005634401610164

29. Boltz AJ, Roby PR, Robison HJ, Morris SN, Collins CL, Chandran A. Epidemiology of Injuries in National Collegiate Athletic Association Men's Track and Field: 2014–2015 Through 2018–2019. *J Athl Train*. 2021;56(7):788-794. doi:10.4085/1062-6050-513-20

30. Cruz CA, Kerbel Y, Smith CM, Prodromo J, Trojan JD, Mulcahey MK. A Sport-specific Analysis of the Epidemiology of Hip Injuries in National Collegiate Athletic Association Athletes From 2009 to 2014. *Arthroscopy: The Journal of Arthroscopic & Related Surgery*. 2019;35(9):2724-2732. doi:10.1016/j.arthro.2019.03.044

31. Lambert C, Reinert N, Stahl L, et al. Epidemiology of injuries in track and field athletes: a cross-sectional study of specific injuries based on time loss and reduction in sporting level. *Phys Sportsmed*. 2022;50(1):20-29. doi:10.1080/00913847.2020.1858701

32. Heil B. Lower Limb Biomechanics Related to Running Injuries. *Physiotherapy*. 1992;78(6):400-406. doi:10.1016/S0031-9406(10)61524-6

33. Hintermann B, Nigg BM. *Pronation in Runners Implications for Injuries*.

34. Neal BS, Griffiths IB, Dowling GJ, et al. Foot posture as a risk factor for lower limb overuse injury: a systematic review and meta-analysis. *J Foot Ankle Res*. 2014;7(1):55. doi:10.1186/s13047-014-0055-4

35. Pohl MB, Mullineaux DR, Milner CE, Hamill J, Davis IS. Biomechanical predictors of retrospective tibial stress fractures in runners. *J Biomech*. 2008;41(6):1160-1165. doi:10.1016/j.jbiomech.2008.02.001

36. Becker J, James S, Wayner R, Osternig L, Chou LS. Biomechanical Factors Associated With Achilles Tendinopathy and Medial Tibial Stress Syndrome in Runners. *Am J Sports Med*. 2017;45(11):2614-2621. doi:10.1177/0363546517708193

37. Kirby K. Biomechanics of the normal and abnormal foot. *J Am Podiatr Med Assoc*. 2000;90(1):30-34. doi:10.7547/87507315-90-1-30

38. Damavandi M, Dixon PC, Pearsall DJ. Ground reaction force adaptations during cross-slope walking and running. *Hum Mov Sci*. 2012;31(1):182-189. doi:10.1016/j.humov.2011.06.004

39. Benca E, Listabarth S, Flock FKJ, et al. Analysis of Running-Related Injuries: The Vienna Study. *J Clin Med*. 2020;9(2):438. doi:10.3390/jcm9020438

40. Noehren B, Davis I, Hamill J. ASB Clinical Biomechanics Award Winner 2006. *Clinical Biomechanics*. 2007;22(9):951-956. doi:10.1016/j.clinbiomech.2007.07.001

41. Foch E, Reinbolt JA, Zhang S, Fitzhugh EC, Milner CE. Associations between iliotibial band injury status and running biomechanics in women. *Gait Posture*. 2015;41(2):706-710. doi:10.1016/j.gaitpost.2015.01.031

42. Sannicandro I, Cofano G, Rosa RA, Piccinno A. Balance training exercises decrease lower-limb strength asymmetry in young tennis players. *J Sports Sci Med*. 2014;13(2):397-402.

43. Vieira TMM, Minetto MA, Hodson-Tole EF, Botter A. How much does the human medial gastrocnemius muscle contribute to ankle torques outside the sagittal plane? *Hum Mov Sci*. 2013;32(4):753-767. doi:10.1016/j.humov.2013.03.003

44. Lee SSM, Piazza SJ. Inversion–eversion moment arms of gastrocnemius and tibialis anterior measured in vivo. *J Biomech*. 2008;41(16):3366-3370. doi:10.1016/j.jbiomech.2008.09.029

45. Knapik JJ, Bauman CL, Jones BH, Harris JMcA, Vaughan L. Preseason strength and flexibility imbalances associated with athletic injuries in female collegiate athletes. *Am J Sports Med*. 1991;19(1):76-81. doi:10.1177/036354659101900113

46. Payne K, Payne J, Larkin TA. Patellofemoral Pain Syndrome and Pain Severity Is Associated With Asymmetry of Gluteus Medius Muscle Activation Measured Via Ultrasound. *Am J Phys Med Rehabil*. 2020;99(7):595-601. doi:10.1097/PHM.0000000000001367

47. Blagrove RC, Bishop C, Howatson G, Hayes PR. Inter-limb strength asymmetry in adolescent distance runners: Test-retest reliability and relationships with performance and running economy. *J Sports Sci*. 2021;39(3):312-321. doi:10.1080/02640414.2020.1820183

48. Piper AD, Knowles EG, Guerra NA, Jones EJ, Joubert DP. Running Economy Strongly Related to Ground Contact Time Imbalances. *International Journal of Exercise Science: Conference Proceedings*. 2019;2(11).

49. Grimston SK, Engsberg JR, Kloiber R, Hanley DA. Bone Mass, External Loads, and Stress Fracture in Female Runners. *International Journal of Sport Biomechanics*. 1991;7(3):293-302. doi:10.1123/ijsb.7.3.293

50. Greene PR. *Sprinting With Banked Turns*.; 1987.

51. Greene PR. Sprinting with banked turns. *J Biomech*. 1987;20(7):667-680. doi:10.1016/0021-9290(87)90033-9

52. White J, Wilson C, von Lieres Und Wilkau H, et al. Does lateral banking and radius affect well-trained sprinters and team-sports players during bend sprinting? *J Sports Sci*. 2023;41(6):519-525. doi:10.1080/02640414.2023.2225026

53. US Track and Field and Cross Country Coaches Assocation. NCAA Indoor Conversion Charts. www.ustfccca.org.

54. Madden R, Sakaguchi M, Tomaras EK, Wannop JW, Stefanyshyn D. Forefoot bending stiffness, running economy and kinematics during overground running. *Footwear Sci*. 2016;8(2):91-98. doi:10.1080/19424280.2015.1130754

55. Ortega JA, Healey LA, Swinnen W, Hoogkamer W. Energetics and Biomechanics of Running Footwear with Increased Longitudinal Bending Stiffness: A Narrative Review. *Sports Medicine*. 2021;51(5):873-894. doi:10.1007/s40279-020-01406-5

56. Stefanyshyn D, Fusco C. Increased shoe bending stiffness increases sprint performance. *Sports Biomech*. 2004;3(1):55-66. doi:10.1080/14763140408522830

57. McLeod AR, Bruening D, Johnson AW, Ward J, Hunter I. Improving running economy through altered shoe bending stiffness across speeds. *Footwear Sci*. 2020;12(2):79-89. doi:10.1080/19424280.2020.1734870

58. McLeod AR, Bruening D, Johnson AW, Ward J, Hunter I. Improving running economy through altered shoe bending stiffness across speeds. *Footwear Sci*. 2020;12(2):79-89. doi:10.1080/19424280.2020.1734870

59. Oh K, Park S. The bending stiffness of shoes is beneficial to running energetics if it does not disturb the natural MTP joint flexion. *J Biomech*. 2017;53:127-135. doi:10.1016/j.jbiomech.2017.01.014

60. Flores N, Delattre N, Berton E, Rao G. Does an increase in energy return and/or longitudinal bending stiffness shoe features reduce the energetic cost of running? *Eur J Appl Physiol*. 2019;119(2):429-439. doi:10.1007/s00421-018-4038-1

61. Beck ON, Golyski PR, Sawicki GS. Adding carbon fiber to shoe soles may not improve running economy: a muscle-level explanation. *Sci Rep*. 2020;10(1):17154. doi:10.1038/s41598-020-74097-7

62. ROY JPR, STEFANYSHYN DJ. Shoe Midsole Longitudinal Bending Stiffness and Running Economy, Joint Energy, and EMG. *Med Sci Sports Exerc*. 2006;38(3):562-569. doi:10.1249/01.mss.0000193562.22001.e8

63. Willwacher S, König M, Braunstein B, Goldmann JP, Brüggemann GP. The gearing function of running shoe longitudinal bending stiffness. *Gait Posture*. 2014;40(3):386-390. doi:10.1016/j.gaitpost.2014.05.005

64. Ortega JA, Healey LA, Swinnen W, Hoogkamer W. Energetics and Biomechanics of Running Footwear with Increased Longitudinal Bending Stiffness: A Narrative Review. *Sports Medicine*. 2021;51(5):873-894. doi:10.1007/s40279-020-01406-5

65. Nurick GN, Martin JB. Deformation of thin plates subjected to impulsive loading—A review. *Int J Impact Eng*. 1989;8(2):159-170. doi:10.1016/0734-743X(89)90014-6

66. Zweben C, Smith W, Wardle M. Test Methods for Fiber Tensile Strength, Composite Flexural Modulus, and Properties of Fabric-Reinforced Laminates. In: *Fifth Conference on Composite Materials: Testing and Design*. ASTM International; :228-228-235. doi:10.1520/STP36912S

67. Yoshioka Y, Siu DW, Cooke TD V., Bryant JT, Wyss U. Geometry of the first metatarsophalangeal joint. *Journal of Orthopaedic Research*. 1988;6(6):878-885. doi:10.1002/jor.1100060612

68. Werd MB, Knight EL. *Athletic Footwear and Orthoses in Sports Medicine*. Springer New York; 2010. doi:10.1007/978-0-387-76416-0

69. Callister WD, Rethwisch DG. *Callister's Materials Science and Engineering*. 10th ed. Wiley; 2019.

70. Wylie CR. *Advanced Engineering Mathematics*. 4th ed. McGraw-Hill; 1975.

71. Frederick EC. Physiological and ergonomics factors in running shoe design. *Appl Ergon*. 1984;15(4):281-287. doi:10.1016/0003-6870(84)90199-6

72. Cook SD, Kester MA, Brunet ME. Shock absorption characteristics of running shoes. *Am J Sports Med*. 1985;13(4):248-253. doi:10.1177/036354658501300406

73. Ireland C, Bowers D, Newton M, Waugh K. A Classification of Object-Relational Impedance Mismatch. In: *2009 First International Confernce on Advances in Databases, Knowledge, and Data Applications*. IEEE; 2009:36-43. doi:10.1109/DBKDA.2009.11

74. Healey LA, Hoogkamer W. Longitudinal bending stiffness does not affect running economy in Nike Vaporfly Shoes. *J Sport Health Sci*. 2022;11(3):285-292. doi:10.1016/j.jshs.2021.07.002

75. Zienkiewicz OC, Taylor RL, Taylor D. *The Finite Element Method for Solid and Structural Mechanics*. Elsevier; 2014. doi:10.1016/C2009-0-26332-X

76. Vaidyanathan A, Banu Rf. Finite element analysis – Concepts for knowledge and implementation in dental research. *The Journal of Indian Prosthodontic Society*. 2022;22(3):211. doi:10.4103/jips.jips_299_22

77. Danielson KT, Browning RS, Adley MD. Comparison of second-order serendipity and Lagrange tetrahedral elements for nonlinear explicit methods. *Finite Elements in Analysis and Design*. 2021;190:103532. doi:10.1016/j.finel.2021.103532

78. Jenkins M. *Materials in Sports Equipment*. Vol 1.; 2003.

79. Allan JJ, McClelland JA, Munteanu SE, et al. First metatarsophalangeal joint range of motion is associated with lower limb kinematics in individuals with first metatarsophalangeal joint osteoarthritis. *J Foot Ankle Res*. 2020;13(1):33. doi:10.1186/s13047-020-00404-0

80. Faul F, Erdfelder E, Lang AG, Buchner A. G*Power 3: A flexible statistical power analysis program for the social, behavioral, and biomedical sciences. *Behav Res Methods*. 2007;39(2):175-191. doi:10.3758/BF03193146

81. Rand MK, Ohtsuki T. EMG analysis of lower limb muscles in humans during quick change in running directions. *Gait Posture*. 2000;12(2):169-183. doi:10.1016/S0966-6362(00)00073-4

82. Joubert DP, Guerra NA, Jones EJ, Knowles EG, Piper AD. Ground Contact Time Imbalances Strongly Related to Impaired Running Economy. *International Journal of Sport Biomechanics*. 2020;13(4):427-437.

83. Kernozek T, Durall CJ, Friske A, Mussallem M. Ankle Bracing, Plantar-Flexion Angle, and Ankle Muscle Latencies During Inversion Stress in Healthy Participants. *J Athl Train*. 2008;43(1):37-43. doi:10.4085/1062-6050-43.1.37

84. Fong DTP, Hong Y, Shima Y, Krosshaug T, Yung PSH, Chan KM. Biomechanics of Supination Ankle Sprain. *Am J Sports Med*. 2009;37(4):822-827. doi:10.1177/0363546508328102

85. Fu W, Fang Y, Liu Y, Hou J. The effect of high-top and low-top shoes on ankle inversion kinematics and muscle activation in landing on a tilted surface. *J Foot Ankle Res*. 2014;7(1):14. doi:10.1186/1757-1146-7-14

86. Kang M, Ragan BG, Park JH. Issues in Outcomes Research: An Overview of Randomization Techniques for Clinical Trials. *J Athl Train*. 2008;43(2):215-221. doi:10.4085/1062-6050-43.2.215

87. World Athletics. World Rankings.

88. Schepers M, Giuberti M, Bellusci G. Xsens MVN: Consistent tracking of human motion using inertial sensing. *Xsens Technology*. 2018;1(8):1-8.

89. Seel T, Raisch J, Schauer T. IMU-Based Joint Angle Measurement for Gait Analysis. *Sensors*. 2014;14(4):6891-6909. doi:10.3390/s140406891

90. Movella. Sensor Placement in Xsens Link System. base.movella.com.

91. Roetenberg D, Luinge H, Slycke P. Xsens MVN: Full 6DOF human motion tracking using miniature inertial sensors. *Xsens Motion Technologies BV, Tech Rep*. 2009;1:1-7.

92. Grood ES, Suntay WJ. A Joint Coordinate System for the Clinical Description of Three-Dimensional Motions: Application to the Knee. *J Biomech Eng*. 1983;105(2):136-144. doi:10.1115/1.3138397

93. Wu G, Siegler S, Allard P, et al. ISB recommendation on definitions of joint coordinate system of various joints for the reporting of human joint motion—part I: ankle, hip, and spine. *J Biomech*. 2002;35(4):543-548. doi:10.1016/S0021-9290(01)00222-6

94. Hermens HJ, Freriks B, Disselhorst-Klug C, Rau G. Development of recommendations for SEMG sensors and sensor placement procedures. *Journal of Electromyography and Kinesiology*. 2000;10(5):361-374. doi:10.1016/S1050-6411(00)00027-4

95. Parker D, Andrews J, Price C. Validity and reliability of the XSENSOR in-shoe pressure measurement system. *PLoS One*. 2023;18(1):e0277971. doi:10.1371/journal.pone.0277971

96. Fong DTP, Chan YY, Hong Y, Yung PSH, Fung KY, Chan KM. Estimating the complete ground reaction forces with pressure insoles in walking. *J Biomech*. 2008;41(11):2597-2601. doi:10.1016/j.jbiomech.2008.05.007

97. Forner Cordero A, Koopman HJFM, van der Helm FCT. Use of pressure insoles to calculate the complete ground reaction forces. *J Biomech*. 2004;37(9):1427-1432. doi:10.1016/j.jbiomech.2003.12.016

98. Aicale R, Tarantino D, Maffulli N. Overuse injuries in sport: A comprehensive overview. *J Orthop Surg Res*. 2018;13(1). doi:10.1186/s13018-018-1017-5

99. Donatelli R. Abnormal Biomechanics of the Foot and Ankle. *Journal of Orthopaedic & Sports Physical Therapy*. 1987;9(1):11-16. doi:10.2519/jospt.1987.9.1.11

100. Duval K, Lam T, Sanderson D. The mechanical relationship between the rearfoot, pelvis and low-back. *Gait Posture*. 2010;32(4):637-640. doi:10.1016/j.gaitpost.2010.09.007

101. Delsys. Delsys Trigno Wireless Biofeedback System User Manual. Delsys.com.

102. De Luca CJ, Donald Gilmore L, Kuznetsov M, Roy SH. Filtering the surface EMG signal: Movement artifact and baseline noise contamination. *J Biomech*. 2010;43(8):1573-1579. doi:10.1016/j.jbiomech.2010.01.027

103. Myers LJ, Lowery M, O'Malley M, et al. Rectification and non-linear pre-processing of EMG signals for cortico-muscular analysis. *J Neurosci Methods*. 2003;124(2):157-165. doi:10.1016/S0165-0270(03)00004-9

104. Fraser GD, Chan ADC, Green JR, MacIsaac D. Removal of electrocardiogram artifacts in surface electromyography using a moving average method. In: *2012 IEEE International Symposium on Medical Measurements and Applications Proceedings*. IEEE; 2012:1-4. doi:10.1109/MeMeA.2012.6226621

105. Chowdhury R, Reaz M, Ali M, Bakar A, Chellappan K, Chang T. Surface Electromyography Signal Processing and Classification Techniques. *Sensors*. 2013;13(9):12431-12466. doi:10.3390/s130912431

106. Naik GR. *Computational Intelligence in Electromyography Analysis: A Perspective on Current Applications and Future Challenges*.; 2012.

107. Parkinson AO, Apps CL, Morris JG, Barnett CT, Lewis MGC. The Calculation, Thresholds and Reporting of Inter-Limb Strength Asymmetry: A Systematic Review. *J Sports Sci Med*. Published online August 10, 2021:594-617. doi:10.52082/jssm.2021.594

108. Davis IS, Bowser BJ, Mullineaux DR. Greater vertical impact loading in female runners with medically diagnosed injuries: a prospective investigation. *Br J Sports Med*. 2016;50(14):887-892. doi:10.1136/bjsports-2015-094579

109. SCHMIDA EA, WILLE CM, STIFFLER-JOACHIM MR, KLIETHERMES SA, HEIDERSCHEIT BC. Vertical Loading Rate Is Not Associated with Running Injury, Regardless of Calculation Method. *Med Sci Sports Exerc*. 2022;54(8):1382-1388. doi:10.1249/MSS.0000000000002917

110. Winter B. Linear models and linear mixed effects models in R with linguistic applications. Published online August 26, 2013.

111. Abdi H, Williams LJ. *Tukey's Honestly Significant Difference (HSD) Test*. http://www.utd.edu/~herve

112. Brooks. Brooks Hyperion Tempo. brooksrunning.com.

113. Neely FG. Biomechanical Risk Factors for Exercise-Related Lower Limb Injuries*. *Sports Medicine*. 1998;26(6):395-413. doi:10.2165/00007256-199826060-00003

114. Wen DY. Risk factors for overuse injuries in runners. *Curr Sports Med Rep*. 2007;6(5):307-313. doi:10.1007/s11932-007-0067-y

115. Ramskov D, Jensen ML, Obling K, Nielsen RO, Parner ET, Rasmussen S. No association between q-angle and foot posture with running-related injuries: a 10 week prospective follow-up study. *Int J Sports Phys Ther*. 2013;8(4):407-415.

116. Hargrave MD, Carcia CR, Gansneder BM, Shultz SJ. Subtalar Pronation Does Not Influence Impact Forces or Rate of Loading During a Single-Leg Landing. *J Athl Train*. 2003;38(1):18-23.

117. Horwood AM, Chockalingam N. Defining excessive, over, or hyper-pronation: A quandary. *The Foot*. 2017;31:49-55. doi:10.1016/j.foot.2017.03.001

118. Kannus VP. Evaluation of abnormal biomechanics of the foot and ankle in athletes. *Br J Sports Med*. 1992;26(2):83-89. doi:10.1136/bjsm.26.2.83

119. Pratt DJ. Mechanisms of shock attenuation via the lower extremity during running. *Clinical Biomechanics*. 1989;4(1):51-57. doi:10.1016/0268-0033(89)90068-5

120. Mann R, Malisoux L, Nührenbörger C, Urhausen A, Meijer K, Theisen D. Association of previous injury and speed with running style and stride-to-stride fluctuations. *Scand J Med Sci Sports*. 2015;25(6). doi:10.1111/sms.12397

121. Ceyssens L, Vanelderen R, Barton C, Malliaras P, Dingenen B. Biomechanical Risk Factors Associated with Running-Related Injuries: A Systematic Review. *Sports Medicine*. 2019;49(7):1095-1115. doi:10.1007/s40279-019-01110-z

122. DeMers MS, Hicks JL, Delp SL. Preparatory co-activation of the ankle muscles may prevent ankle inversion injuries. *J Biomech*. 2017;52:17-23. doi:10.1016/j.jbiomech.2016.11.002

123. Kyröläinen H, Avela J, Komi P V. Changes in muscle activity with increasing running speed. *J Sports Sci*. 2005;23(10):1101-1109. doi:10.1080/02640410400021575

124. Moore IS, Ashford KJ, Cross C, Hope J, Jones HSR, McCarthy-Ryan M. Humans Optimize Ground Contact Time and Leg Stiffness to Minimize the Metabolic Cost of Running. *Front Sports Act Living*. 2019;1. doi:10.3389/fspor.2019.00053

125. Wright IC, Neptune RR, van den Bogert AJ, Nigg BM. Passive regulation of impact forces in heel-toe running. *Clinical Biomechanics*. 1998;13(7):521-531. doi:10.1016/S0268-0033(98)00025-4

126. Johnson CD, Tenforde AS, Outerleys J, Reilly J, Davis IS. Impact-Related Ground Reaction Forces Are More Strongly Associated With Some Running Injuries Than Others. *Am J Sports Med*. 2020;48(12):3072-3080. doi:10.1177/0363546520950731

127. Johnson CD, Sara LK, Bradach MM, et al. Relationships between tibial accelerations and ground reaction forces during walking with load carriage. *J Biomech*. 2023;156:111693. doi:10.1016/j.jbiomech.2023.111693

128. Gruber AH, Boyer KA, Derrick TR, Hamill J. Impact shock frequency components and attenuation in rearfoot and forefoot running. *J Sport Health Sci*. 2014;3(2):113-121. doi:10.1016/j.jshs.2014.03.004

129. SCHMIDA EA, WILLE CM, STIFFLER-JOACHIM MR, KLIETHERMES SA, HEIDERSCHEIT BC. Vertical Loading Rate Is Not Associated with Running Injury, Regardless of Calculation Method. *Med Sci Sports Exerc*. 2022;54(8):1382-1388. doi:10.1249/MSS.0000000000002917

130. Pataky TC. Generalized n-dimensional biomechanical field analysis using statistical parametric mapping. *J Biomech*. 2010;43(10):1976-1982. doi:10.1016/j.jbiomech.2010.03.008

131. Gottschalk F, Kourosh S, Leveau B. The functional anatomy of tensor fasciae latae and gluteus medius and minimus. *J Anat*. 1989;166:179-189.

132. Lino H, Perry D, Bertschy M, Price M, Hoogkamer W. Effects of longitudinal bending stiffness and midsole foam on running energetics and biomechanics. *Footwear Sci*. 2023;15(sup1):S122-S124. doi:10.1080/19424280.2023.2199393

APPENDICES

APPENDIX A

RUNNING SHOE TERM DEFINITION

A typical shoe consists of many parts. In this study, it is important to define several terms relating to running shoe anatomy (fig. A1). The outsole of a shoe is the lowermost portion of the shoe that contacts the running surface and is usually made of a tough, durable rubber. The midsole is one layer up from the outsole and makes up the bulk of a running shoe. The midsole is usually made from a lightweight foam that is effective at shock absorption and energy return, such as ethylene-vinyl acetate (EVA) or polyurethane (PU) foam. Typically, a running shoe that utilizes a stiff plate to enhance running performance and energetics will embed the plate within the midsole of a shoe, termed a midsole plate. The final layer of the shoe base is called the insole and is often removable from the running shoe entirely. Commercial insoles exist that utilize a stiff imbedded insole mid-plate. Finally, the upper of a shoe is the portion that holds the athlete's foot in place, typically consisting of a mesh material, laces, and the tongue.

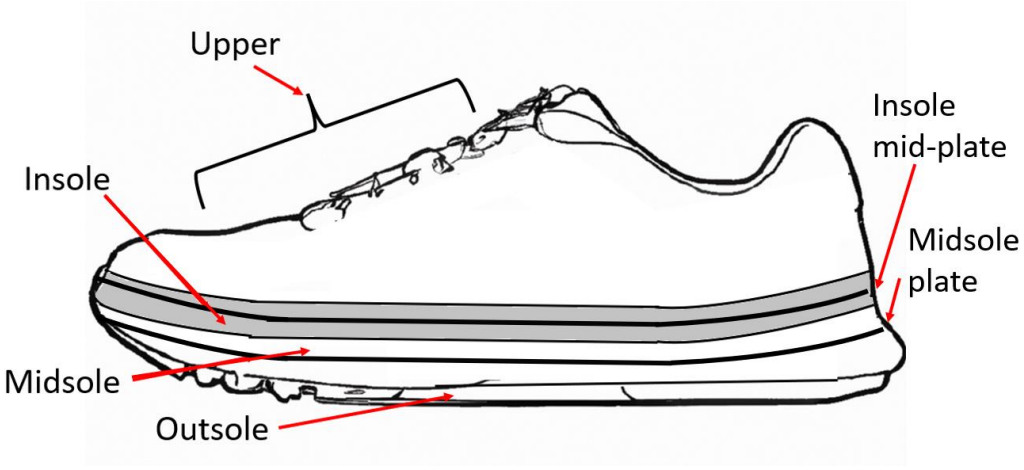

Figure A1. A diagram of the different parts of a standard running shoe.

APPENDIX B

TURN RUNNING THEORY

Some of Peter R. Greene's initial work regarding track turn running involved the compilation and cohesion of several existing theories describing turn running motion to relate track turn radius and velocity. Through the process of developing this relationship, several other dependencies can be observed. By starting with ground reaction force and ground contact time, the average forces of running in the vertical and horizontal directions can be generalized to the equations

$$\overline{F_v} = F_v t_1/(t_1 + t_2) \tag{B1}$$

$$\overline{F_h} = F_h t_1/(t_1 + t_2) \tag{B2}$$

where F_v is vertical force, F_h is horizontal force, t_1 is ground contact time, and t_2 is the time spent in the air when neither foot contacts the ground. These equations stand if the vertical and horizontal force-time curves are idealized as a train of square impulses. Now, applying Newton's second law in the vertical and horizontal directions, we can define the average forces as

$$\overline{F_v} = mg \tag{B3}$$

$$\overline{F_h} = mv^2/R \tag{B4}$$

where m is mass, v is running velocity, g is the gravitational constant, and R is turn radius. Then, to relate speed, stride length, and ground-time we can use a relationship defined by Cavagna, et al.

$$v(L, t_1) = L/t_1 \tag{B5}$$

$$L = constant \neq L(R) \tag{B6}$$

where L is stride length. In addition, we assume that stride length is constant, and that maximum running effort is mechanically realized, bring us to

$$F_v{}^2 + F_h{}^2 = F_{max}{}^2 = constant \tag{B7}$$

We can then define total stride time as the sum of t_1 and t_2, which, under the assumption of constant stride length, is also constant.

$$T = t_1 + t_2 = constant \tag{B8}$$

With all basic equations now defined, we can now solve for a speed-radius relationship. First, we can substitute equations 8, 9, 10, and 11 into equation 14 to get

$$\left[(mg)^2 + \left(\frac{mv^2}{R}\right)^2\right] \times \left(\frac{T}{t_1}\right)^2 = {F_{max}}^2 \tag{B9}$$

In a straight running condition, we can take the limit as R -> inf, driving v -> v_0.

$${F_{max}}^2 = (mg)^2 \times \left(\frac{T}{t_1}\right)^2 = \left(\frac{Tv_0}{t_1}\right)^2 \times (mg)^2 \tag{B10}$$

Substituting equation B10 into B9 yields

$$R(v) = \frac{v^3}{g\sqrt{{v_0}^2 - v^2}} \tag{B11}$$

Rearranging brings us to the dimensionless speed-radius relation

$$\frac{Rg}{{v_0}^2} = \frac{(v/v_0)^3}{\sqrt{1 - \left(\frac{v}{v_0}\right)^2}} \tag{B12}$$

Then, Greene highlights that the left side of equation B12 is the reciprocal Froude number, a property that typically appears in fluid mechanics. Other research has shown that the Froude number based on leg length is an important factor for describing human locomotion.

$$Fr^{-1} = \frac{Rg}{{v_0}^2} \tag{B13}$$

Following a similar process, the relationship between turn radius and ground contact time and turn radius and stride length. We again start with equation B5, this time defined separately for general velocity v and top speed v_0

$$v = L/t_1 \tag{B14}$$

$$v_0 = L_0/t_1^0 \tag{B15}$$

Dividing equation B14 by B15 yields

$$v/v_0 = t_1^0/t_1 \tag{B16}$$

Substituting equation B16 into B12 gives us the relationship between radius and ground contact time.

$$\frac{Rg}{{v_0}^2} = \frac{(t_1^0/t_1)^3}{\sqrt{1-\left(\frac{t_1^0}{t_1}\right)^2}} \tag{B17}$$

Now, we can define stride length as the velocity times the stride length

$$S(R) = v(R)T(R) \tag{B18}$$

For straight running conditions, or as R -> inf, this relationship is defined in terms of maximal velocity, stride length, and stride time

$$S_0 = v_0 T_0 \tag{B19}$$

Dividing equation B18 by B19 yields

$$S/S_0 = (v/v_0)(T/T_0) \tag{B20}$$

Continuing with the assumption that stride time is constant and plugging the resulting equation into equation B12 once again gives us a new relationship.

$$\frac{Rg}{{v_0}^2} = \frac{(S/S_0)^3}{\sqrt{1-\left(\frac{S}{S_0}\right)^2}} \tag{B21}$$

Through this analysis, it should be noted that turn radius shows a direct correlation to running velocity, stride length, and ground contact time. In addition, the consistent appearance of the inverse Froude number lays the groundwork for future investigation. It is possible that the effects of the insoles also vary as a function of inverse Froude number. While the linear mixed effects model showed no correlation with any single variable, a mixed effects model based on a nonlinear equation may prove more useful in predicting insole efficacy based on personal identifiers like height, weight, stride length, or running velocity. It is also possible that linear relationships exist between certain performance metrics and unknown linear variable combinations, another topic for future research.

APPENDIX C

ENGINEERING DRAWINGS

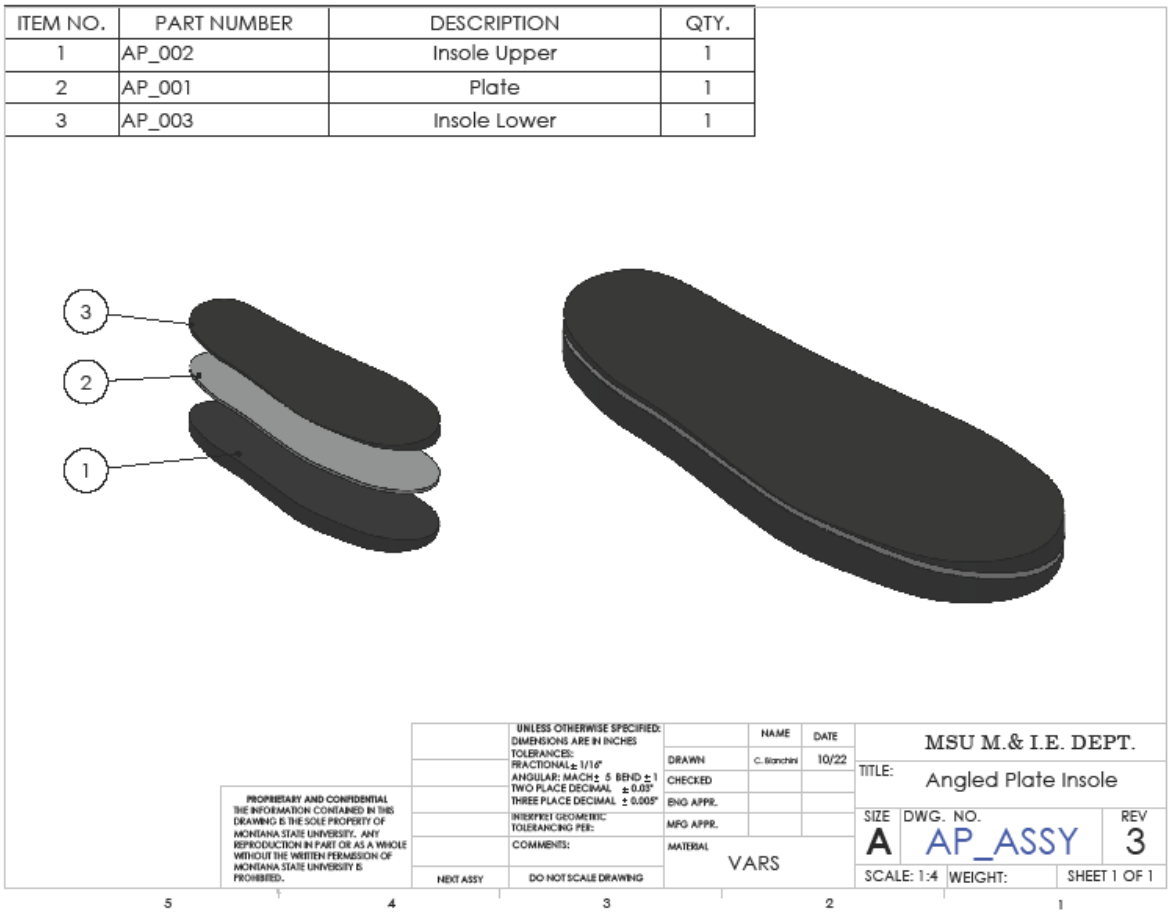

Figure C1. Assembly drawing of the angled plate insole.

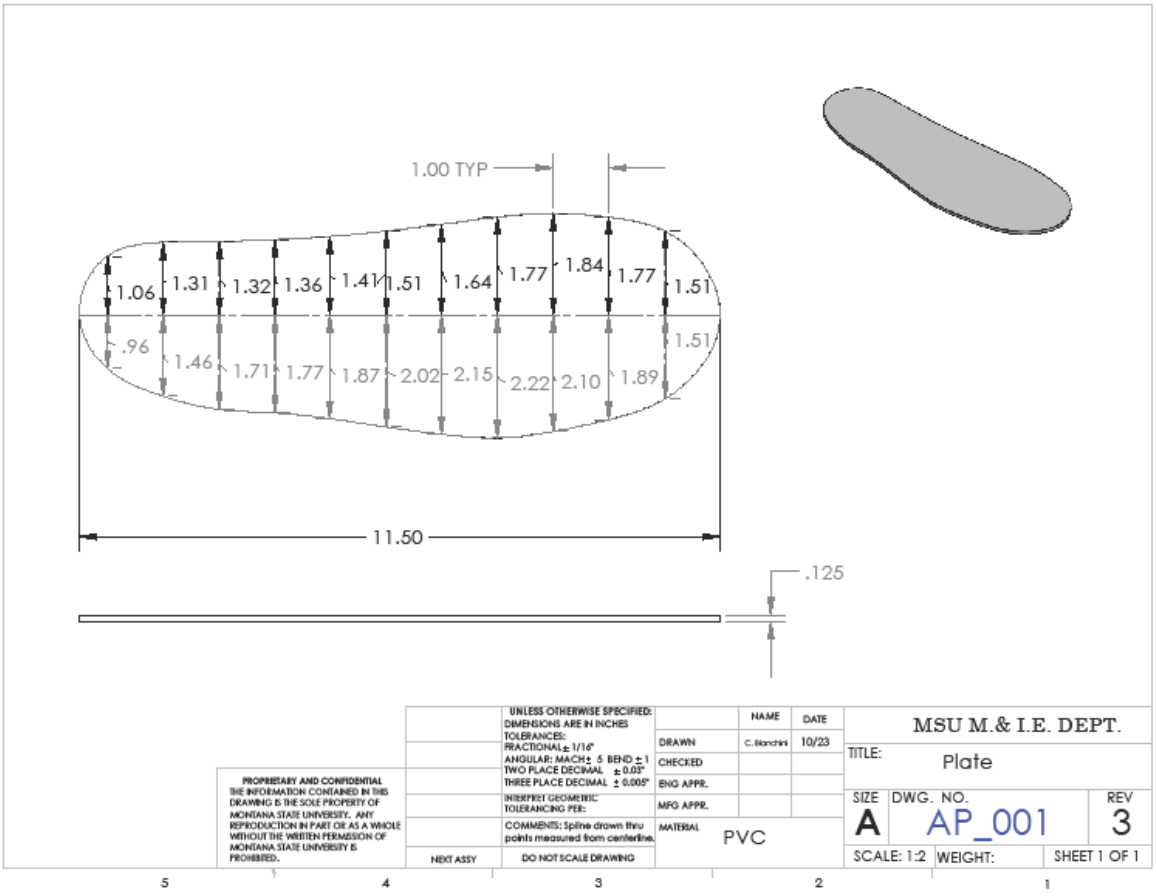

Figure C2. Part drawing of the plate used in the angled plate insole.

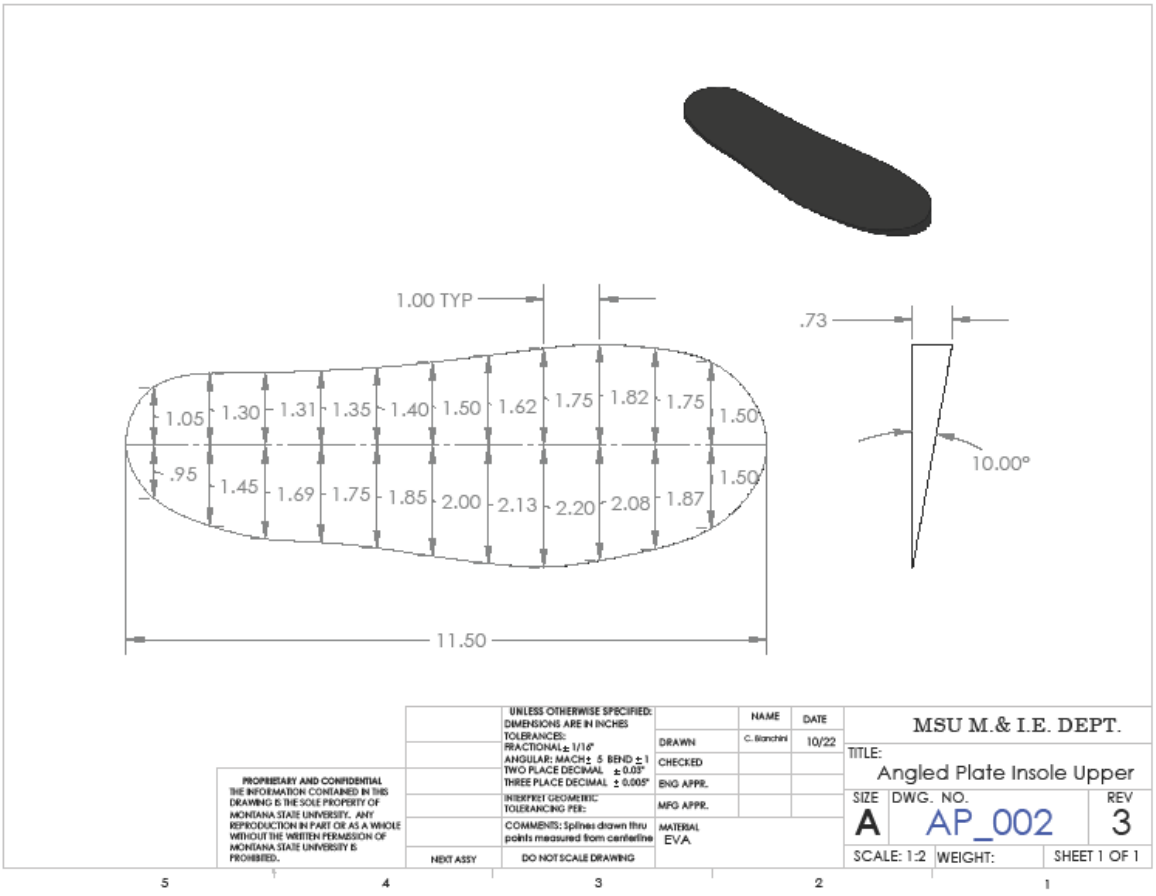

Figure C3. Part drawing of the upper foam portion of the angled plate insole.

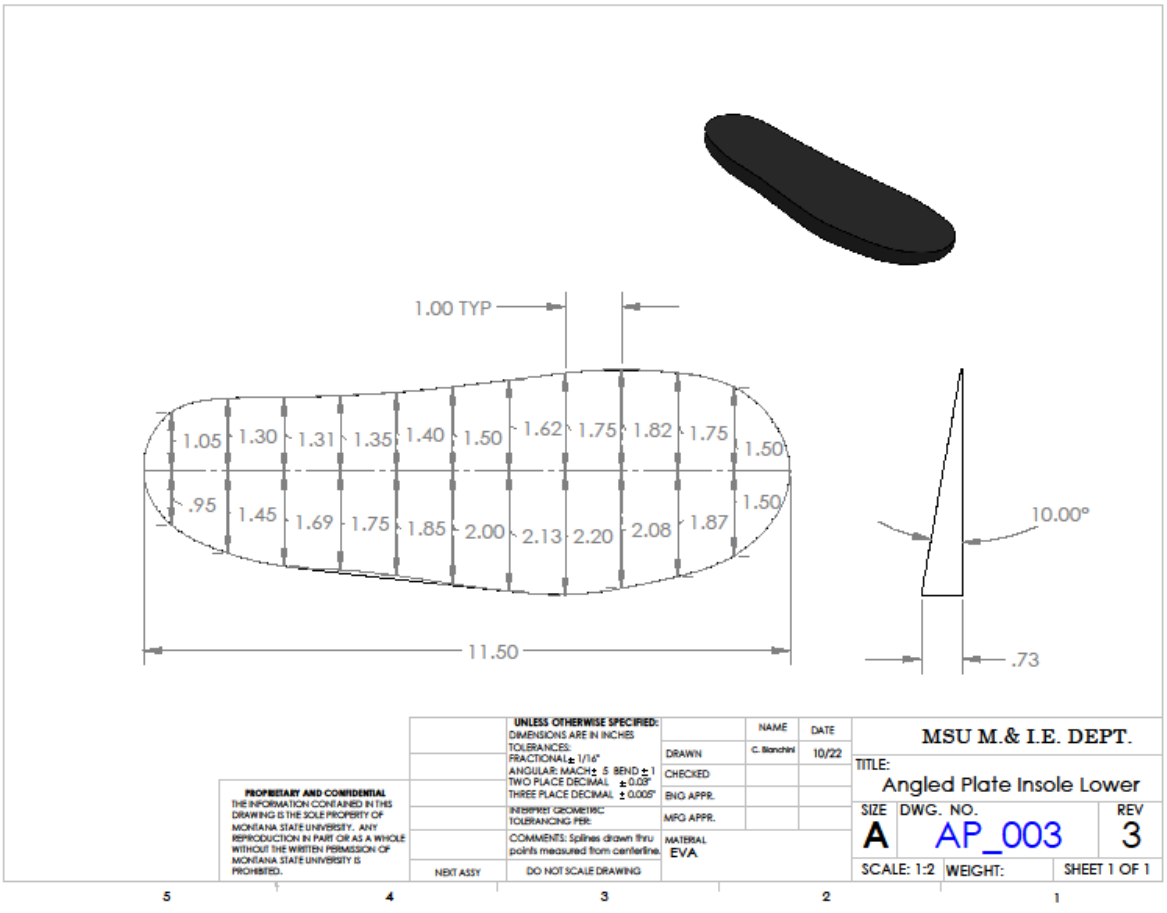

Figure C4. Part drawing of the lower foam portion of the angled plate insole.

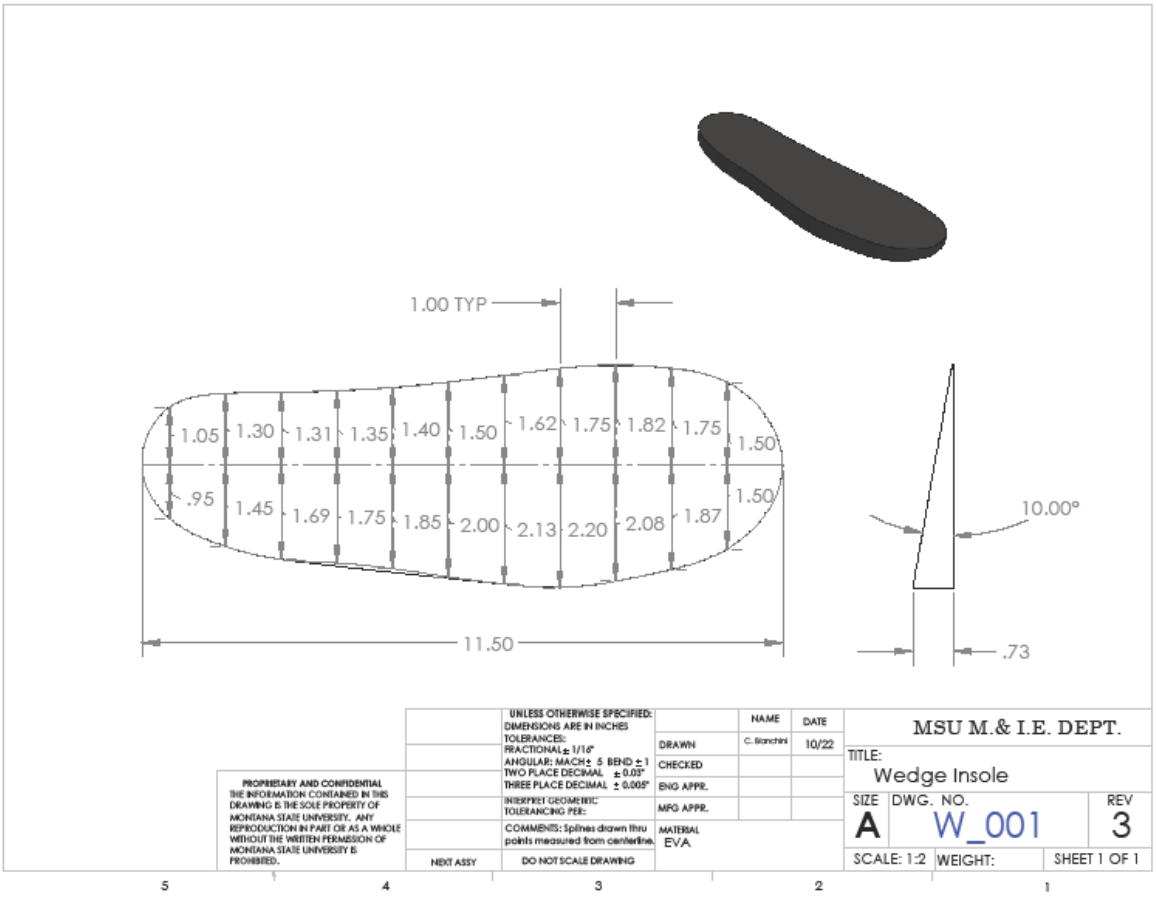

Figure C5. Part drawing of the wedge insole.

APPENDIX E

INTERNATIONAL REVIEW BOARD APPLICATION

Full Committee Review ☐
Expedited Review ☐

MONTANA STATE UNIVERSITY
Institutional Review Board Application for Review
(revised 12/12/22)

****

THIS AREA IS FOR INSTITUTIONAL REVIEW BOARD USE ONLY. DO NOT WRITE IN THIS AREA

Application Number: Approval Date:
Disapproved: IRB Chair's Signature:

****

Date:

I. Investigators and Associates (list all investigators involved; application will be filed under name of first person listed)

NAME: Corey Pew TITLE: Assistant Professor
DEPT: Mechanical and Industrial Engineering PHONE #: 406-994-6769
112 Roberts Hall
Bozeman, MT 59717
E-MAIL ADDRESS: Corey.Pew@montana.edu
DATE TRAINING COMPLETED: __In Progress_ *[Required training: CITI Training; see website for link]*

SIGNATURE (PI or ADVISOR): _____

NAME: Christopher Bianchini TITLE: Student
DEPT: Mechanical and Industrial Engineering PHONE #:
COMPLETE ADDRESS: 212 Roberts Hall, Bozeman, MT 59717
E-MAIL ADDRESS: Christophe.bianchini@student.montana.edu
DATE TRAINING COMPLETED: 5/10/21 [*Required training: CITI Training; see website for link]*

II. Title of Proposal: **The Effects of Angled Midsole Plates on Indoor Short Track Running Mechanics**

III. Beginning Date for Use of Human Subjects: 12/1/2022

IV. Type of Grant and/or Project (if applicable)
Research Grant:
Contract:
Training Grant:
Classroom Experiments/Projects:
Thesis Project:
Other (Specify):

V. Name of Funding Agency to which Proposal is Being Submitted (if applicable): NA

VI. Signatures

Submitted by Investigator
Typed Name: Corey Pew
Signature:
Date: 1/22/2020

VII. Summary of Activity.

A. RATIONALE AND PURPOSE OF RESEARCH.

Indoor track running can also lead to higher rates of injury. When training and competing on the smaller turn radii of an indoor 200m flat track as opposed to a typical 400m outdoor track, an athlete experiences asymmetrical strength changes and variations to their natural running gait that result in higher stresses throughout the lower extremities. Physically angled (wedged) shoes can increase running performance and mechanics for strictly curve-only running by allowing an athlete to exert a force directly perpendicular to the surface on which they are running. With a ground reaction force perpendicular to the athlete, an athlete's gait becomes more like that of straight, flat running, and many of the issues introduced by corner running are resolved. However, a wedged shoe is impractical for a flat indoor track where straight running is also prevalent. Our goal is to demonstrate that an athlete may be able to receive benefit during both straight and curved running by introducing an angled and asymmetrically stiff carbon fiber plate into competition shoes while not requiring an athlete's ankles to be physically tilted by a wedge or a banked track.

B. RESEARCH PROCEDURES INVOLVED.

This study will utilize an experimental, human subject protocol. Recruitment will consist of the research coordinator (Chris Bianchini) approaching Montana State Track & Field athletes individually. Potential participants will be provided with the research coordinator's email address and phone number and will be instructed to reach out if they are interested in participating. Initial conversations will consist of a verbal interview to determine their eligibility. If eligibility requirements are met, a time will be scheduled for their data collection. Participants will arrive at the Brick Breeden Fieldhouse (free parking provided) and will first complete the informed consent process. Next, they will be interviewed for self-report information. Specifically, we will ask their age, gender, height, weight, the number of miles they run per week, their primary race distance (defined by their highest national ranking by event), their average primary race pace, and if they have sustained any injury in the last six months that would inhibit their ability to run. We will then have them change into tight fitting clothing and shorts to prevent interference with the inertial measurement unit (IMU) components and allow the placement of electromyography (EMG) units on legs. We will then measure their height and weight. Inertial measurement units will be secured to the participants body via a custom-made set of tight-fitting clothing with pockets secured to crucial points. The IMU components are contained in these pockets and are wirelessly connected to the researcher's computer. EMG units will be attached to each participant's medial gastrocnemius muscle and gluteus medias muscle with a double-sided sticky tape. Subjects will start by performing a ten-minute run at their self-selected pace as a warmup. The individual will then be allowed to rest for a minimum of five minutes and will be given as much rest as necessary until they indicate they are ready to continue testing. During this rest period, we will review the testing process with them. There are two different inserts that will be tested with each participant: an insert with a flat plate and an insert with an angled plate. The participant will be blind to which insert they are currently running in so as to prevent altered running gait based on the participant's expectations of outcomes with each insert. At this point, the participant will be randomly given one of the inserts to complete the first phase of testing. Participants will provide their own preferred running shoes to the researcher and the first insert will be placed into the shoes. The participant will then put their shoes back on with the insert inside. Participants will then be instructed to begin running. For each insert, 3 corners and 3 straights need to be recorded, resulting in a total of 12 50-meter runs. The participant will begin by running 50 meters at their selected race pace, followed by a 100-meter jog or walk for recovery, as decided by the participant. At the end of the 100-meter recovery portion, the participant will be instructed to run another 50 meters at their selected race pace. This will be repeated until 3 straights and 3 corners have been recorded. If at any point the participant asks for additional rest, rest will be

allowed as necessary. The participant will then provide their shoes to the researcher again to allow the second insert to be applied. The participant will then repeat the first portion of testing, completing 3 corners and 3 straights at race-pace. The participant's original inserts will then be put back into their shoes and the participant will be instructed to run for another 5 minutes at a self-selected pace as a cool down. IMU and EMG data will be collected and stored in a locked file to be seen only by the researcher and researcher's assistant. The total testing time will be less than 60 minutes, and total running time will be no more than 25 minutes.

C. DECEPTION

None.

D. SUBJECTS

1. Approximate number and ages
   How Many Subjects: 50
   Age Range of Subjects: 18-23 years old

2. Criteria for selection:

   Subjects are required to be experienced runners, who compete regularly on a 200m flat track and run 40-100 miles per week for at least 40 weeks out of the year.

3. Criteria for exclusion:

   Recent history of musculoskeletal injury that would inhibit running performance by self-report.

4. Source of Subjects (including patients):

   Montana State University Track and Field team, distance and mid-distance event groups

5. Who will approach subjects and how? Explain steps taken to avoid coercion.

   The Montana State Track and Field team members will be approached. We will reach out to the coach, Lyle Weese, to provide information and allow him to relay the information to the athletes. By allowing the coach to provide the information we will not be able to directly coerce individuals.

6. Will subjects receive payments, service without charge, or extra course credit? Yes or (No)
   (If yes, what amount and how? Are there other ways to receive similar benefits?)

7. Location(s) where procedures will be carried out:

   Montana State University indoor track and field complex in Brick Breeden fieldhouse at 1 Bobcat Cir, Bozeman, MT 59717

E. RISKS AND BENEFITS (ADVERSE EFFECTS)

1. Describe nature and amount of risk and/or adverse effects (including side effects), substantial stress, discomfort, or invasion of privacy involved.

   Risks include fatigue from running and falling. Participants will be allowed to rest or stop

testing at any point they feel uncomfortable. Risk of falling will be no greater than an individual running on a 200m flat track.

2. Will this study preclude standard procedures (e.g., medical or psychological care, school attendance, etc.)? If yes, explain.

   No

3. Describe the expected benefits for individual subjects and/or society.

   No benefit to participants. Societal benefits include a better understanding of how an angled midsole plate may function as a temporary intervention during injury rehabilitation from injuries sustained while participating in indoor track and field.

F. ADVERSE EFFECTS

1. How will possible adverse effects be handled?

   By investigator(s):
   Referred by investigator(s) to appropriate care: Participants will see their own care provider
   Other (explain):

2. Are facilities/equipment adequate to handle possible adverse effects? Yes or No
   (If no, explain.)

3. Describe arrangements for financial responsibility for any possible adverse effects.

   MSU compensation (explain):
   Sponsoring agency insurance:
   Subject is responsible: Subject is financially responsible for adverse effects.
   Other (explain):

G. CONFIDENTIALITY OF RESEARCH DATA

1. Will data be coded? Yes or No

2. Will master code be kept separate from data? Yes or No

3. Will any other agency have access to identifiable data? Yes or No
   (If yes, explain.)

4. How will documents, data be stored and protected?
   Locked file: Master List will be kept in locked file
   Computer with restricted password: Experimental data (deidentified) will be kept on password protected computer
   Other (explain):

VIII. Checklist to be completed by Investigator(s)

A. Will any group, agency, or organization be involved? Yes or No
   (If yes, please confirm that appropriate permissions have been obtained.)

B. Will materials with potential radiation risk be used (e.g. x-rays, radioisotopes)? Yes or No

1. Status of annual review by MSU Radiation Sources Committee (RSC). Pending or Approved
   (If approved, attach one copy of approval notice.)

2. Title of application submitted to MSU RSC (if different).

C. Will human blood be utilized in your proposal? Yes or No
   (If yes, please answer the following)

   1. Will blood be drawn? Yes or No
      (If yes, who will draw the blood and how is the individual qualified to draw blood?
      What procedure will be utilized?)

   2. Will the blood be tested for HIV? Yes or No

   3. What disposition will be made of unused blood?

   4. Has the MSU Occupational Health Officer been contacted? Yes or No

D. Will non-investigational drugs or other substances be used for purposes of the research? Yes or No

   Name:
   Dose:
   Source:
   How Administered:
   Side effects:

E. Will any investigational new drug or other investigational substance be used? Yes or No
   [*If yes, provide information requested below and one copy of: 1) available toxicity data; 2) reports of animal studies; 3) description of studies done in humans; 4) concise review of the literature prepared by the investigator(s); and 5) the drug protocol.]*

   Name:
   Dose:
   Source:
   How Administered:
   IND Number:
   Phase of Testing:

F. Will an investigational device be used? Yes or No
   (If yes, provide name, source description of purpose, how used, and status with the U.S. Food and Drug Administration FDA). Include a statement as to whether or not device poses a significant risk. Attach any relevant material.)

G. Will academic records be used? Yes or No

H. Will this research involve the use of:
   Medical, psychiatric and/or psychological records Yes or No
   Health insurance records Yes or No
   Any other records containing information regarding personal health and illness Yes or No

   If you answered "Yes" to any of the items under "H.", you must complete the **HIPAA worksheet**.

I. Will audio-visual or tape recordings or photographs be made? Yes or No

J. Will written consent form(s) be used? (Yes or No. If no, explain.) (Please use accepted format from our website. Be sure to indicate that participation is voluntary. Provide a stand-alone copy; do not include the form here.)

APPENDIX E

CONSENT FORM

SUBJECT CONSENT FORM FOR PARTICIPATION IN HUMAN RESEARCH AT MONTANA STATE UNIVERSITY

We are asking you to participate in a research study. This form is designed to give you information about this study. We will describe this study to you and answer any of your questions.

Project Title: The Effects of Angled Midsole Plates on Indoor Short Track Running Mechanics

Principal Investigator: Corey Pew, PhD
Mechanical and Industrial Engineering
(406)-994-6769

What the study is about
Indoor track running can lead to higher rates of injury compared to outdoor track running. When training and competing on the smaller turn radii of an indoor, 200m flat track as opposed to a typical, 400m outdoor track, an athlete experiences asymmetrical strength changes and variations to their natural running gait that result in higher stresses throughout the lower extremities. The purpose of this research study is to determine whether a new shoe insole is an effective intervention to mitigate the negative effects of indoor flat track running.

What we will ask you to do
We will begin by asking you 5 questions regarding personal details and running background. The 5 questions are:

1. On average, how many miles do you run per week during a typical training cycle?
2. What are your fastest times ever achieved in official competition for 800m, 1500m, 1 mile, 3000m, 3000m steeplechase, 5000m, and 10,000m?
3. What is your height?
4. What is your weight?
5. In the last 12 months, have you incurred a significant musculoskeletal injury that resulted in a surgery or more than 2 weeks away from training?

You will perform multiple running trials. We will ask you to run straight and around corners, with different shoe insoles. The experiment will consist of alternating 50-meter test portions and 100-meter recovery portions. For the test portions, you are required to run at your primary race pace. Your primary race is defined as the distance at which you would have the highest World Athletics score. If you are unsure of your primary race distance, we will help you identify it before testing. You may run slowly or walk during your recovery period.

You will begin with a 10-minute warm up at a self-selected pace. We will then set up the data collection equipment and move into the testing phase. EMG sensors will be placed on your

medial gastrocnemius (inside calf) and gluteus medias (outside upper hip region) on your skin using light adhesive tape. We will also attach small inertial measurement units to each segment of your body using Velcro straps. Then, you will be asked to put on a pair of tights and a tight-fitting shirt in order to contain any wires and mitigate unwanted movement of data collection devices.

You will be tested for a total of 750 meters, broken up into 15 repetitions of 50 meters, 6 straight and 9 around a corner. The figure below will familiarize you with the data collection process.

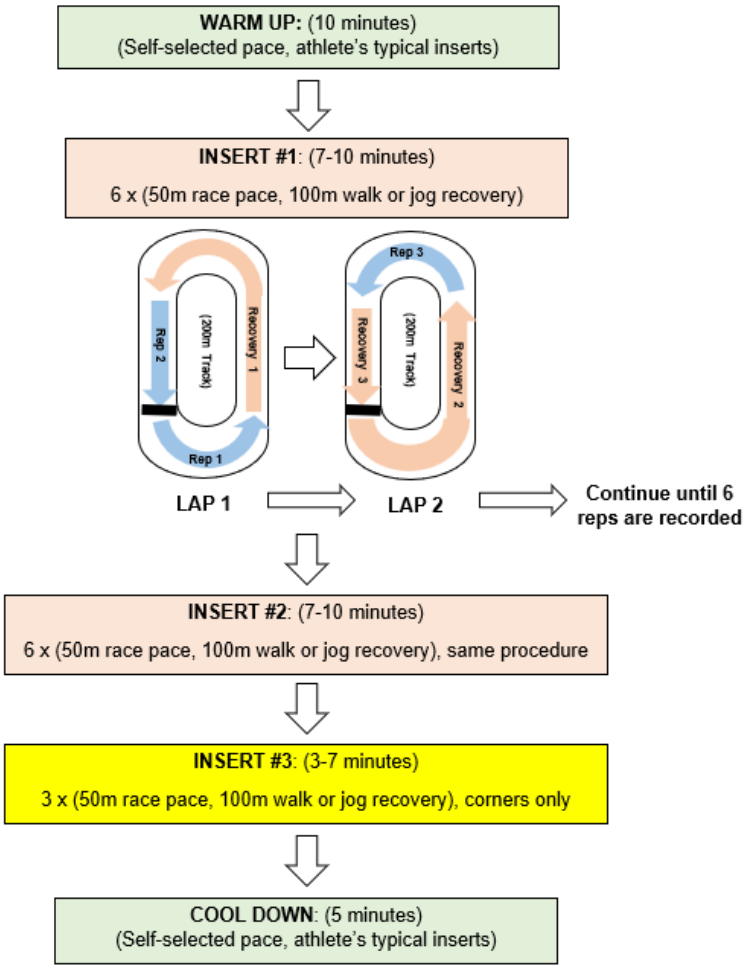

Risks and discomforts

While you are doing study activities on the track, there is a risk that you may fall and hurt yourself. This risk is not any higher than it would be when running normally. In addition, due to the physical nature of these tests you may become tired or fatigued and experience muscle pain.

You may experience slight discomfort when the sensors and markers are removed. This discomfort will not be greater than removing a band-aid.

When placing the EMG sensors, a sensor will need to be placed on your gluteus medius muscles, which are on the top outside portion of the hip. This will require a researcher to be very close to your personal space. A female researcher will place EMGs on female participants and a male researcher will place EMGs on male participants. If the placement of the EMG devices makes you too uncomfortable to continue, this step can be skipped.

Benefits
There will be no direct benefit to you by participating in the study. However, runners like yourself may benefit from the data collected in this study in the future.

Payment for participation
You will not receive any compensation for this study.

Audio/Video Recording
During this study, we may take photographs or video recordings of you while you run. These images will exclude your head so that your face will not be visible. Additionally, we will cover any tattoos or other identifying marks with an easy-to-remove tape, and any video recording will be done with the camera on mute so that we will not record your voice. These measures are in place to protect your identity and privacy. You will be given an opportunity to review the photographs and video recordings and erase any that you wish. If we use any videos during a scientific presentation or publication, none of your personal identifiers will be included.

Please sign below if you are willing to be recorded (video and audio). You may still participate in this study if you are not willing to have the study recorded.

☐ I do not want to have this study recorded.
☐ I am willing to have this study recorded:

Signed: _____

Date: _____

If you are injured by this research
In the event that any research-related activities result in an injury, treatment will be made available including first aid, emergency treatment, and follow-up care as needed. Cost for such care will be billed in the ordinary manner to you or your insurance company. No reimbursement, compensation, or free medical care is offered by Montana State University. If you think that you have suffered a research-related injury, contact Corey Pew right away at (406)-994-6769.

Privacy/Confidentiality

We will take every precaution to maintain the confidentiality of your data. Your identity (including any photographs or video recordings, which will be taken in a way to protect your identity and privacy) will be strictly confidential. Only the study staff will have access to the information that we collect from you. The data will be stored on secured computers and in file cabinets in locked offices or in the lab. All the personal information you provide will be confidential. However, if we learn that you intend to harm yourself or others, we must report that to appropriate authorities. To ensure only study personnel can match you to your data, we will use a unique study code instead of identifying information such as your name.

Data Sharing

De-identified data from this study may be shared with the research community at large to advance science and health. We will remove or code any personal information that could identify you before files are shared with other researchers to ensure that, by current scientific standards and known methods, no one will be able to identify you from the information we share. Despite these measures, we cannot guarantee anonymity of your personal data.

Taking part is voluntary

You do not have to take part in this study. If you are in this study, you can withdraw at any time. You will not be penalized for your decision to not participate or withdraw if you decide to do so. If you decide to withdraw from the study, no new information will be collected from you; however, data already collected will continue to be part of the analyses. If you decide to withdraw, or if you are terminated from the study, a person from the study team may need to meet with you to discuss the necessary steps that you may need to take to end your participation in the study.

Withdrawal by investigator, physician, or sponsor

The investigators, physicians or sponsors may stop the study or take you out of the study at any time should they judge that it is in your best interest to do so, if you experience a study-related injury, if you need additional or different medication/treatment, or if you do not comply with the study plan. They may remove you from the study for various other administrative and medical reasons. They can do this without your consent.

If you have questions

The main researcher conducting this study is Corey Pew, a professor at Montana State University. Please ask any questions you have now. If you have questions later, you may contact Corey Pew at Corey.Pew@Montana.edu or at (406)-994-6769. If you have any questions or concerns regarding your rights as a subject in this study, you may contact the Institutional Review Board (IRB) for Human Participants at 406-994-4706 or access their website at http://www.montana.edu/orc/irb/index.html.

You will be given a copy of this form to keep for your records.

Statement of Consent

I have read the above information and have received answers to any questions I asked. I consent to take part in the study.

Your Signature_____ Date_____

Your Name (printed)_____

Signature of person obtaining consent_____ Date_____

Printed name of person obtaining consent_____

This consent form will be kept by the researcher for at least five years beyond the end of the study.